Strain-boost and Diffusive Molecular Dynamics

Ju Li, Sina Ardakani, Shuhei Shinzato, Sanket Sarkar,
Shotaro Hara, Akio Ishii, Shigenobu Ogata, Yunzhi Wang

http://Li.mit.edu/mapp

Workshop on New algorithms for exploring structure and dynamics of interfaces,
The University of British Columbia, July 31-Aug 1, 2017.

long-timescale atomic-resolution evolution of interfacial structure, tied to macroscopic properties

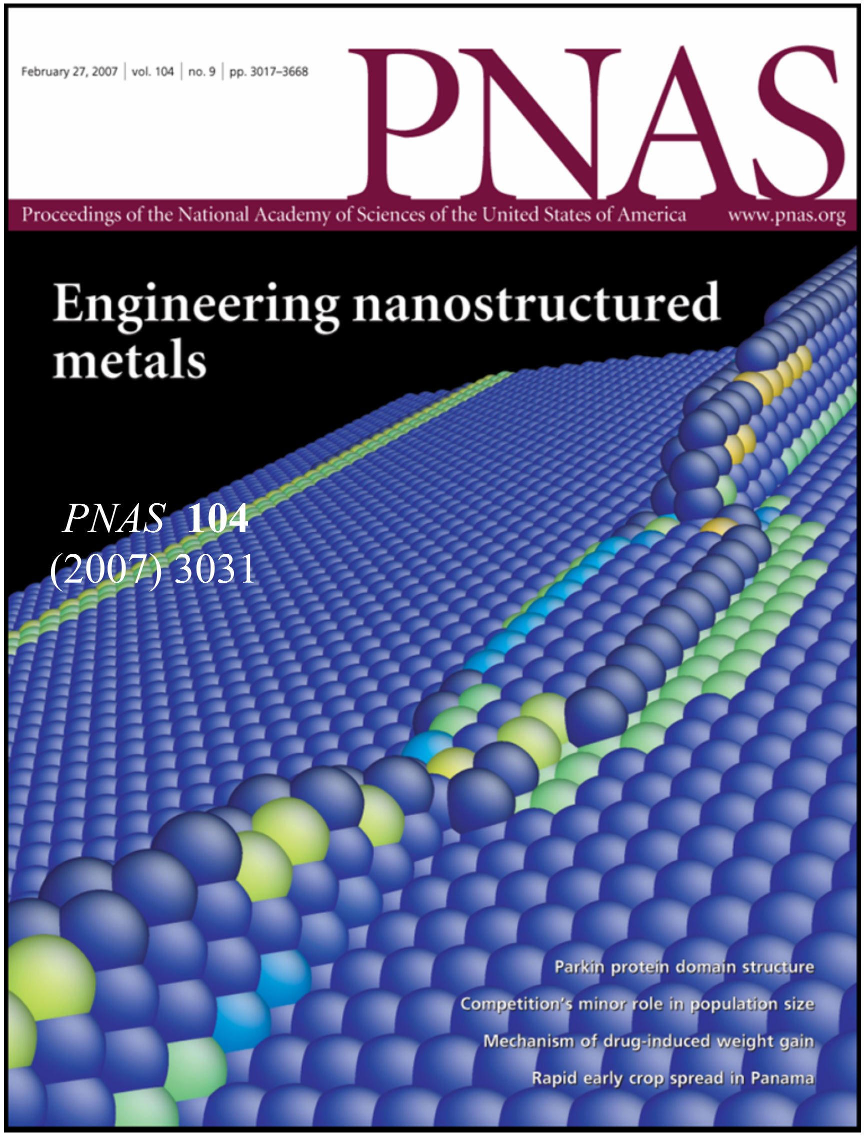

February 27, 2007 | vol. 104 | no. 9 | pp. 3017–3668

PNAS

Proceedings of the National Academy of Sciences of the United States of America www.pnas.org

Engineering nanostructured metals

Parkin protein domain structure

Competition's minor role in population size

Mechanism of drug-induced weight gain

Rapid early crop spread in Panama

PNAS **104** (2007) 3031

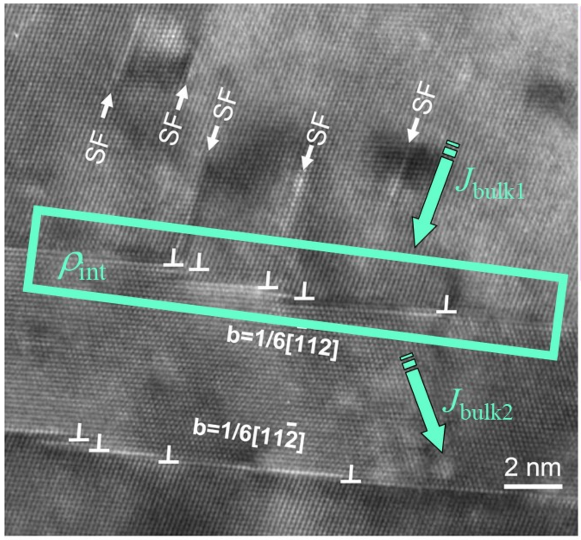

Absorption-Desorption-Transmission kinetics for interfacial dislocation density ρ_{int} evolution:

$$J_{\text{bulk1}} = J_{\text{abs}}(\tau,\rho_{\text{int}}) + J_{\text{tms}}(\tau,\rho_{\text{int}})$$

$$J_{\text{bulk2}} = J_{\text{tms}}(\tau,\rho_{\text{int}}) + J_{\text{des}}(\tau,\rho_{\text{int}})$$

$$\frac{d\rho_{\text{int}}}{dt} = J_{\text{abs}}(\tau,\rho_{\text{int}}) - J_{\text{des}}(\tau,\rho_{\text{int}})$$

$-\log J(\tau,\rho_{\text{int}}) \propto Q(\tau,\rho_{\text{int}})$:

Atomistic calculation	Exp't measurement
$\frac{\partial Q(\tau,\rho_{\text{int}})}{\partial \tau} \propto -\Omega \longrightarrow$	strain-rate sensitivity *m*
$\frac{\partial Q(\tau,\rho_{\text{int}})}{\partial \rho_{\text{int}}} \propto \Pi \longrightarrow$	strain-hardening coefficient Θ

Comparison of yield stress, activation volume and strain-rate sensitivity between experimental measurements and atomistic calculation

		yield stress	activation volume Ω	strain-rate sensitivity *m*
Nano-twinned Copper	Uniaxial tension [Lu04]	~ 1 GPa		$m \equiv \frac{\partial \ln \sigma}{\partial \ln \dot{\varepsilon}} = \frac{k_B T}{\sigma \Omega}$
	Nanoindentation [Lu05]	> 700 MPa*	$12 - 22b^3$	$0.025 - 0.036$
	Atomistic calculation	780 MPa	$24 - 44b^3$	$0.013 - 0.023$
Diffusion-controlled processes			$\sim 0.1b^3$	~ 1
Bulk forest hardening		$\sim \mu b\sqrt{\rho_{\text{bulk}}}$	$100 - 1000b^3$	$0 - 0.005$

* extracted from measured hardness H as $\frac{H}{3}$.

PNAS **104** (2007) 3031

Stress-driven activated process

MRS Bulletin **32** (2007) 151

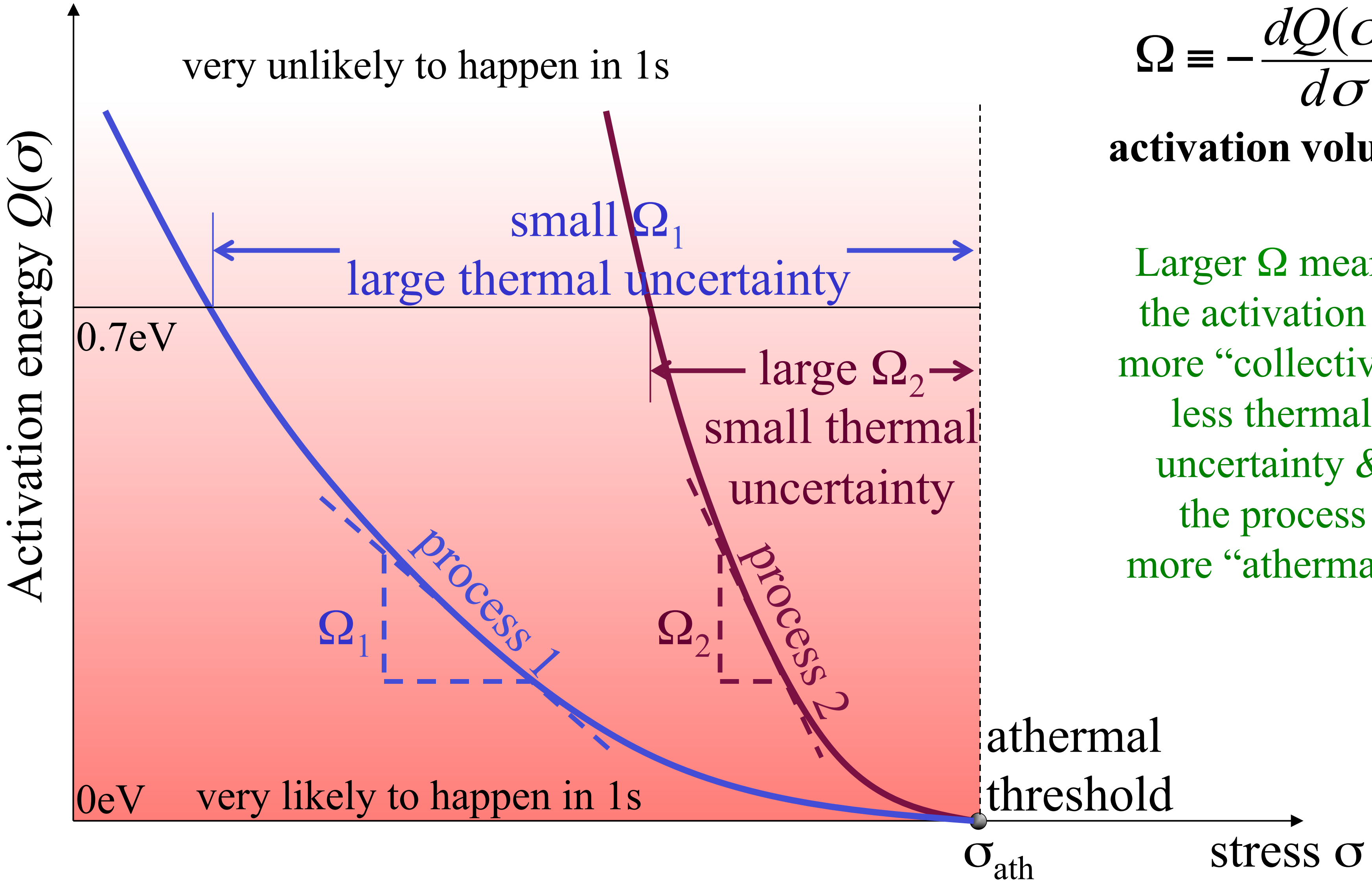

$$\Omega \equiv -\frac{dQ(\sigma)}{d\sigma}$$

activation volume

Larger Ω means the activation is more “collective”, less thermal uncertainty & the process more “athermal”.

point defect diffusion: ~0.02-1b^3 forest dislocation cutting: ~$10^3 b^3$

Free-end nudged elastic band (FENEB) method connecting to unstable final state to probe driven, thermally activated processes:

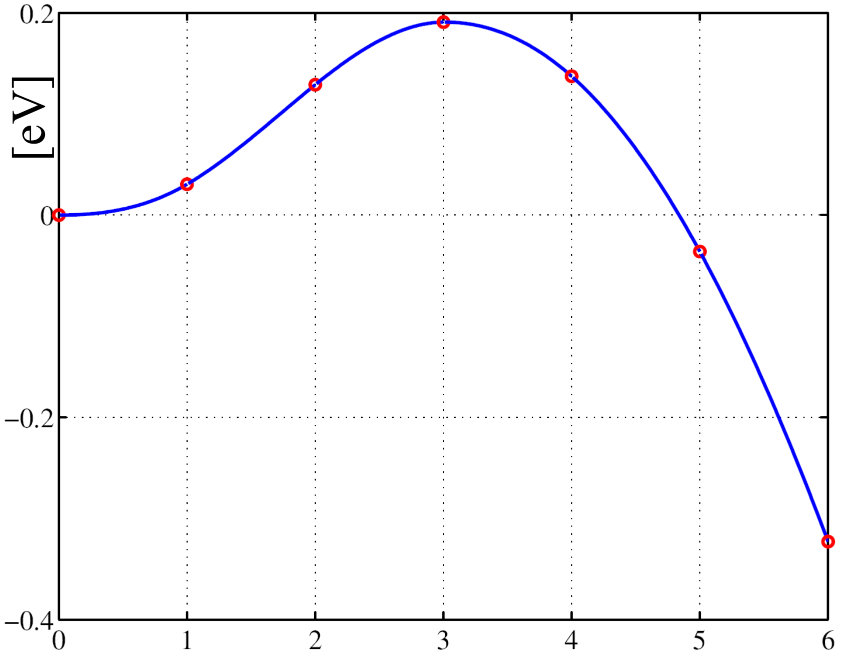

minimum energy path of homogeneous dislocation nucleation in Cu

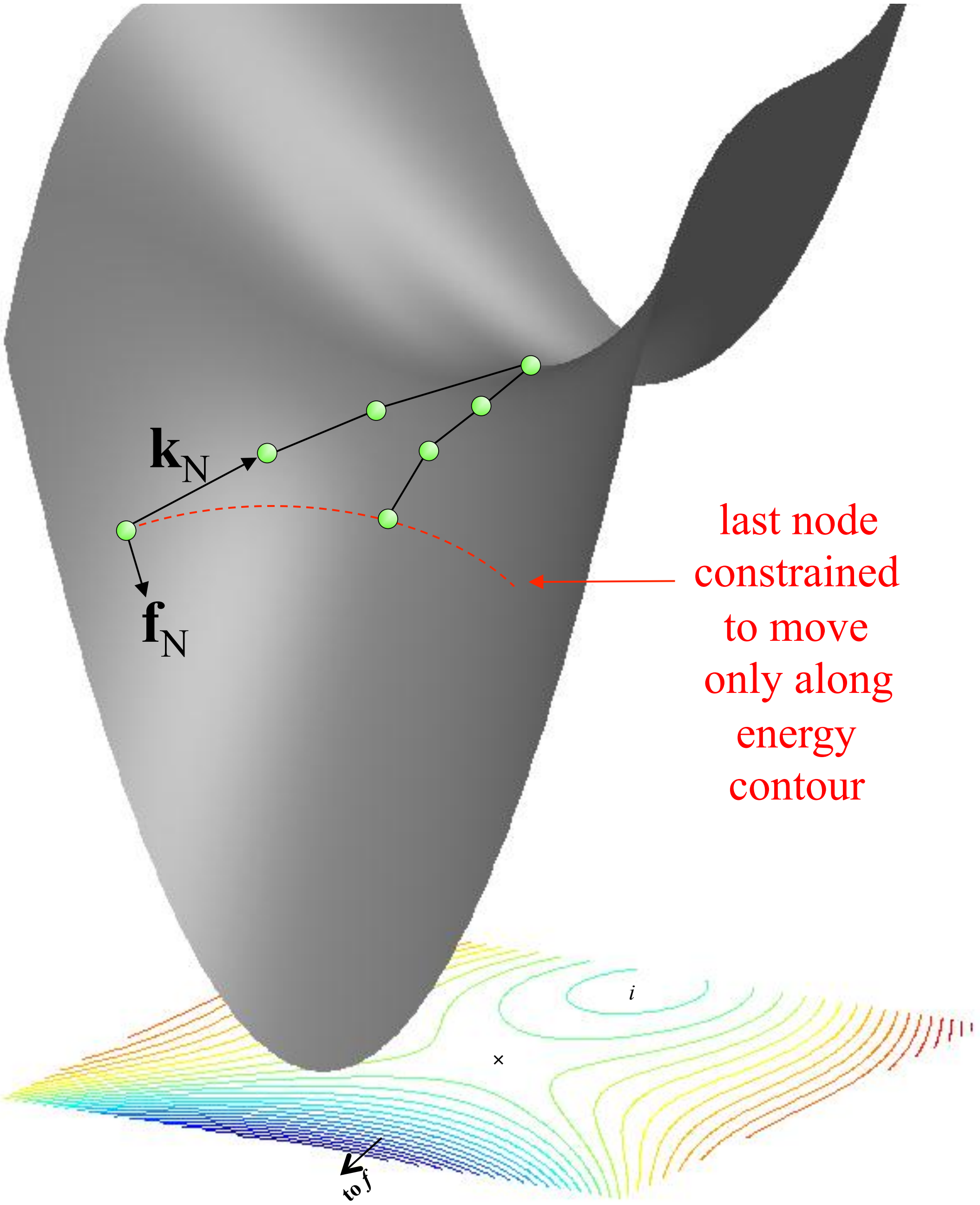

last node constrained to move only along energy contour

PNAS **104** (2007) 3031

$$\Delta \mathbf{x}_N = \nu \left(\mathbf{k}_N - \frac{(\mathbf{k}_N \cdot \mathbf{f}_N)\mathbf{f}_N}{|\mathbf{f}_N|^2} \right) + \alpha(E_N - E_N^{\mathrm{desired}}) \frac{\mathbf{f}_N}{|\mathbf{f}_N|^2}$$

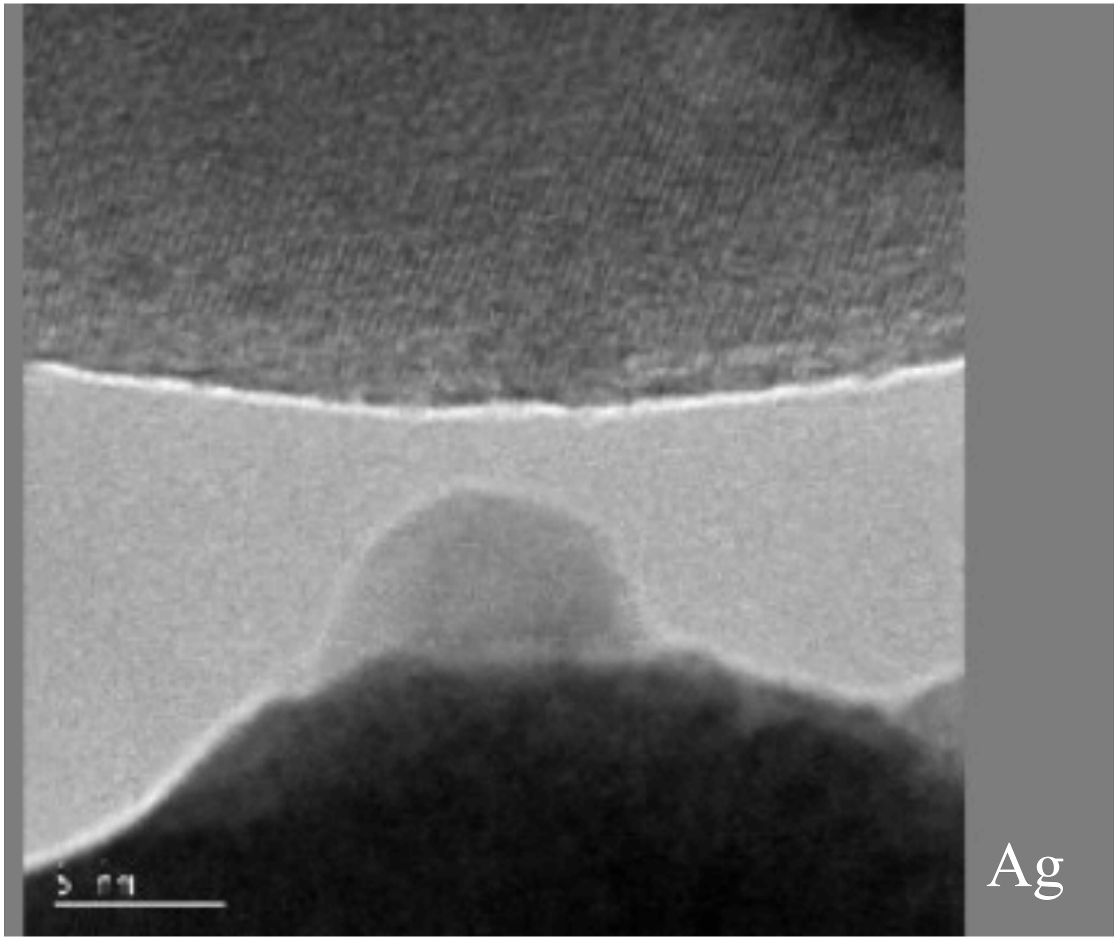

“Liquid-like pseudoelasticity of sub-10-nm crystalline silver particles”, *Nature Materials* **13** (2014) 1007

Room-temperature Diffusive deformation of nanoscale objects

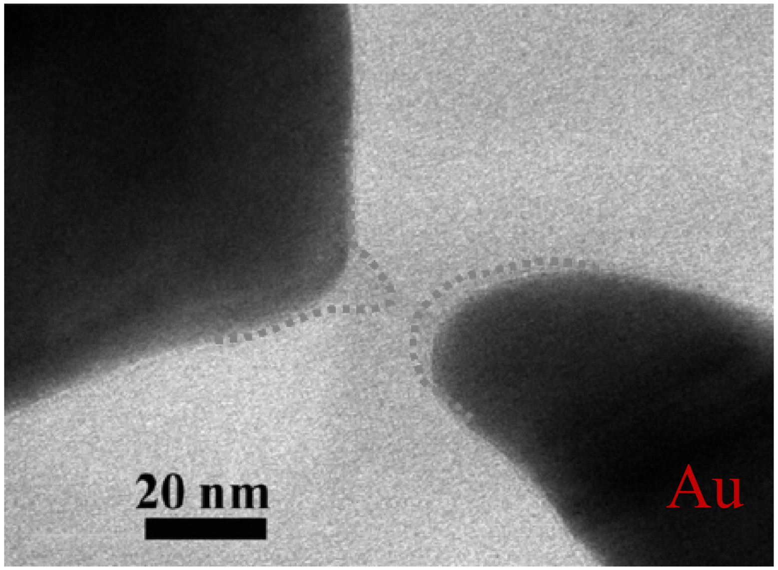

Nanogap in Au after leaving the sample for 4 months at room temperature.
Strachan et al, *Nano Letters* **6** (2006) 441

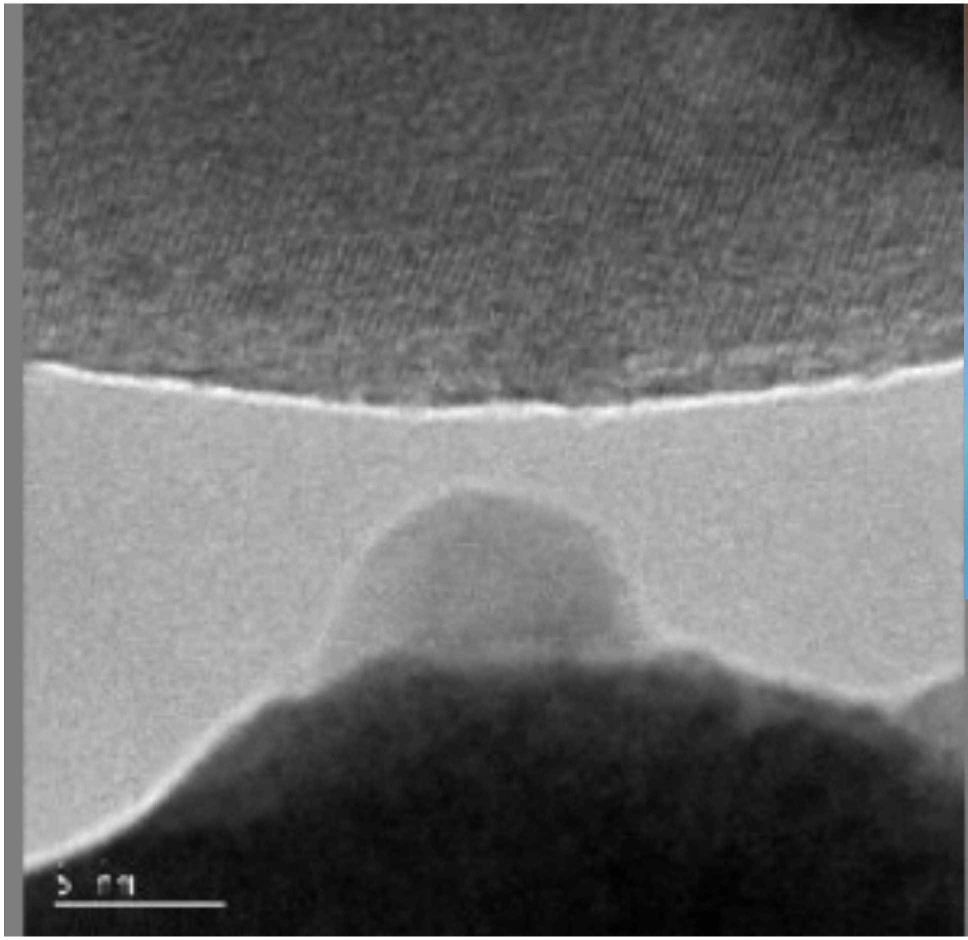

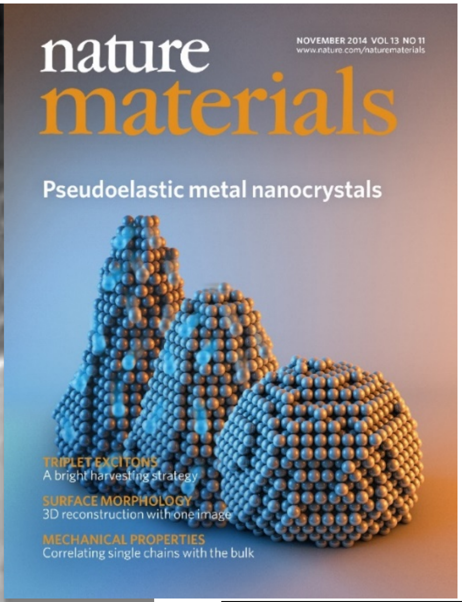
NOVEMBER 2014 VOL 13 NO 11
www.nature.com/naturematerials

nature materials

Pseudoelastic metal nanocrystals

TRIPLET EXCITONS
A bright harvesting strategy

SURFACE MORPHOLOGY
3D reconstruction with one image

MECHANICAL PROPERTIES
Correlating single chains with the bulk

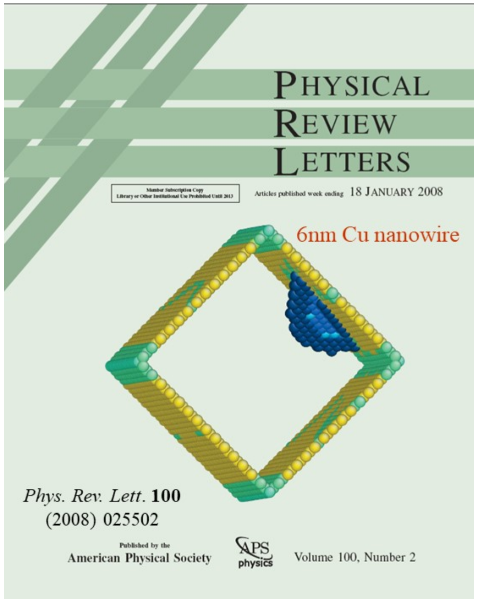
PHYSICAL REVIEW LETTERS

Articles published week ending 18 JANUARY 2008

6nm Cu nanowire

Phys. Rev. Lett. **100**
(2008) 025502

Published by the American Physical Society

APS physics

Volume 100, Number 2

Ag

Diffusive vs Displacive

“Liquid-like pseudoelasticity of sub-10-nm crystalline silver particles”, *Nature Materials* **13** (2014) 1007

Room-temperature Diffusive deformation of nanoscale objects

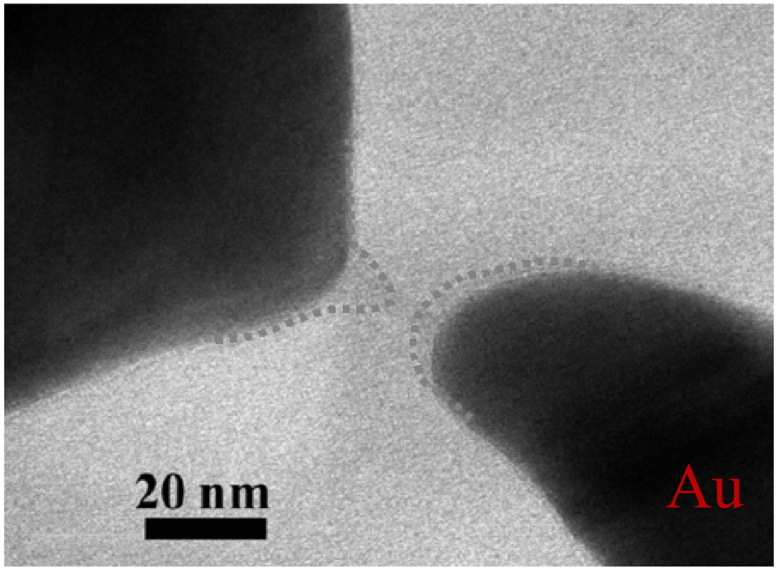

Nanogap in Au after leaving the sample for 4 months at room temperature.
Strachan et al, *Nano Letters* **6** (2006) 441

How well does Transition State Theory (TST) work?

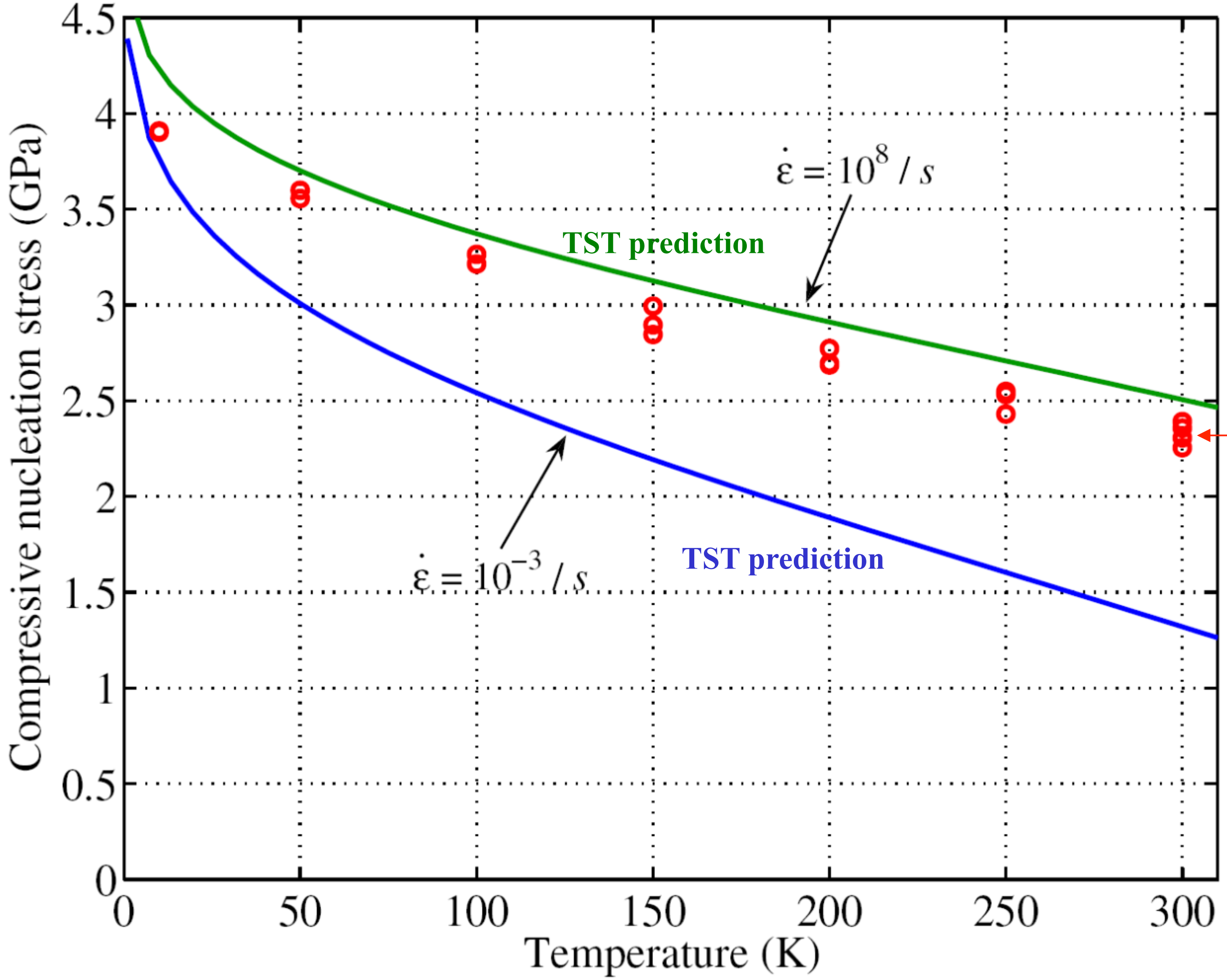

Direct MD simulations at 10^8/s

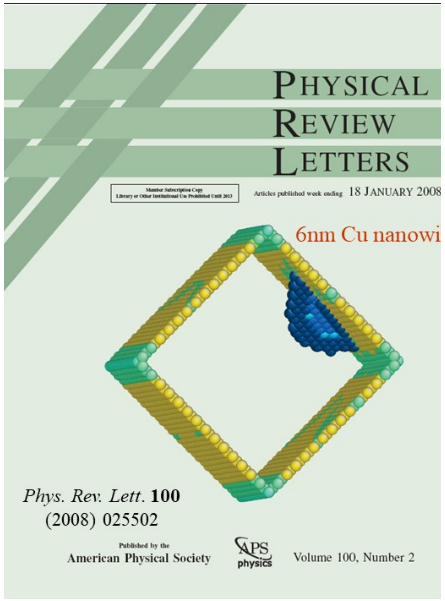

Physical Review Letters

Articles published week ending 18 January 2008

Phys. Rev. Lett. **100** (2008) 025502

Published by the American Physical Society

Volume 100, Number 2

Autonomous PES Explorations by Hyperdynamics / Metadynamics

A. F. Voter, *Phys. Rev. Lett.* **78** (1997) 3908

Potential Energy Surface

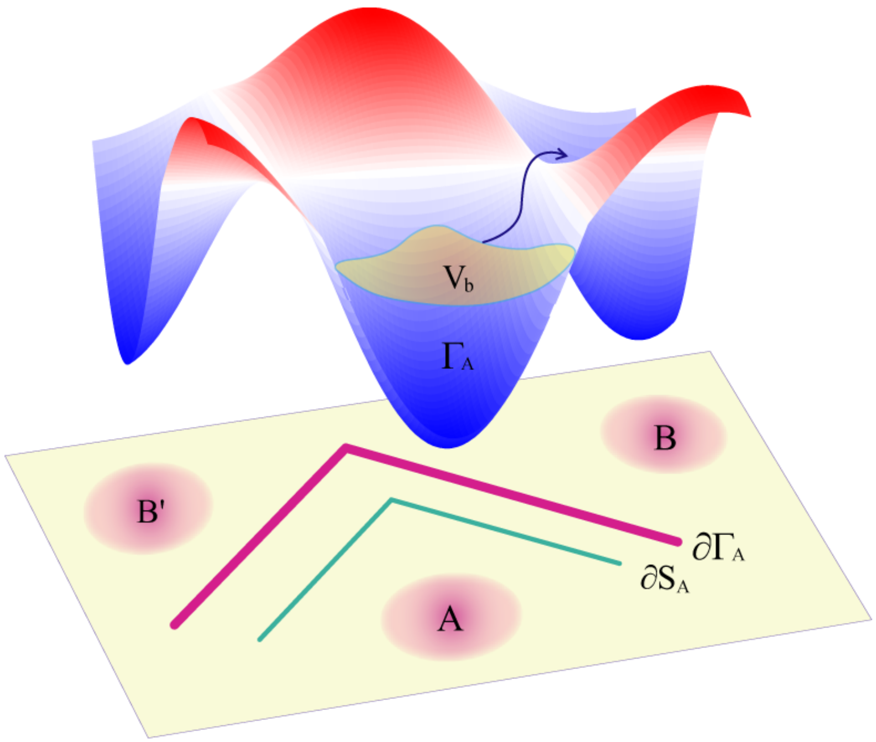

- Add a positive boost potential around basin A

$$V_b = V + \boxed{\Delta V}$$

- Must satisfy hyperdynamics requirement.

At all the dividing surface, $\Delta V=0$

Speed-up factor

Time evolution :

$$\Delta t_{\text{Phys}} = \Delta t_{\text{MD}} \boxed{e^{\Delta V / k_B T}}$$

How we design an effective and robust boost-potential?

Geometry-based Hyperdynamics: Boost potential depends on local atomic geometry

- **Bond-boost method**

Miron & Fichthorn, *J. Chem. Phys.* **119** (2003) 6210

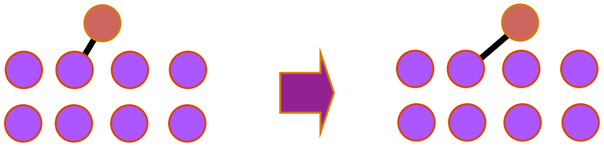

$$\varepsilon_i \equiv (r_i - r_{\text{eq}})/r_{\text{eq}}$$

- **Eshelby Transformation**

Hara & Li, *Phys. Rev. B* **82** (2010) 184114

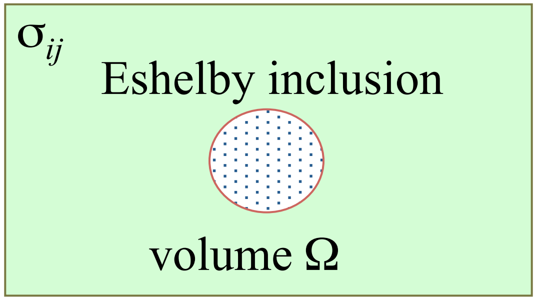

inelastic transformation of continuum ellipsoid

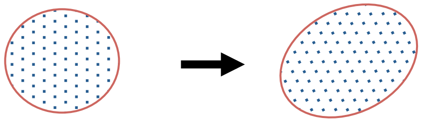

transformation strain η_{ij}

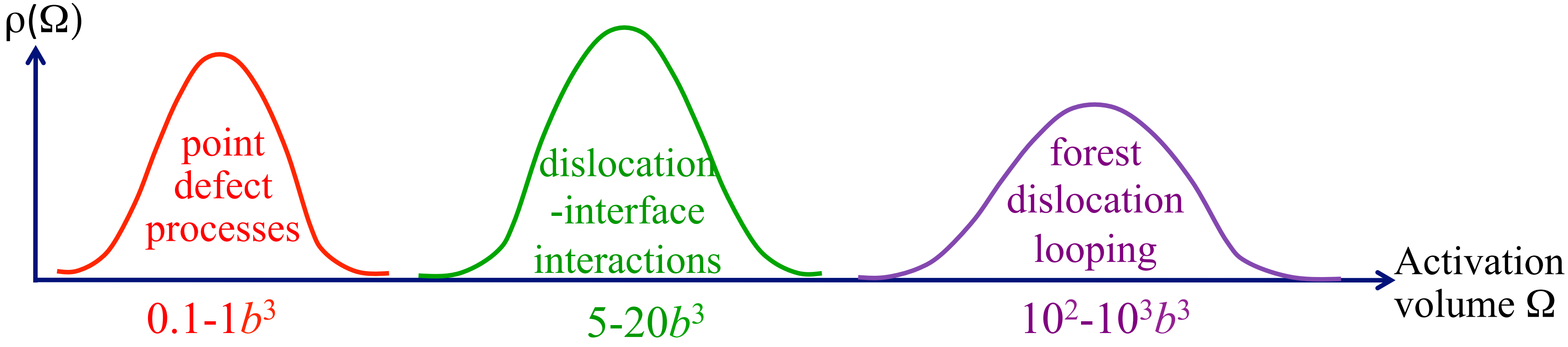

Least-Square Atomic Strain

Hara & Li, *Phys. Rev. B* **82** (2010) 184114

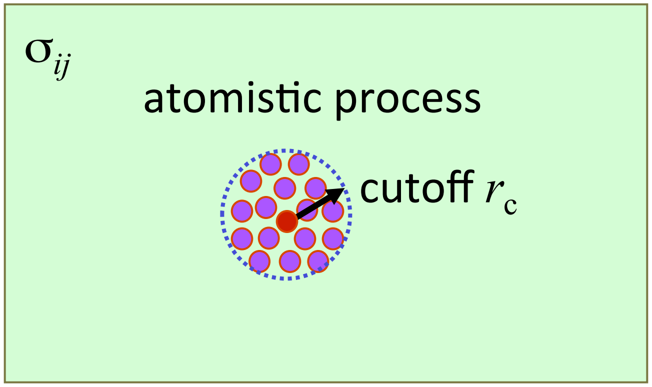

small r_c (small Ω)

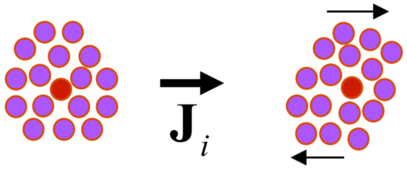

$$\min_{\mathbf{J}_i} \sum_{j\in N_i} \left| \mathbf{d}^0_{ji}\mathbf{J}_i - \mathbf{d}_{ji} \right|^2$$

$$\eta_i^{\mathrm{hydro}} \equiv \mathrm{Tr}(\boldsymbol{\eta}_i)/3$$

$$\boldsymbol{\eta}_i \equiv (\mathbf{J}_i\mathbf{J}_i^{\mathrm{T}} - \mathbf{I})/2$$

$$\eta_i^{\mathrm{Mises}} \equiv \sqrt{\mathrm{Tr}(\boldsymbol{\eta}_i - \eta_i^{\mathrm{hydro}}\mathbf{I})^2/2}$$

$$= \sqrt{\eta_{iyz}^2 + \eta_{ixz}^2 + \eta_{ixy}^2 + \frac{(\eta_{iyy} - \eta_{izz})^2 + (\eta_{ixx} - \eta_{izz})^2 + (\eta_{ixx} - \eta_{iyy})^2}{6}}$$

r_c chosen to match the (experimentally known) **activation volume spectral range**

Surface dislocation nucleation

Cu nano-pillar compression

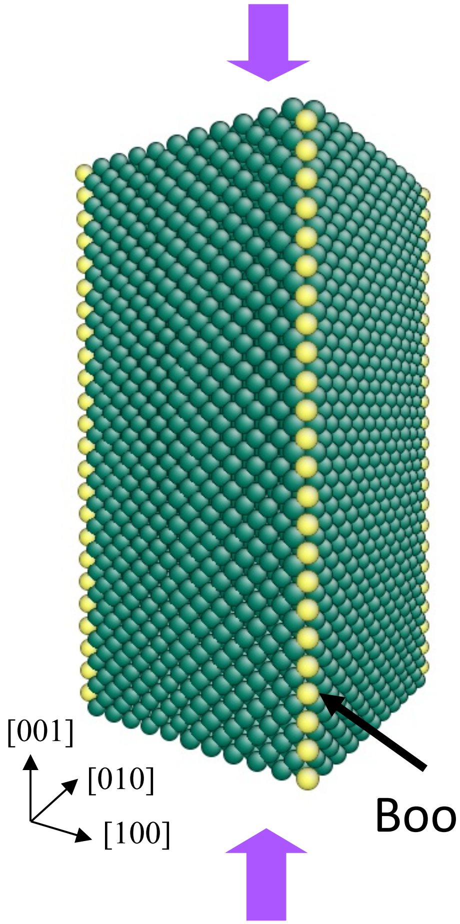

Boost atoms

- 14000 atoms
- Mishin potential
- 1 million simulation steps (maximum)
- Applied stress (σ: 1.75-2.50 GPa)
- Temperature (T: 100-450 K)

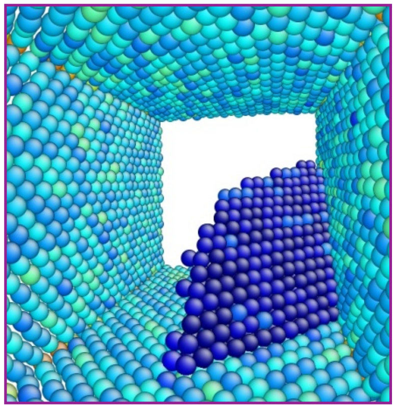

Partial dislocation nucleation from corner

$T = 180$ [K]
$\sigma = 1.75$ [GPa]
$t_{\mathrm{Phys}} = 70$ [sec]

$$\Delta V = \boxed{A(\eta_{\max}^{\text{Mises}})} \sum_{N_a} \frac{\delta V_i(\eta_i^{\text{Mises}})}{N_a}$$

η_i^{Mises} : atomic shear strain Mises invariant

N_a : the number of boost atoms

Shutdown Function

$$\eta_{\max}^{\text{Mises}} = \max\{\eta_i^{\text{Mises}}\}$$

$$A = 0 \quad \text{when} \quad \eta_{\max}^{\text{Mises}} > \boxed{q_c}$$

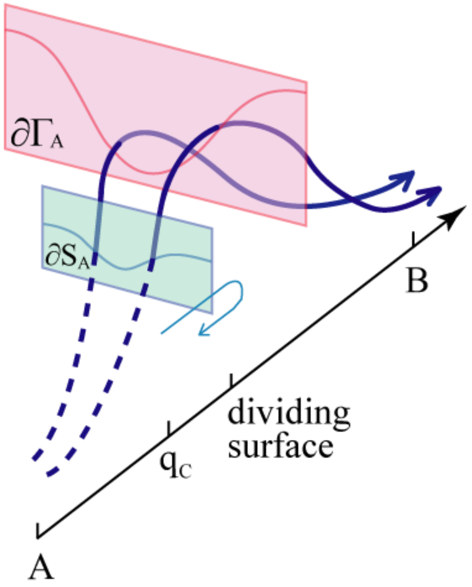

dividing surface

boundary surface of boost potential

q_c should be small enough to satisfy the hyperdynamics requirement

q_c should be large as possible to gain a maximum efficiency

Adaptive Strain-Boost Potential

Hara & Li, *Phys. Rev. B* **82** (2010) 184114

Acceleration (Boost) Factor

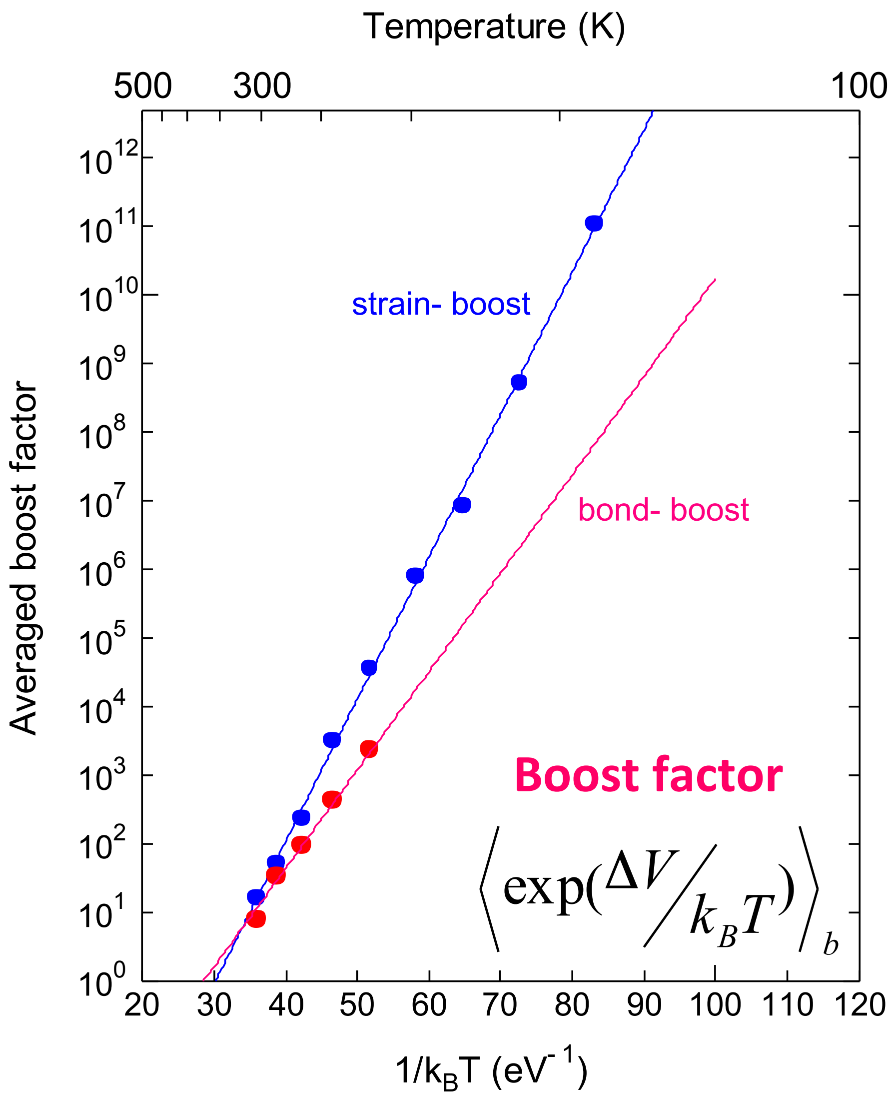

Strain-boost speed-up:
11 orders of magnitude

Ability to track dynamics over time scale of seconds.

Strain-boost is more suitable for exploring the collective stress-driven process.

Arrhenius plot

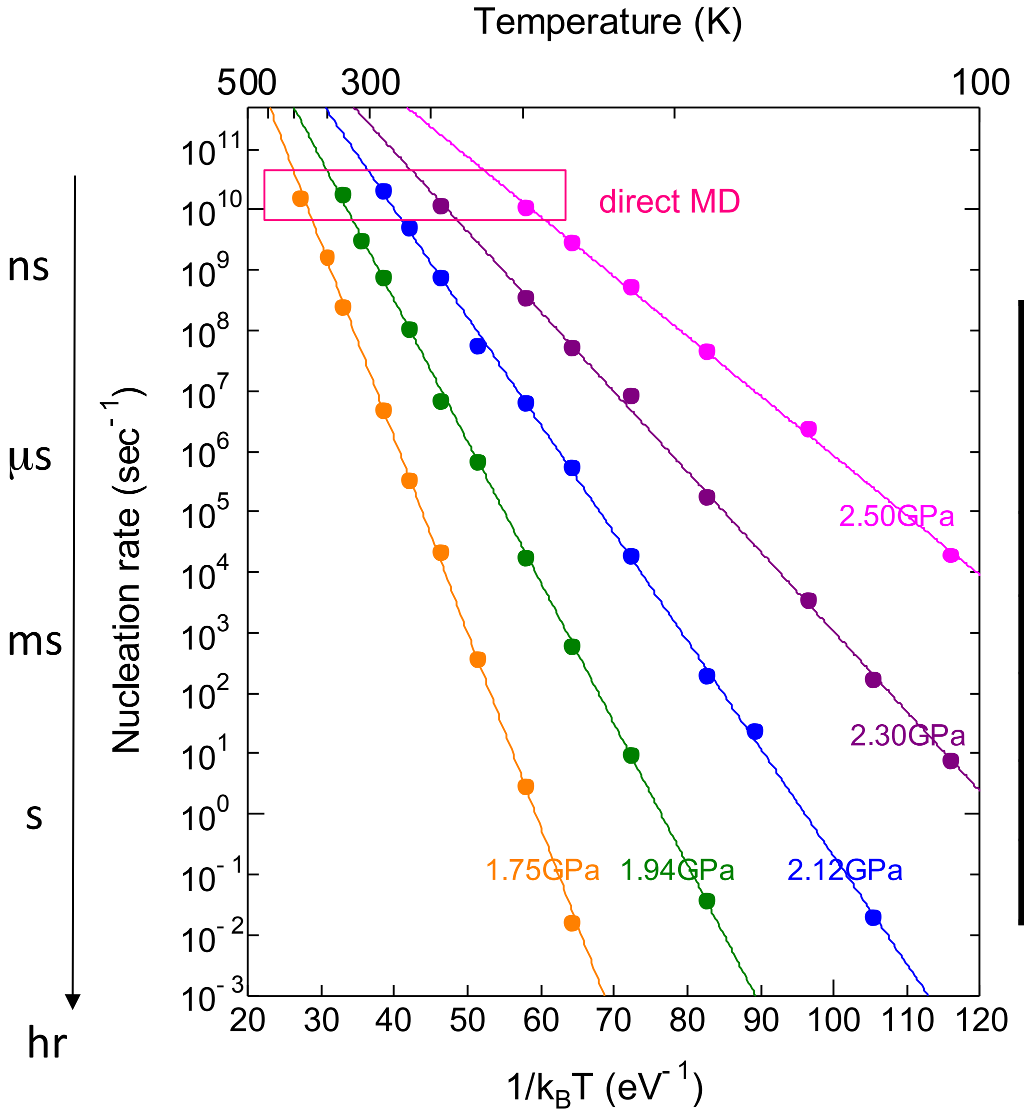

$$R(\sigma,T) = R_0(\sigma)\exp(-\frac{\Delta H(\sigma)}{k_B T})$$

Stress [GPa]	Activation Enthalpy [eV] **This work**	Activation Enthalpy [eV] **NEB**
1.75	0.74	0.72
1.94	0.54	0.55
2.12	0.41	0.42
2.3	0.31	0.32
2.5	0.23	0.25

Pre-factor → Activation Entropy

$$R = M\nu_{\mathrm{M}}(\boldsymbol{\sigma})\exp\left(-\frac{\Delta G(\boldsymbol{\sigma},T)}{k_{\mathrm{B}}T}\right) \rightarrow \Delta H(\boldsymbol{\sigma},T) = -k_{\mathrm{B}}\left.\frac{\partial(\ln R)}{\partial(1/T)}\right|_{\boldsymbol{\sigma}}$$

van't Hoff equation

Activation *Free Energy* Activation *Enthalpy* Activation *Entropy*

$$\Delta G(\boldsymbol{\sigma},T) = \Delta H(\boldsymbol{\sigma},T) - T\Delta S(\boldsymbol{\sigma},T)$$

$$R = \boxed{M\nu_{\mathrm{M}}(\boldsymbol{\sigma})\exp\left(\frac{\Delta S(\boldsymbol{\sigma},T)}{k_{\mathrm{B}}}\right)}\exp\left(-\frac{\Delta H(\boldsymbol{\sigma},T)}{k_{\mathrm{B}}T}\right)$$

M : the number of equivalent nucleation sites

ν_{M}: initial curvature of MEP

Stress-dependent Activation Entropy

Meyer-Neldel rule
Iso-kinetic law

$$\Delta S(\boldsymbol{\sigma}) \approx \frac{\Delta H(\boldsymbol{\sigma})}{T_{\mathrm{MN}}}$$

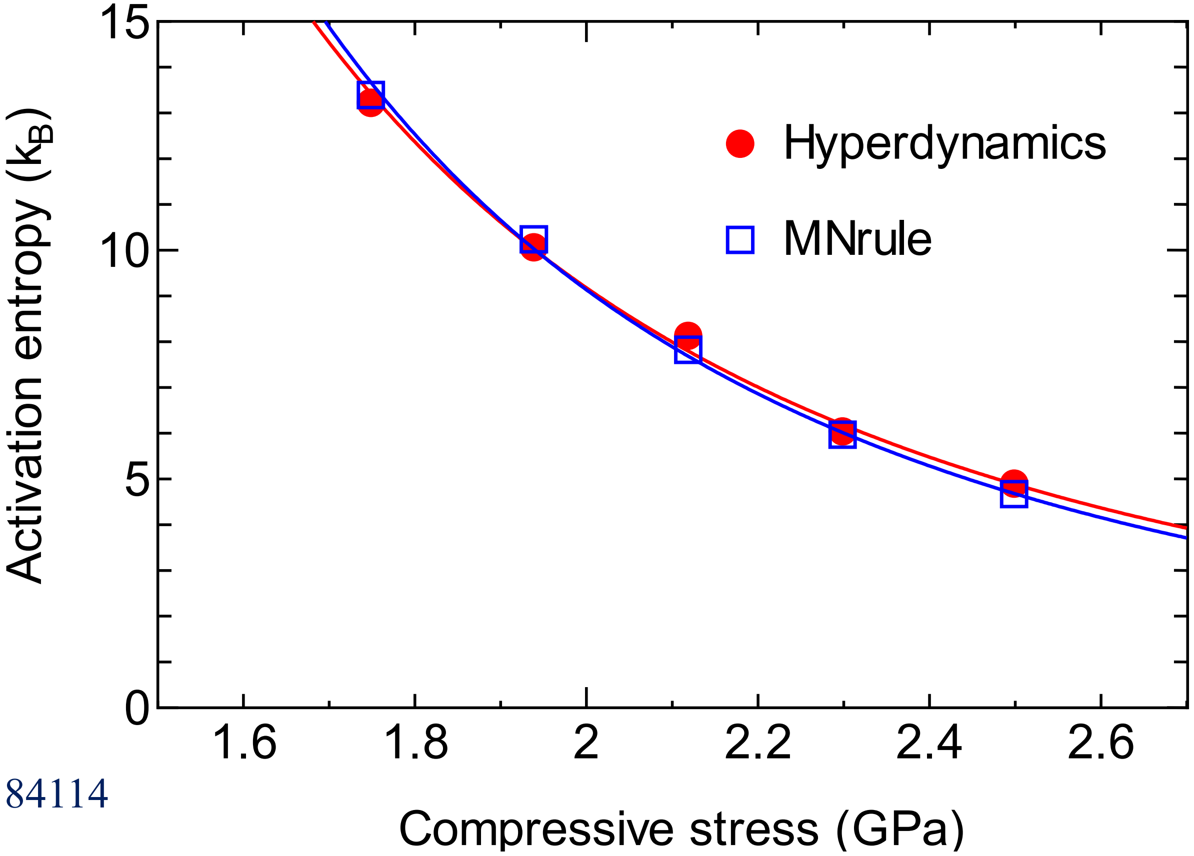

Hara & Li, *Phys. Rev. B* **82** (2010) 184114

$T_{\mathrm{MN}} = 625$ K (best fitting)

Half of bulk melting point (1320 K):
around surface premelting temperature

What if **Many Many Many** Barriers ?

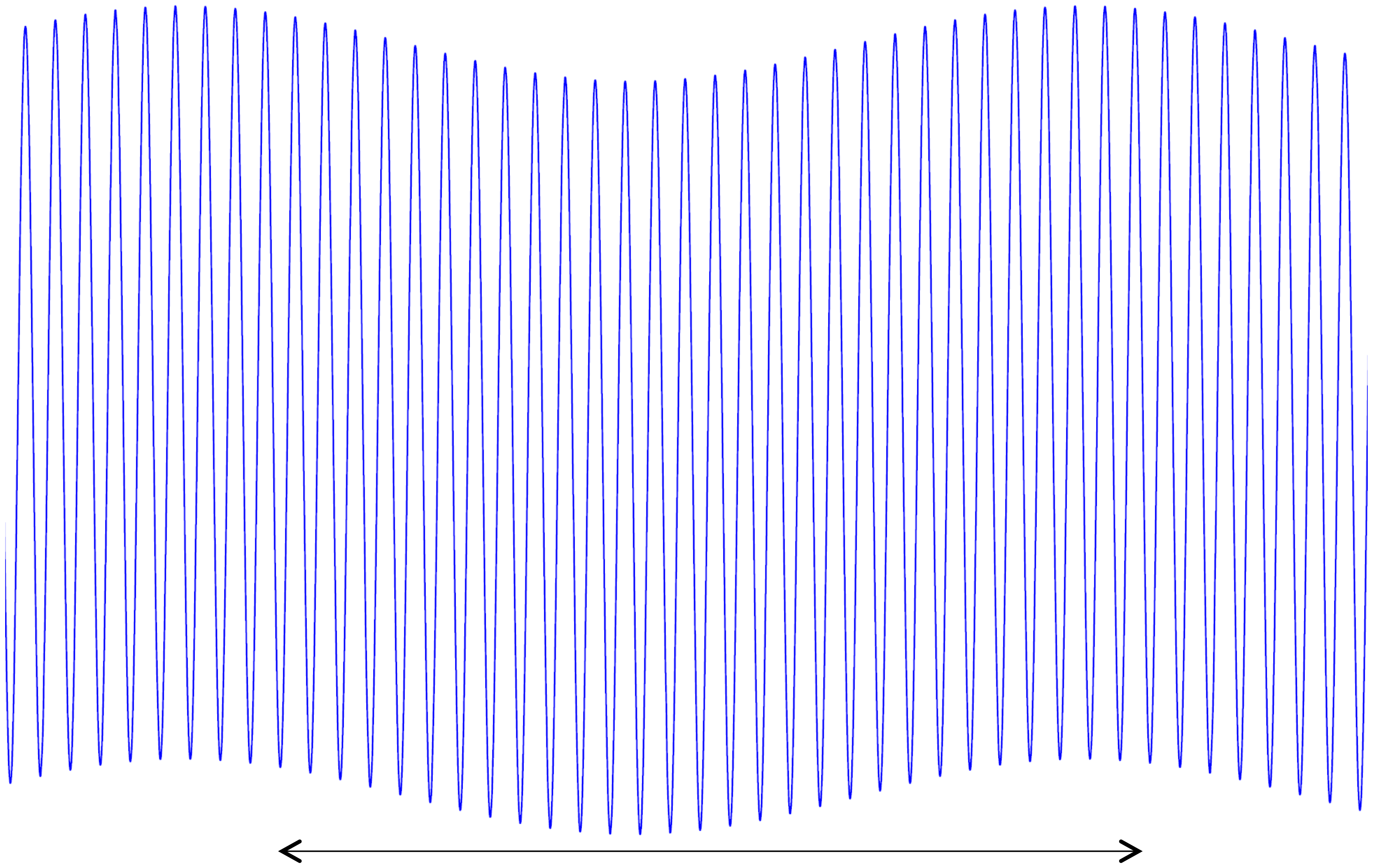

Trillions of barriers

- DMD thermodynamics formulated as a **density functional theory**. Atomic realization of regular solution model, w/ gradient thermodynamics, long-range elastic & short-range coordination interactions

- Pair, triplet, … **correlations** ignored. **Cluster expansion** calculation should give more accurate $F_{\mathrm{DMD}}(\{\mathbf{X}_i,\alpha_i,\mathbf{c}_i\})$

- DMD kinetics "solves Cahn-Hilliard equation on a moving atom grid", with **atomic spatial resolution**, but at **diffusive timescales**. *Time-Dependent DFT*

- Another view: DMD guides **atom creation** and **atom annihilation operators** in MD or VG simulations by chemical potential gradient

Li et al, *Phys. Rev. B* **84** (2011) 054103; Sarkar et al., *Phys. Rev. B* **86** (2012) 014115

Diffusive MD: Basic Idea

Variational Gaussian Method

$\{\mathbf{X}_i, \alpha_i\}, i=1..N$

Lesar, Najafabadi, Srolovitz,
Phys. Rev. Lett. **63** (1989) 624.

⬇

DMD

$\{\mathbf{X}_i, \alpha_i, \mathbf{c}_i\}, i=1..N$

$\mathbf{c}_i$: occupation probability
(vacancy, solutes)

Define $\boldsymbol{\mu}_i$ for each atomic site,
to drive diffusion

Ferris wheel seen with long
camera exposure time

Phase-Field Crystal: **Elder, Grant, et al.**
Phys. Rev. Lett. **88** (2002) 245701
Phys. Rev. E **70** (2004) 051605
Phys. Rev. B **75** (2007) 064107

basis: planewave → Gaussian

Advantage of a **continuous** site-probability representation at **atomic resolution**

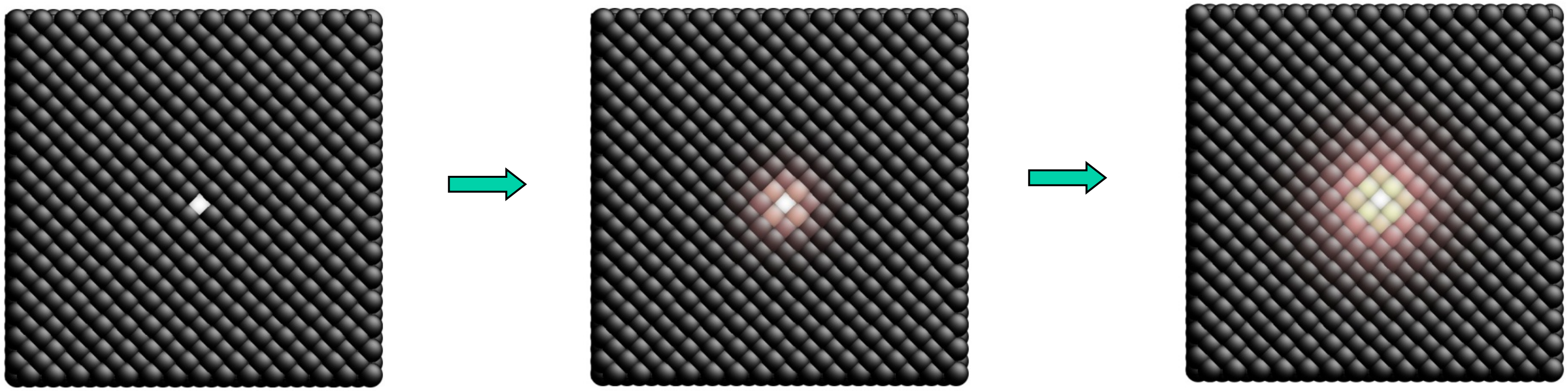

Probability Wave of Vacancy Random Walker

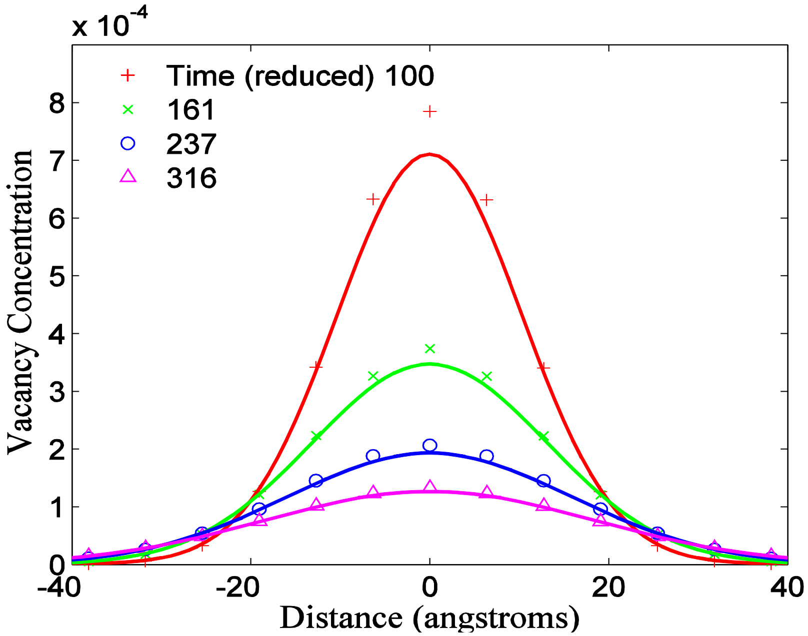

Representing **long-range mass transport** by vacancy random walk with MD, hyper-MD or kinetic Monte Carlo could require trillions of vacancy hops – impractical and unnecessary

Vacancy concentration: $c_{\mathrm{V}}(\Delta X,\tau) = \Omega\left(\tau b^2\right)^{-d/2} \exp\left[-\pi \Delta X^2 / \left(\tau b^2\right)\right]$

“**particle creation**” and “**particle annihilation**” operators in atomistic simulations

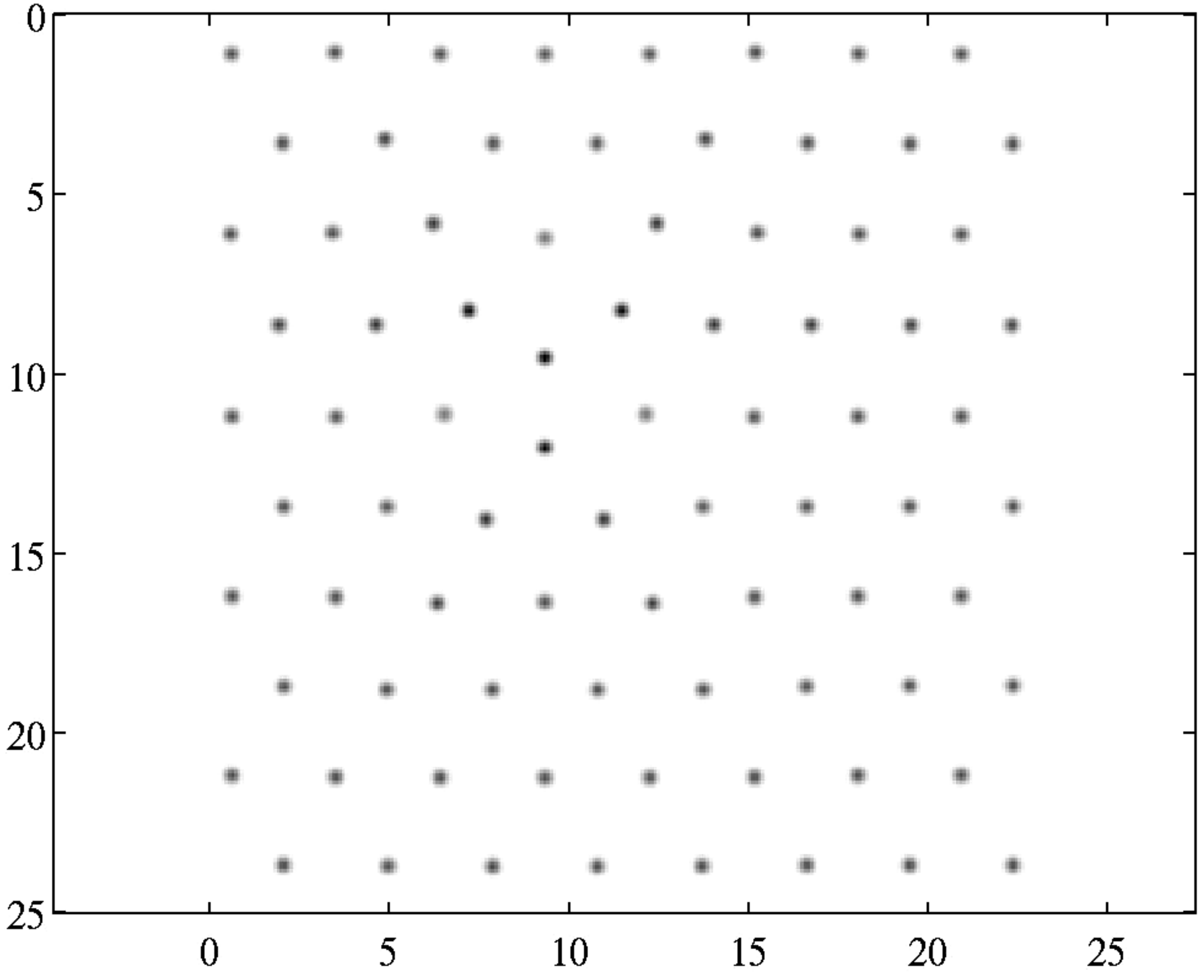

Variational Gaussian: reference to Einstein crystals

Gibbs-Bogoliubov Free Energy Bound:

$$F \le F_0 + \left\langle U - U_0 \right\rangle_0$$

$$= \frac{1}{2}\sum_{i=1}^{N}\sum_{i\neq j}\overbrace{\left(\frac{\alpha_i}{\pi}\right)^{3/2}\left(\frac{\alpha_j}{\pi}\right)^{3/2}\int_{-\infty}^{\infty}\int_{-\infty}^{\infty}\exp\left[-\alpha_i\left(\mathbf{x}_i-\mathbf{X}_i\right)^2\right]\exp\left[-\alpha_j\left(\mathbf{x}_j-\mathbf{X}_j\right)^2\right]u\left(|\,\mathbf{x}_i-\mathbf{x}_j\,|\right)d\mathbf{x}_i d\mathbf{x}_j}^{w(|\mathbf{X}_i-\mathbf{X}_j|,\alpha_i,\alpha_j)}$$

$$+\frac{3}{2}k_{\mathrm{B}}T\sum_{i=1}^{N}\ln\frac{\alpha_i\Lambda_T^2}{\pi e} \qquad \left(\text{thermal wavelength } \Lambda_T = \hbar\sqrt{\frac{2\pi}{mk_{\mathrm{B}}T}}\right)$$

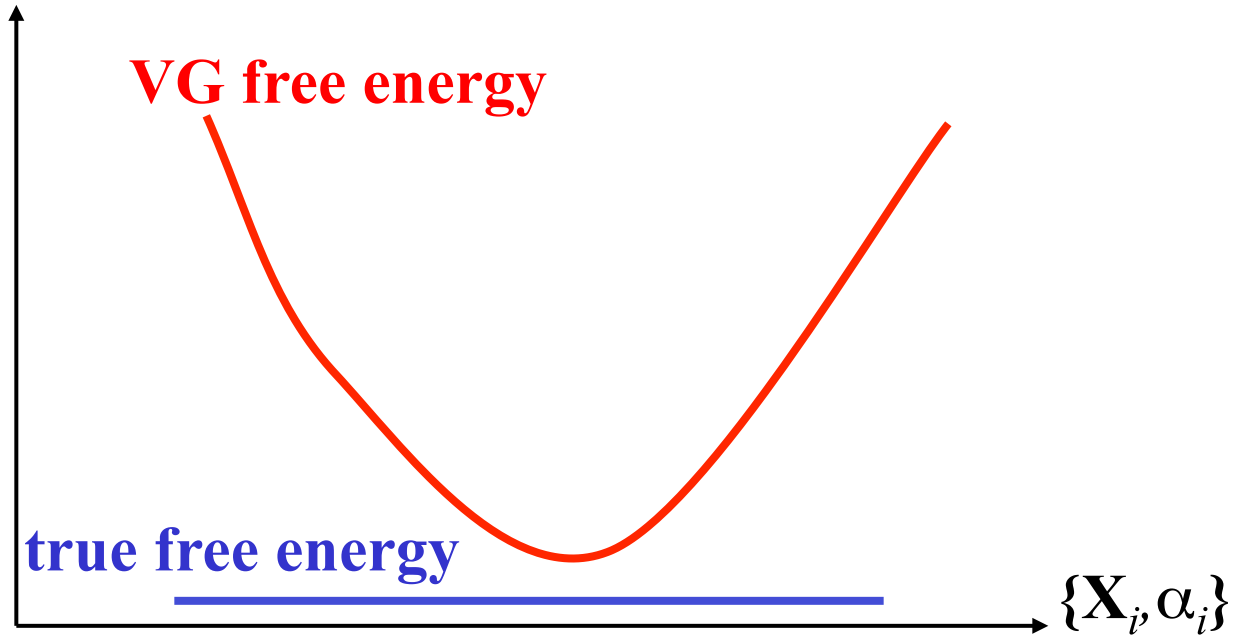

Variational Gaussian compared with Frenkel-Ladd Monte Carlo

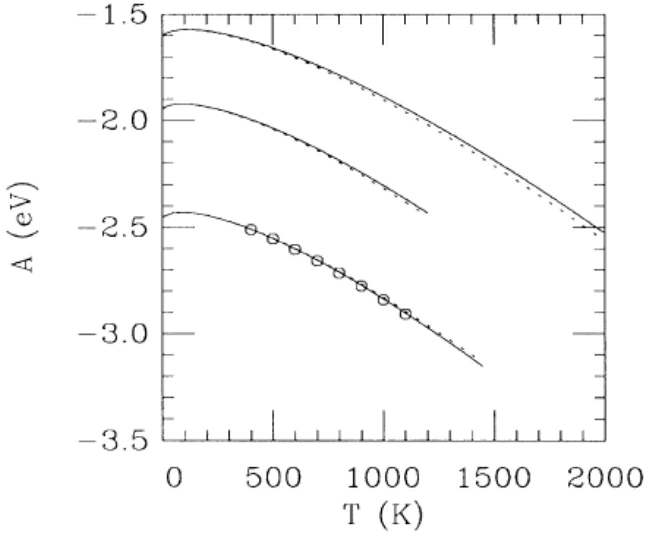

FIG. 1. Calculated free energy vs temperature for a perfect Cu crystal using a truncated Morse potential. The upper curve is for a pressure of 80 GPa, the middle curve for −3.2 GPa, and the lower curve for zero pressure. The values for the −3.2-GPa results have been shifted by +0.5 eV to separate them from the zero-pressure results. The solid curves are from the local harmonic model, the dashed curves from the variational Gaussian method, and the circles from the Frenkel-Ladd Monte Carlo procedure. We note that the MC results require ten full length simulations per point. The estimated errors in the MC calculations are smaller than the symbol size.

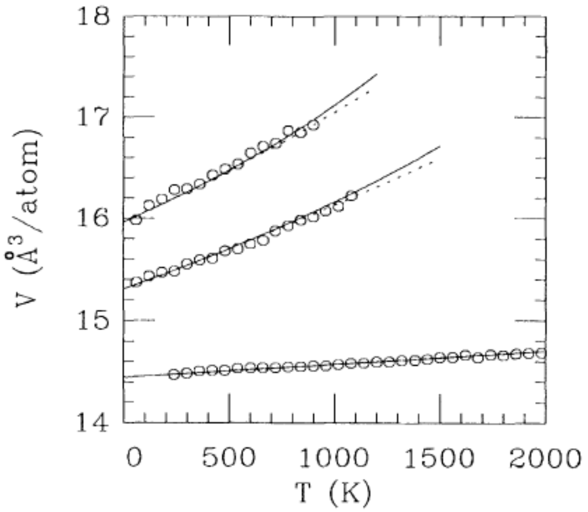

FIG. 2. Calculated volume per atom for a perfect Cu crystal using a Morse potential truncated at the second-nearest neighbors. The upper curve is for a pressure of −3.2 GPa, the middle curve at zero pressure, and the lower curve at 80 GPa. The values for the 80-GPa results have been shifted up by 4 Å^3/atom to compress the scale. The line and symbol types are the same as for Fig. 1.

Lesar, Najafabadi, Srolovitz,
Phys. Rev. Lett. **63** (1989) 624.

Embedded atom potential:

$$F_{\mathrm{VG}} = \frac{1}{2}\sum_{i=1}^{N}\sum_{j\neq i} w(X_{ij},\alpha_{ij}) + \sum_{i=1}^{N} E\left(\sum_{j\neq i}\psi(X_{ij},\alpha_{ij})\right) + \frac{3}{2}k_{\mathrm{B}}T\sum_{i=1}^{N}\ln\frac{\alpha_i\Lambda_T^2}{\pi e}$$

$$\Lambda_T = \hbar\sqrt{\frac{2\pi}{mk_{\mathrm{B}}T}}, \quad X_{ij} \equiv \left|\mathbf{X}_i - \mathbf{X}_j\right|, \quad \alpha_{ij} \equiv \frac{1}{\alpha_i^{-1} + \alpha_i^{-1}}$$

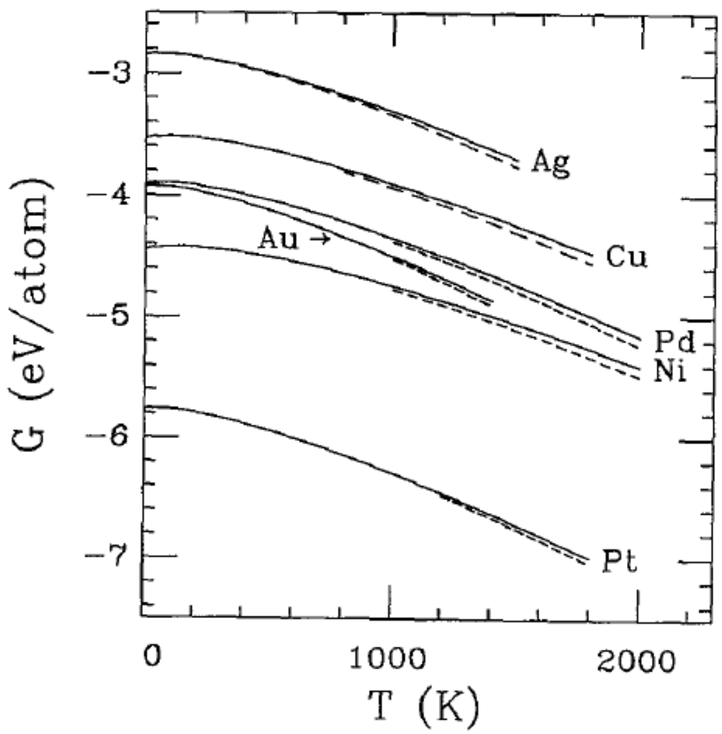

—— Variational Gaussian

- - - - Foiles-Adams Monte Carlo

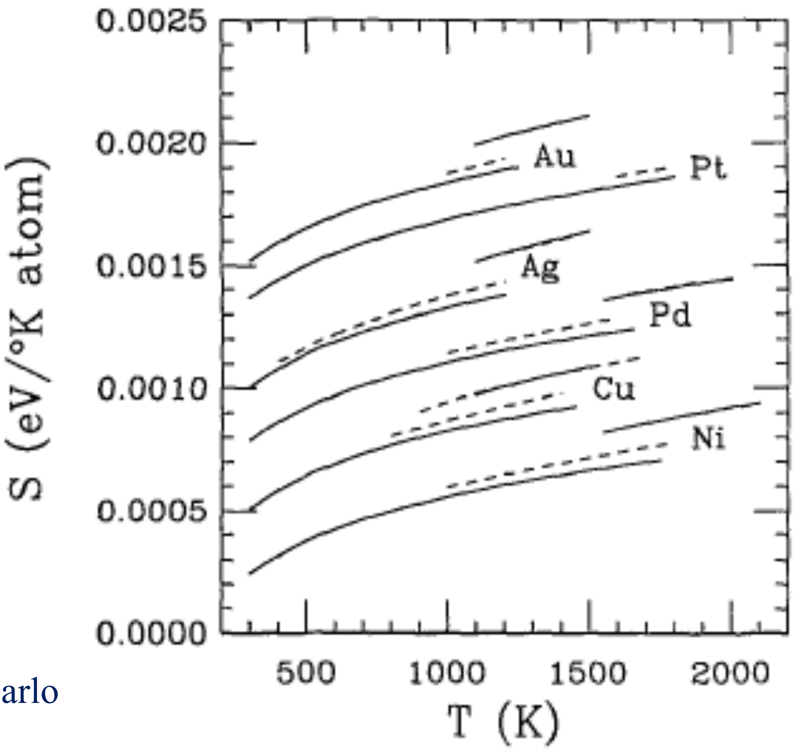

LeSar, Najafabadi and Srolovitz, "Thermodynamics of solid and liquid embedded-atom-method metals: A variational study," *J. Chem. Phys*. **94** (1991) 5090. Foiles & Adams, *Phys. Rev. B* **40** (1989) 5909.

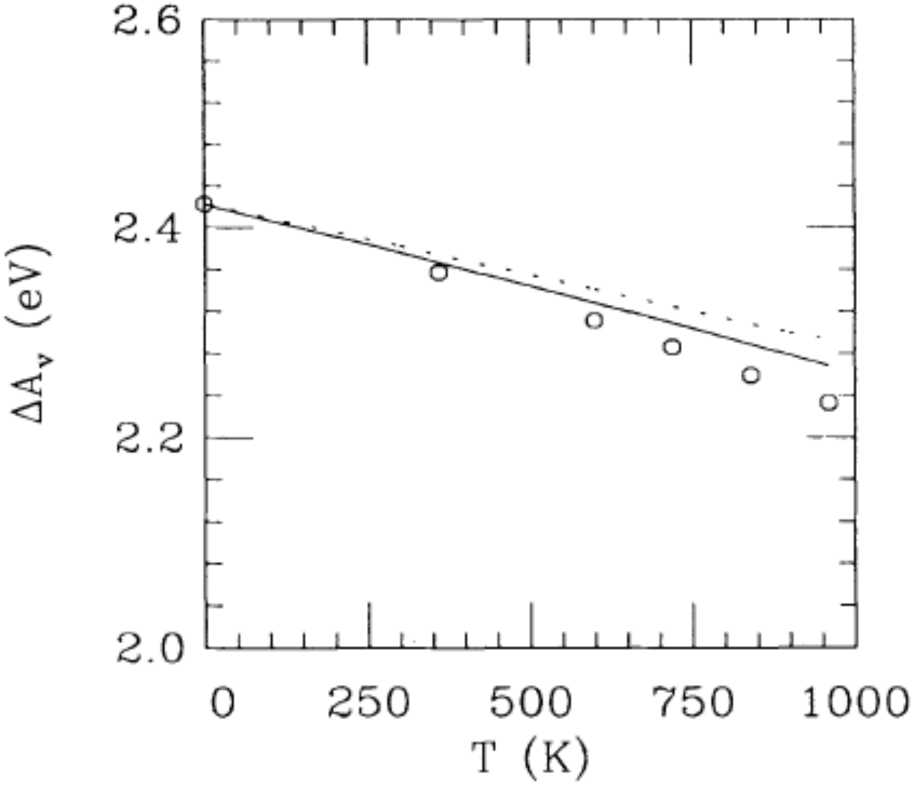

FIG. 3. Vacancy formation free energy for one atom removed from a 108-particle system (periodic boundary conditions), $\Delta A_v = (107/108)A_p - A_v$, where A_p is the free energy of a perfect 108-particle system and A_v is the free energy of the 107-particle system with a vacancy at the same volume. The solid curves are from the local harmonic model, the dashed curves from the variational Gaussian method, and the circles from the Frenkel-Ladd Monte Carlo procedure. The estimated errors in the MC results are smaller than the symbol size.

Displacement Correlation Effect

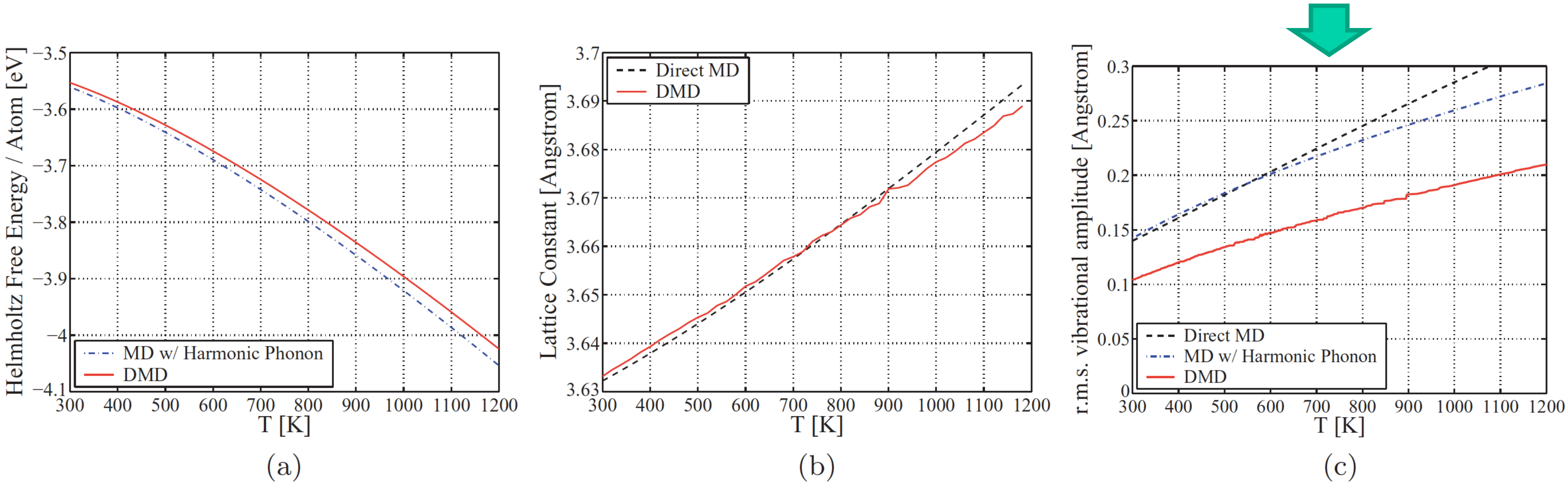

(a) (b) (c)

FIG. 1. (Color online) Benchmarking VG/DMD with Mishin EAM potential (Ref. 10) for Cu. Calculations were performed with $(1-c) = 10^{-20}$ on occupied sites of a perfect crystal. (a) Helmholtz free energy per atom F_{DMD}/atom (red solid line), in comparison with analytical free energy $e_0 + N^{-1}\sum_{k=1}^{3N} k_{\mathrm{B}}T \ln(\hbar\omega_k/k_{\mathrm{B}}T)$ based on harmonic phonon theory (blue dash-dotted line), with phonon frequencies $\{\omega_k\}$ extracted from $T \approx 0$ MD simulations. (b) Lattice parameter a_0 from DMD calculation (red solid line), in comparison with direct MD simulations (black dashed line). (c) Root mean square displacement $(\langle|\mathbf{x}_i - \mathbf{X}_i|^2\rangle)^{1/2}$ per atom, based on DMD calculation $(=[3(2\alpha)^{-1}]^{1/2}$, red solid line), full-spectrum harmonic phonon theory $(=[N^{-1}\sum_{k=1}^{3N} k_{\mathrm{B}}T(m\omega_k^2)^{-1}]^{1/2}$, blue dash-dotted line), and direct MD simulations (black dashed line).

Similar in spirit to electronic DFT, where Kohn-Sham orbitals are of *fictitious reference electronic system* without electron-electron interactions, but giving the same single-e density as the *real interacting-electrons system*.

Li et al., *Phys. Rev. B* **84** (2011) 054103

DMD thermodynamics

Add occupation probability ("color") to sites:

$$\{\mathbf{X}_i, \alpha_i, \mathbf{c}_i\},\ i=1..N$$

VG view

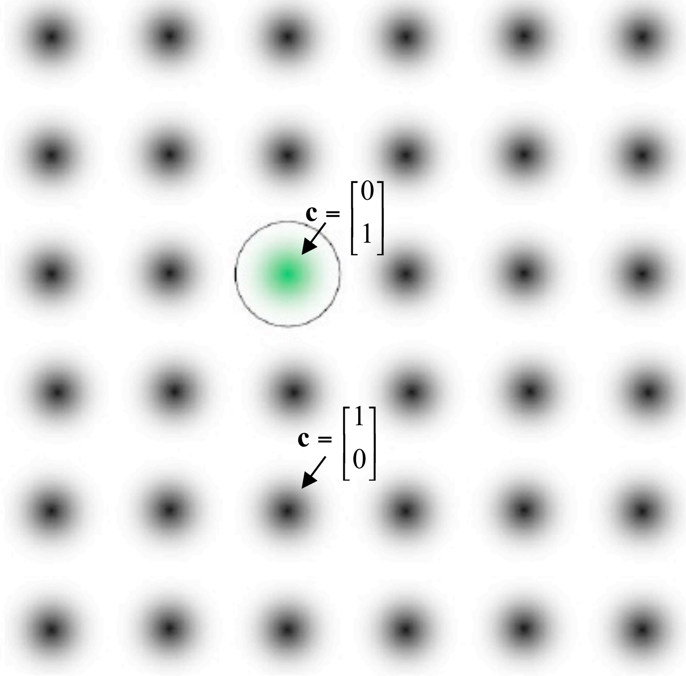

DMD view

$$F_{\mathrm{DMD}} = \sum_{i=1}^{N} c_i E\left(\sum_{j\neq i} c_j \psi(X_{ij},\alpha_{ij})\right) + \frac{\sum_{j\neq i} c_i c_j w(X_{ij},\alpha_{ij})}{2} + k_{\mathrm{B}} T \sum_{i=1}^{N} \left\{ \frac{3c_i}{2} \ln\left[\frac{\alpha_i \Lambda^2}{\pi e}\right] + c_i \ln c_i + (1-c_i)\ln(1-c_i) \right\}$$

DMD Timestepping

- Step 1: Fix $\{\mathbf{c}_i\}$, minimize $F_{\mathrm{DMD}}(\{\mathbf{X}_i, \alpha_i, \mathbf{c}_i\})$ with respect to $\{\mathbf{X}_i, \alpha_i\}$ instantaneously (mechanical, thermal equilibria much faster than chemical equilibrium by diffusive "mass action")

- Step 2: At optimized $\{\mathbf{X}_i, \alpha_i\}$, compute $\{\boldsymbol{\mu}_i\}$: drive mass exchange : update $\{\mathbf{c}_i\}$ by master equation

Because displacive and thermalization updates are "instantaneous", timestep limited only by chemical diffusivity.

Li et al, *Phys. Rev. B* **84** (2011) 054103

DMD kinetics

The chemical potential for each atomic site is easily derived:

$$\mu_i \equiv \frac{\partial F_{\mathrm{DMD}}(\{\mathbf{X}_i,\alpha_i,\mathbf{c}_i\})}{\partial c_i} = \frac{1}{2}\sum_{i=1}^{N}\sum_{i\neq j} c_j w(X_{ij},\alpha_{ij}) + k_{\mathrm{B}}T\sum_{i=1}^{N}\left\{\frac{3}{2}\ln\left[\frac{\alpha_i\Lambda^2}{\pi e}\right]+\ln\left(\frac{c_i}{1-c_i}\right)\right\}$$

$$f_i \equiv \mu_i - k_{\mathrm{B}}T\ln\left[\frac{c_i}{1-c_i}\right]$$

$$f_{ij} \equiv f_i - f_j$$

$$Q_{\mathrm{m}} = F^*_{ij} - (f_i + f_j)/2$$

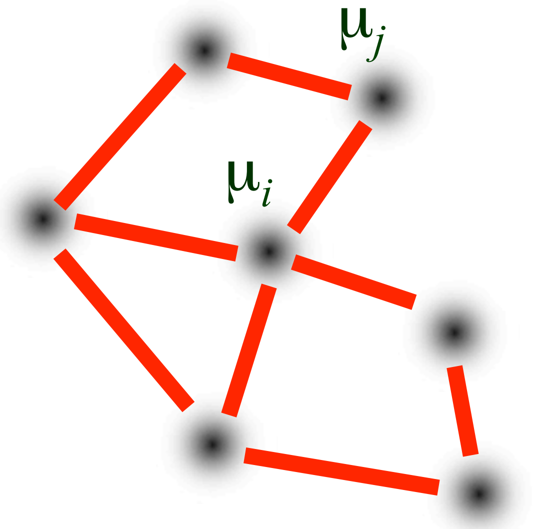

$$\frac{dc_i}{dt} = \sum_j{}' \nu \exp\left[-\frac{Q_{\mathrm{m}}}{k_{\mathrm{B}}T}\right]\left\{c_j(1-c_i)\exp\left[-\frac{f_{ij}}{2k_{\mathrm{B}}T}\right] - c_i(1-c_j)\exp\left[\frac{f_{ij}}{2k_{\mathrm{B}}T}\right]\right\},$$

Calibrate Q_{m} against experimental diffusivity

nearest-neighbor network

$$D_{\mathrm{V}} = \frac{Z}{2d}\nu b^2\exp\left[-\frac{Q_{\mathrm{m}}}{k_{\mathrm{B}}T}\right]$$

Li et al, *Phys. Rev. B* **84** (2011) 054103

Atomic Environment-Dependent Diffusivity

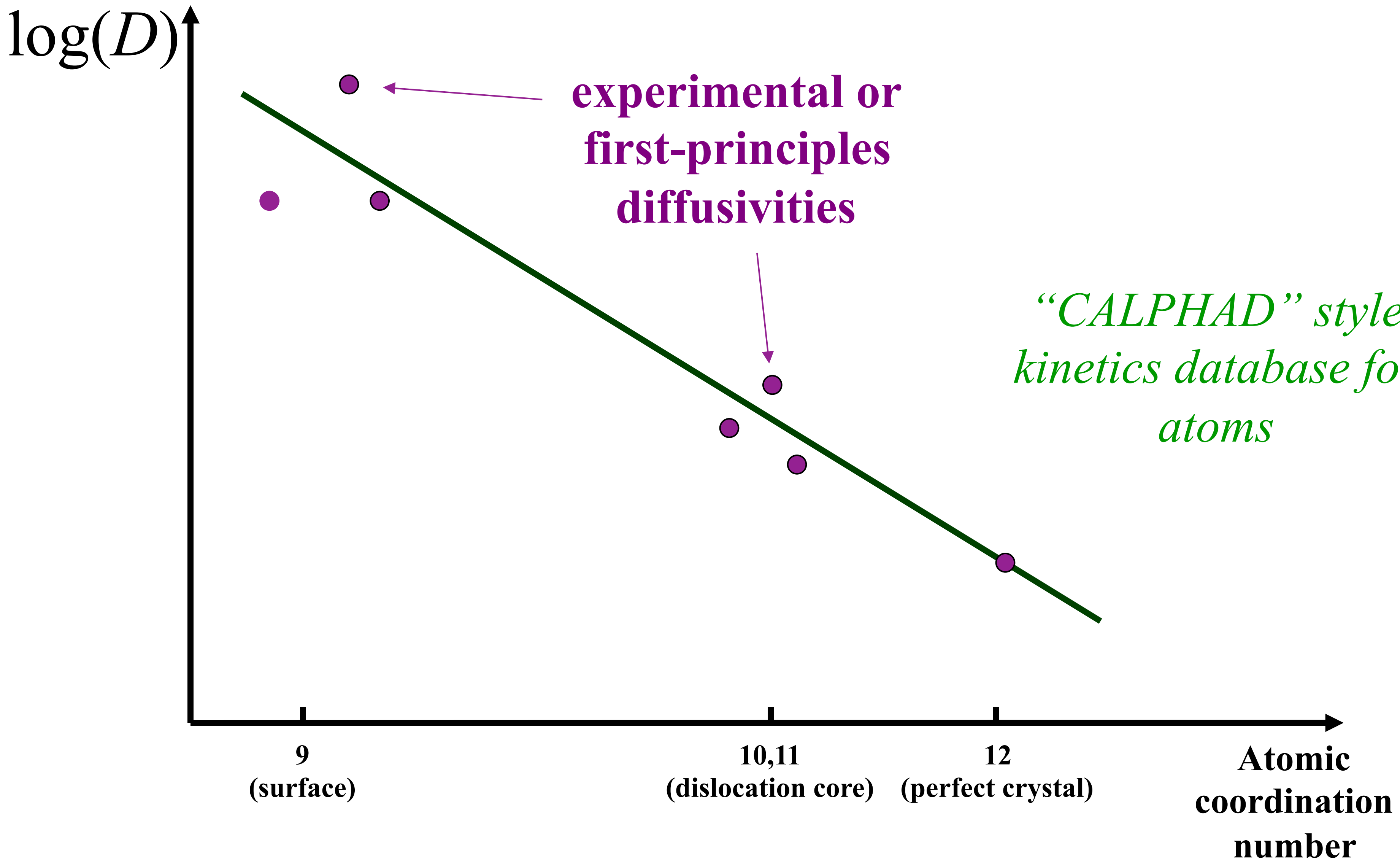

experimental or first-principles diffusivities

"CALPHAD" style kinetics database for atoms

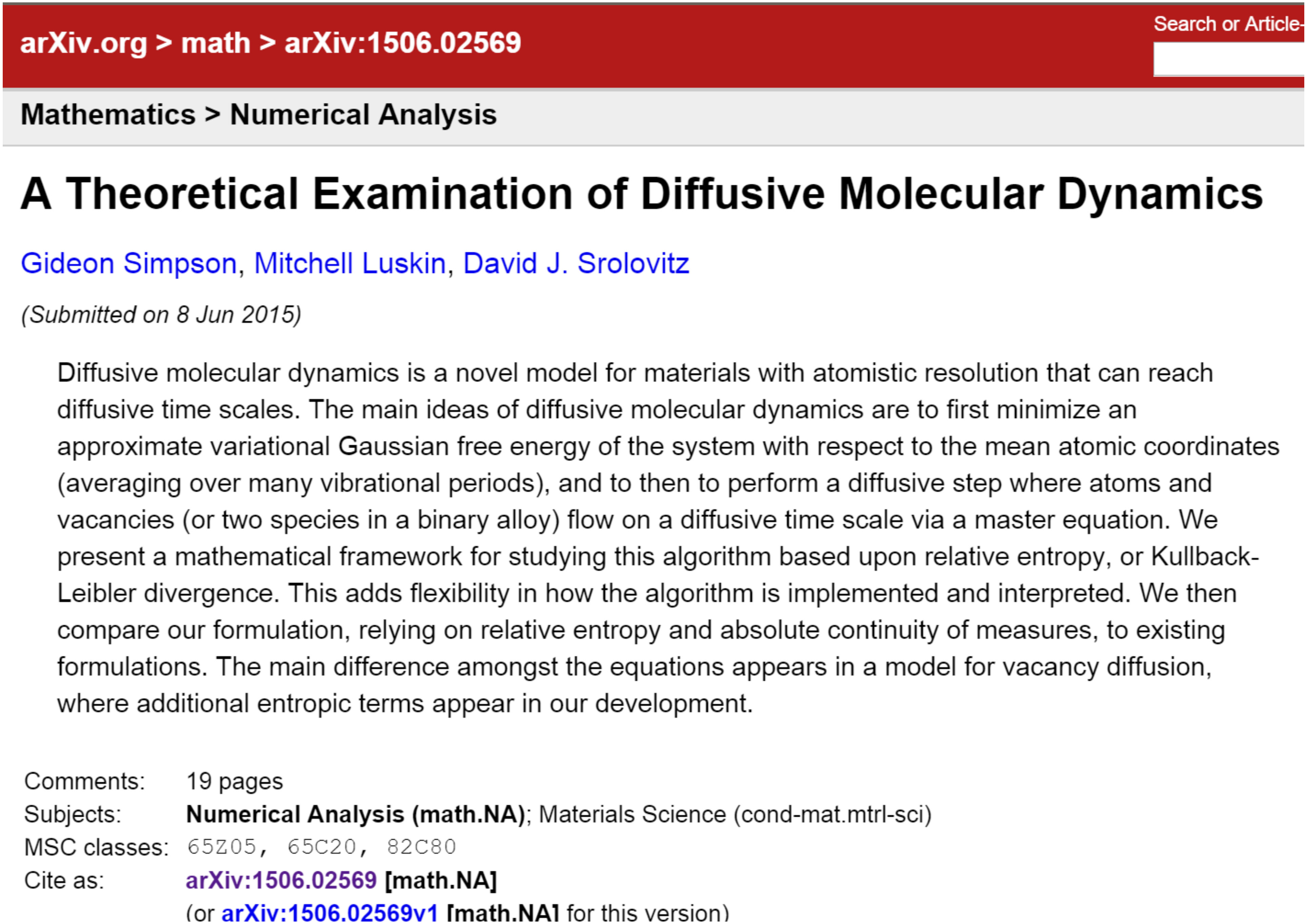

arXiv.org > math > arXiv:1506.02569

Mathematics > Numerical Analysis

A Theoretical Examination of Diffusive Molecular Dynamics

Gideon Simpson, Mitchell Luskin, David J. Srolovitz

(Submitted on 8 Jun 2015)

Diffusive molecular dynamics is a novel model for materials with atomistic resolution that can reach diffusive time scales. The main ideas of diffusive molecular dynamics are to first minimize an approximate variational Gaussian free energy of the system with respect to the mean atomic coordinates (averaging over many vibrational periods), and to then to perform a diffusive step where atoms and vacancies (or two species in a binary alloy) flow on a diffusive time scale via a master equation. We present a mathematical framework for studying this algorithm based upon relative entropy, or Kullback-Leibler divergence. This adds flexibility in how the algorithm is implemented and interpreted. We then compare our formulation, relying on relative entropy and absolute continuity of measures, to existing formulations. The main difference amongst the equations appears in a model for vacancy diffusion, where additional entropic terms appear in our development.

Comments:	19 pages
Subjects:	**Numerical Analysis (math.NA)**; Materials Science (cond-mat.mtrl-sci)
MSC classes:	`65Z05, 65C20, 82C80`
Cite as:	**arXiv:1506.02569 [math.NA]**
	(or **arXiv:1506.02569v1 [math.NA]** for this version)

Li et al, *Phys. Rev. B*
84 (2011) 054103

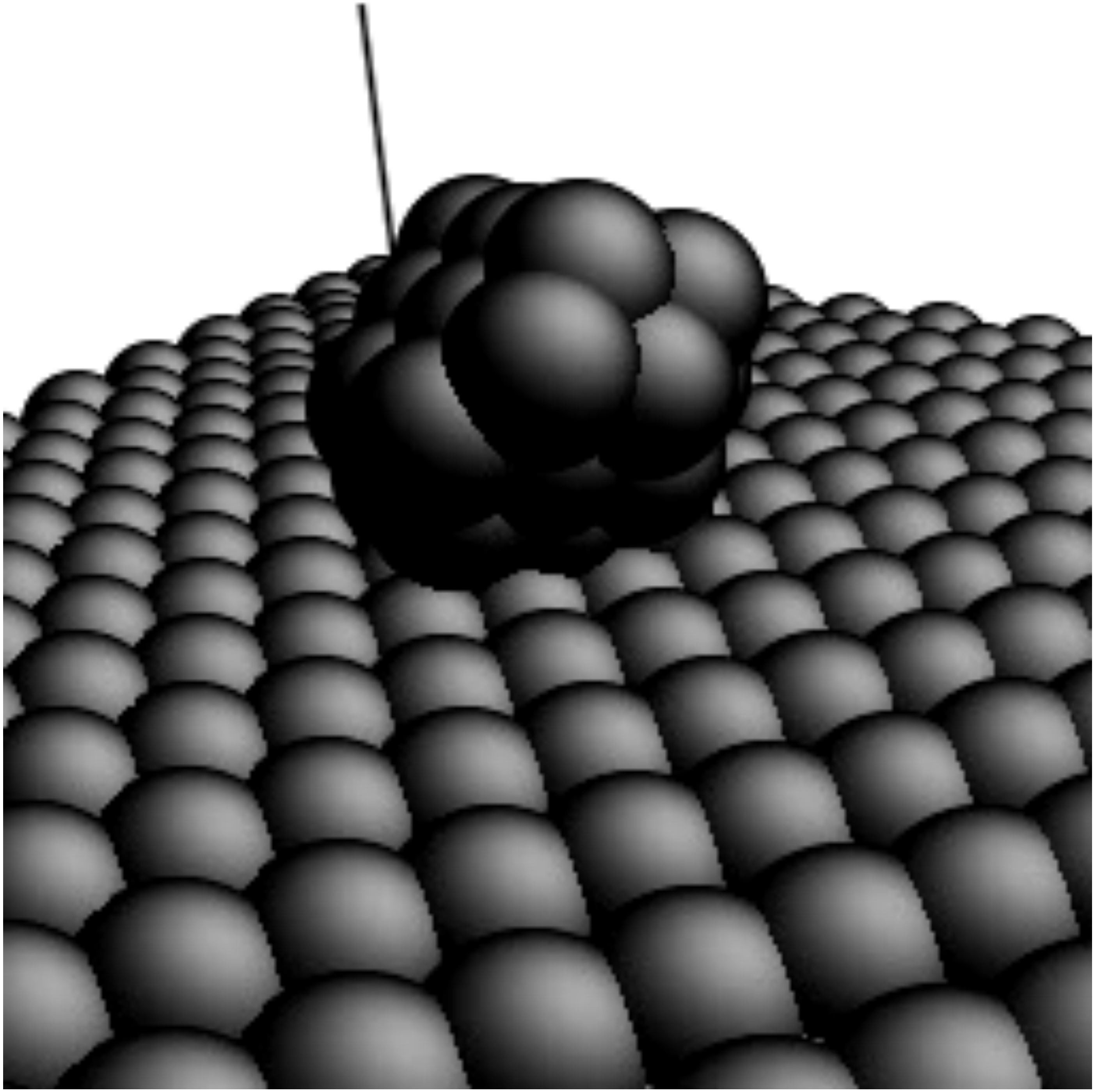

Small particle
on surface

Li et al, *Phys. Rev. B*
84 (2011) 054103

Larger particle on surface

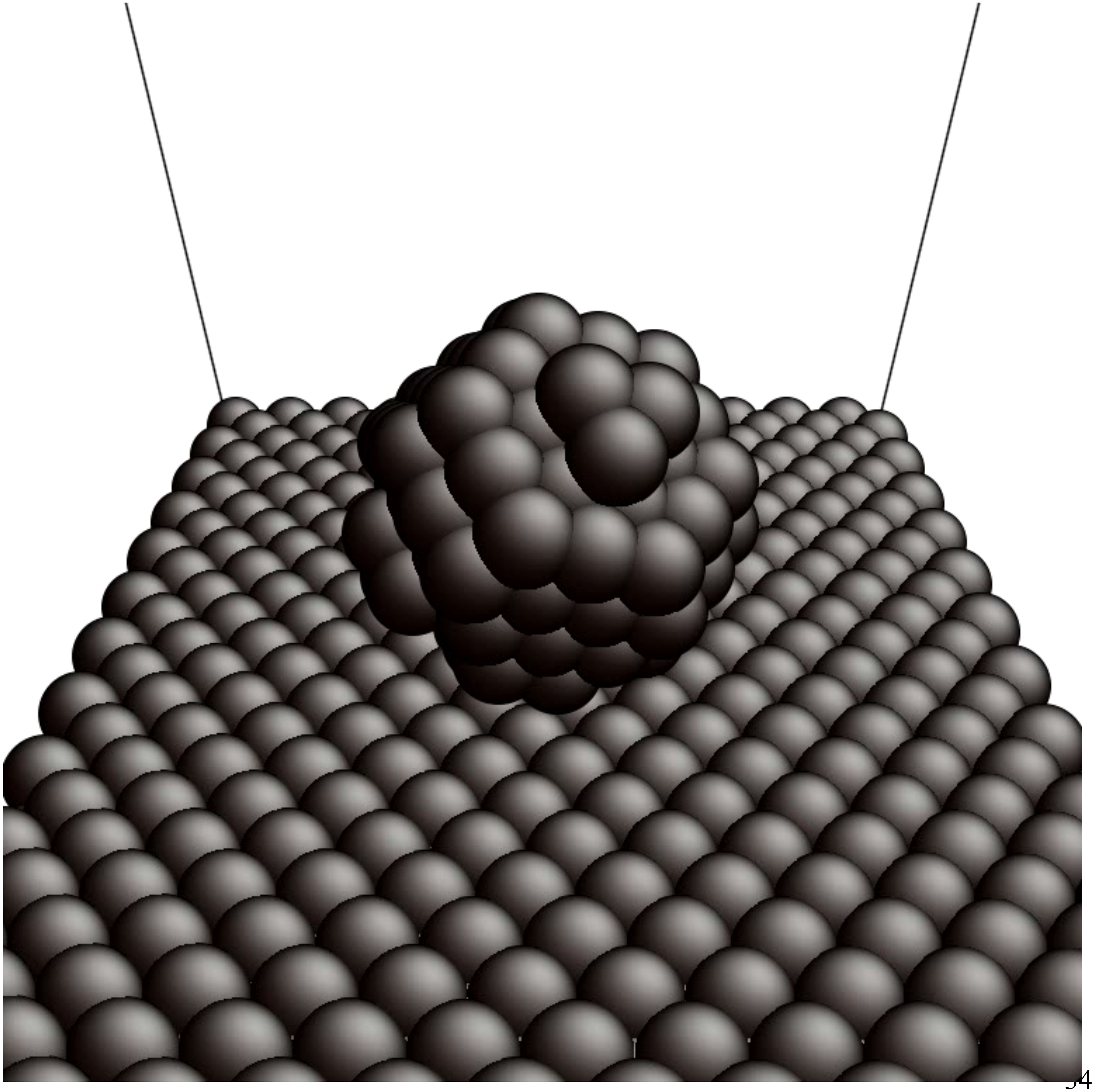

Li et al, *Phys. Rev. B* **84** (2011) 054103

Sintering

Particle rotation

plastic deformation

rapid neck formation

breakup of long thin pore into pore droplets

grains coarsening

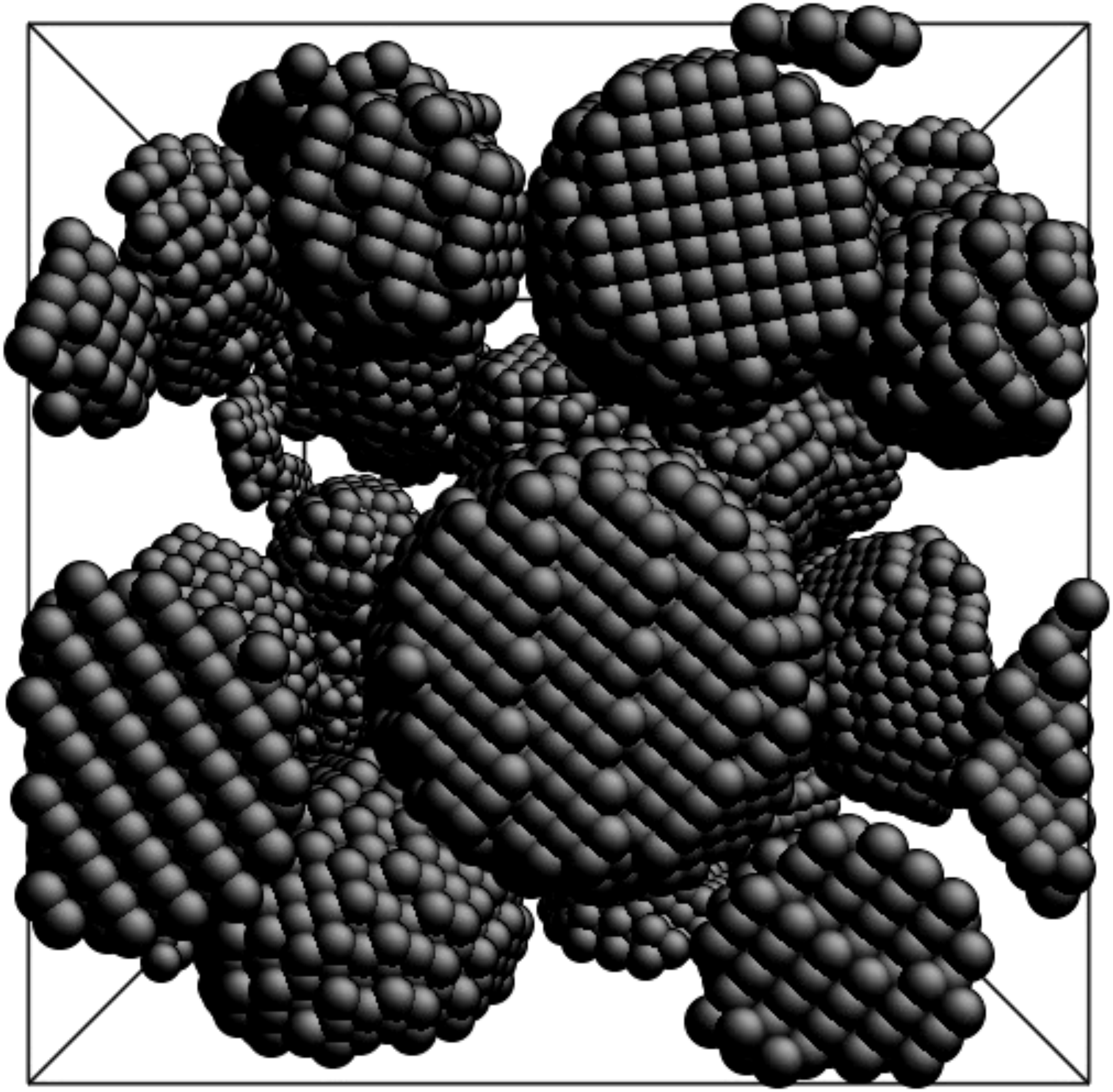

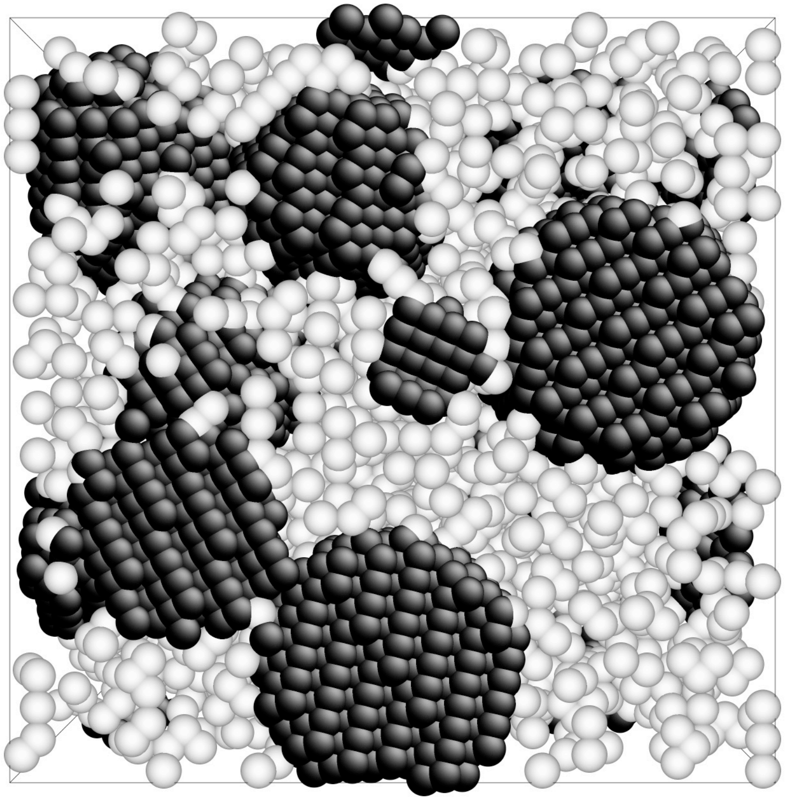

“Ghost sites” gas around grains

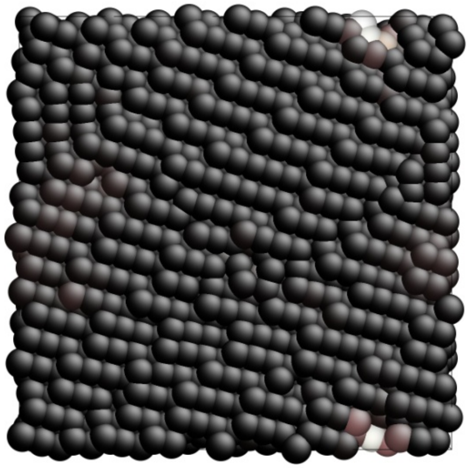

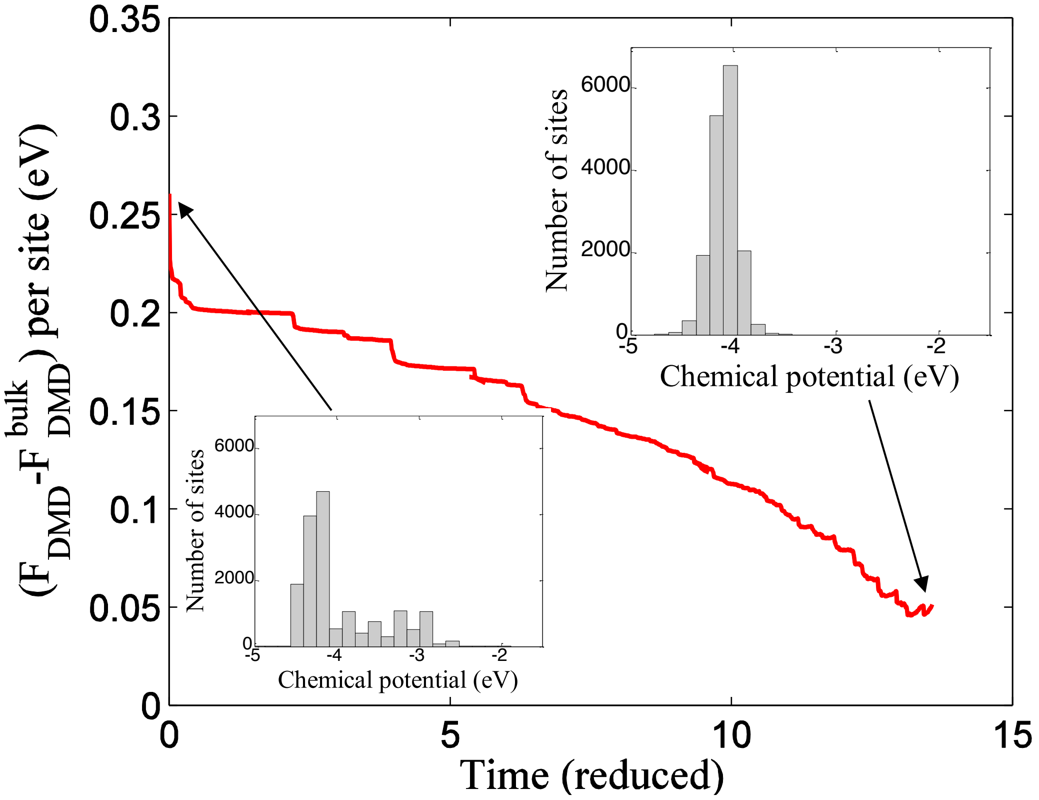

Climb of Edge Dislocation in FCC metals

Figure taken from: Cherns, Hirsch, Saka, "Mechanism of climb of dissociated dislocations," Proc. R. Soc. Lond. A **371** (1980) 213

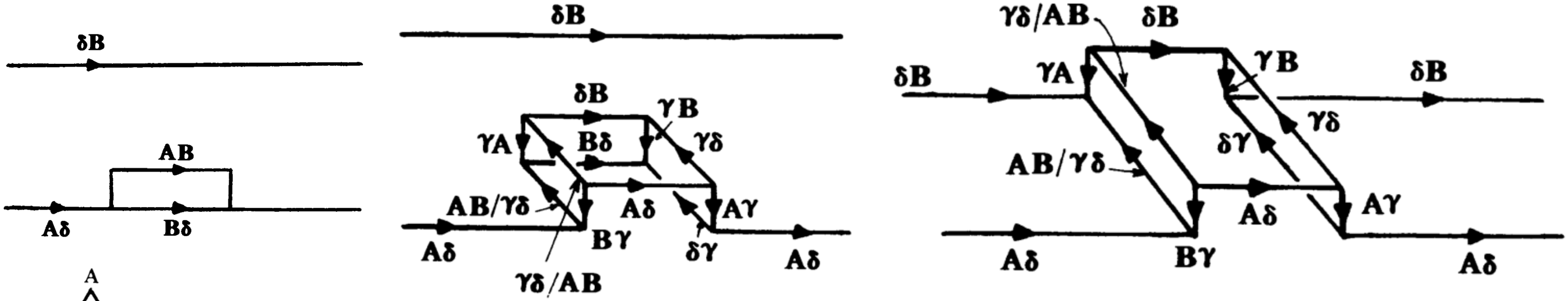

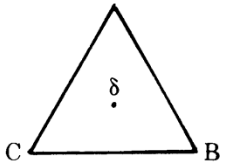

D: below

Thomson & Balluffi (*J. Appl. Phys*. **33** (1962) 803) double jog on an extended edge dislocation:

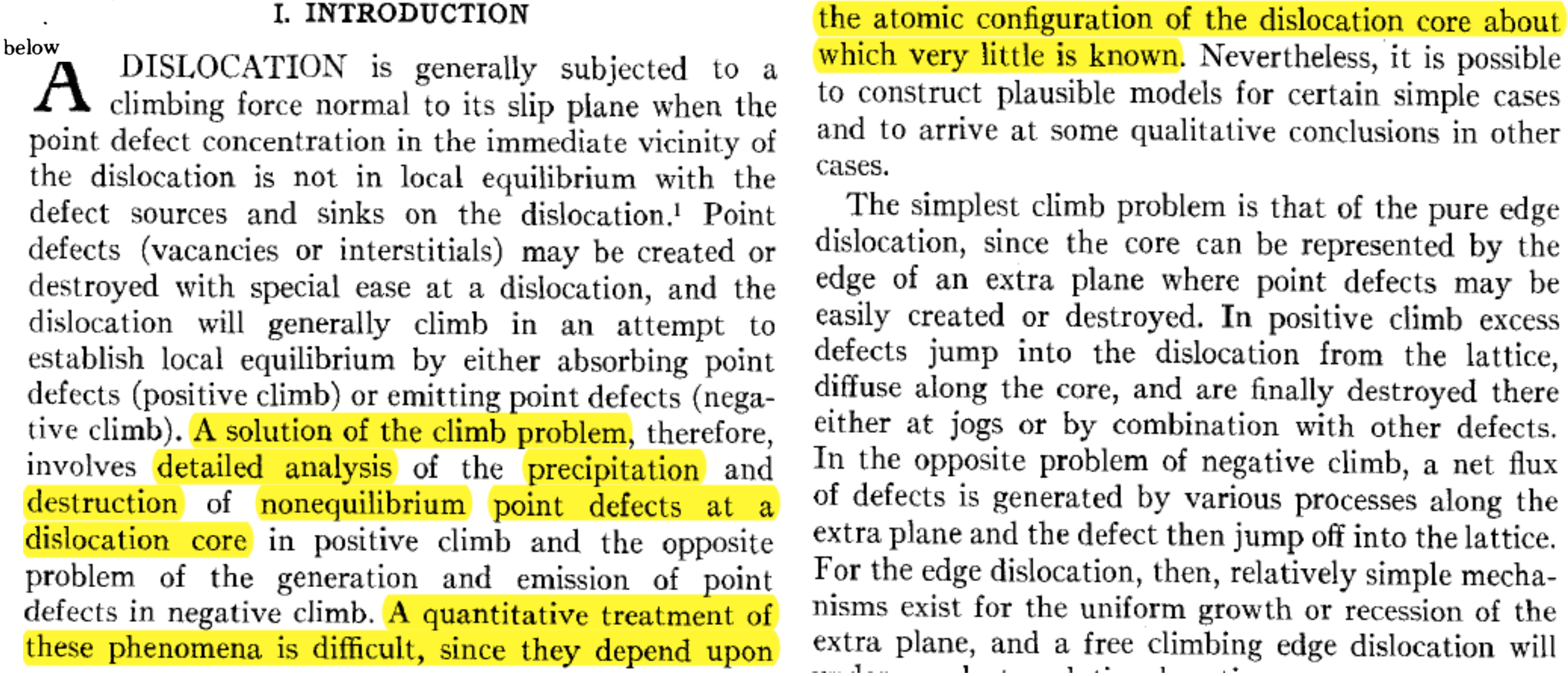

I. INTRODUCTION

A DISLOCATION is generally subjected to a climbing force normal to its slip plane when the point defect concentration in the immediate vicinity of the dislocation is not in local equilibrium with the defect sources and sinks on the dislocation.[1] Point defects (vacancies or interstitials) may be created or destroyed with special ease at a dislocation, and the dislocation will generally climb in an attempt to establish local equilibrium by either absorbing point defects (positive climb) or emitting point defects (negative climb). A solution of the climb problem, therefore, involves detailed analysis of the precipitation and destruction of nonequilibrium point defects at a dislocation core in positive climb and the opposite problem of the generation and emission of point defects in negative climb. A quantitative treatment of these phenomena is difficult, since they depend upon the atomic configuration of the dislocation core about which very little is known. Nevertheless, it is possible to construct plausible models for certain simple cases and to arrive at some qualitative conclusions in other cases.

The simplest climb problem is that of the pure edge dislocation, since the core can be represented by the edge of an extra plane where point defects may be easily created or destroyed. In positive climb excess defects jump into the dislocation from the lattice, diffuse along the core, and are finally destroyed there either at jogs or by combination with other defects. In the opposite problem of negative climb, a net flux of defects is generated by various processes along the extra plane and the defect then jump off into the lattice. For the edge dislocation, then, relatively simple mechanisms exist for the uniform growth or recession of the extra plane, and a free climbing edge dislocation will

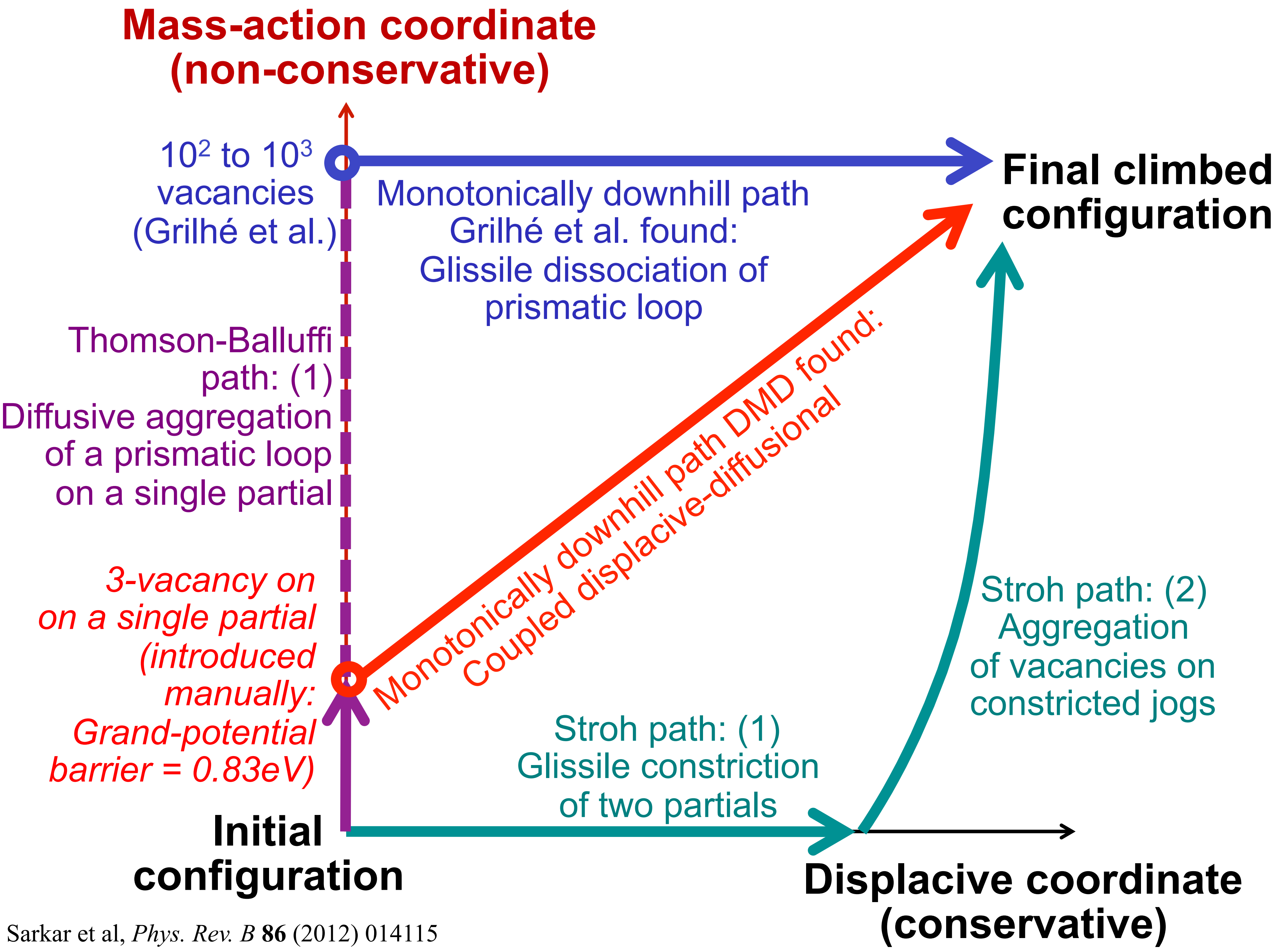

Mass-action coordinate (non-conservative)

10^2 to 10^3 vacancies (Grilhé et al.)

Monotonically downhill path Grilhé et al. found: Glissile dissociation of prismatic loop

Final climbed configuration

Thomson-Balluffi path: (1) Diffusive aggregation of a prismatic loop on a single partial

3-vacancy on on a single partial (introduced manually: Grand-potential barrier = 0.83eV)

Monotonically downhill path DMD found: Coupled displacive-diffusional

Stroh path: (2) Aggregation of vacancies on constricted jogs

Stroh path: (1) Glissile constriction of two partials

Initial configuration

Displacive coordinate (conservative)

Sarkar et al, *Phys. Rev. B* **86** (2012) 014115

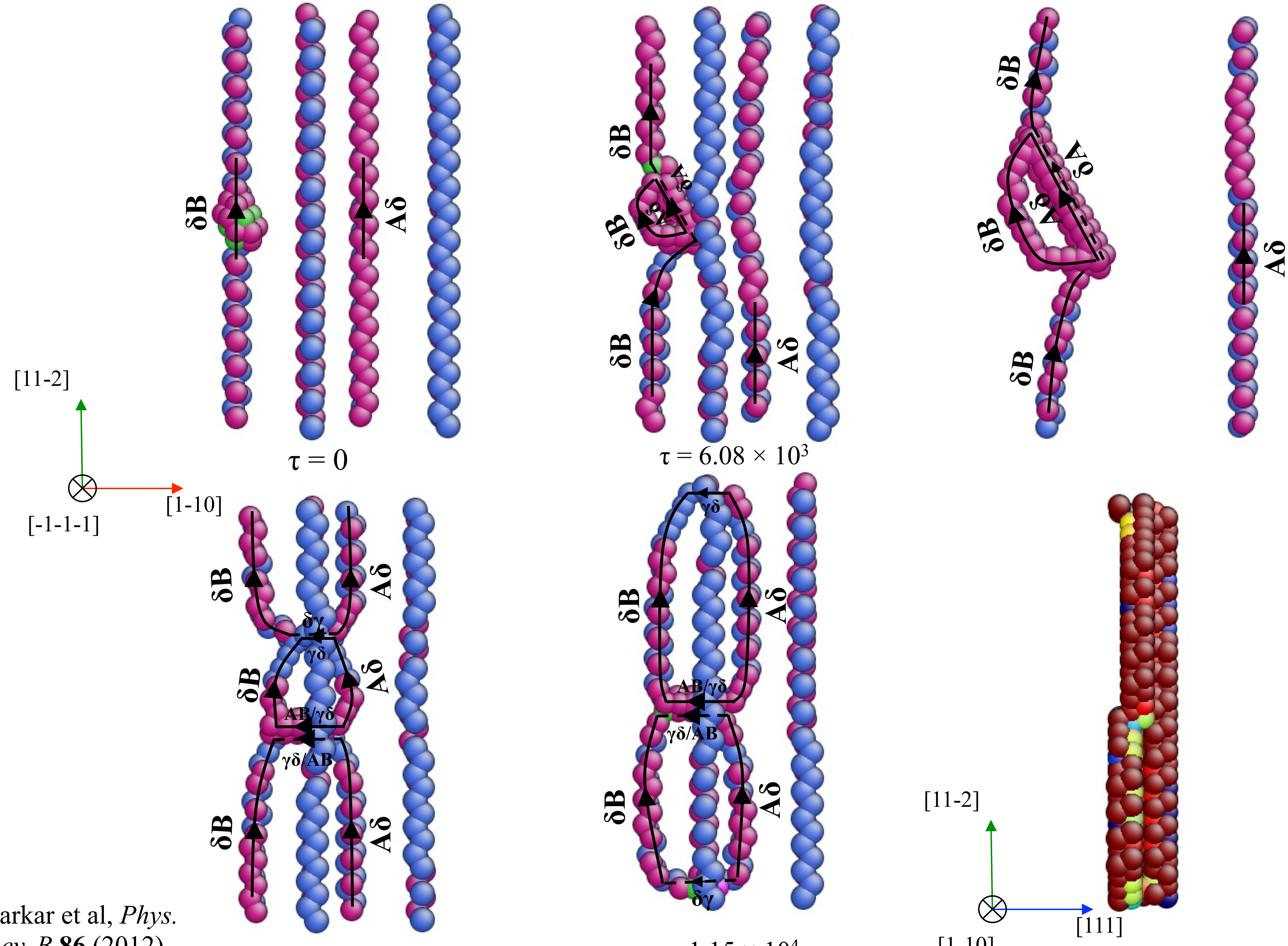

τ = 0

τ = 6.08 × 10^3

τ = 1.04 × 10^4

τ = 1.15 × 10^4

Centrosymmetry plot

Sarkar et al, *Phys. Rev. B* **86** (2012) 014115

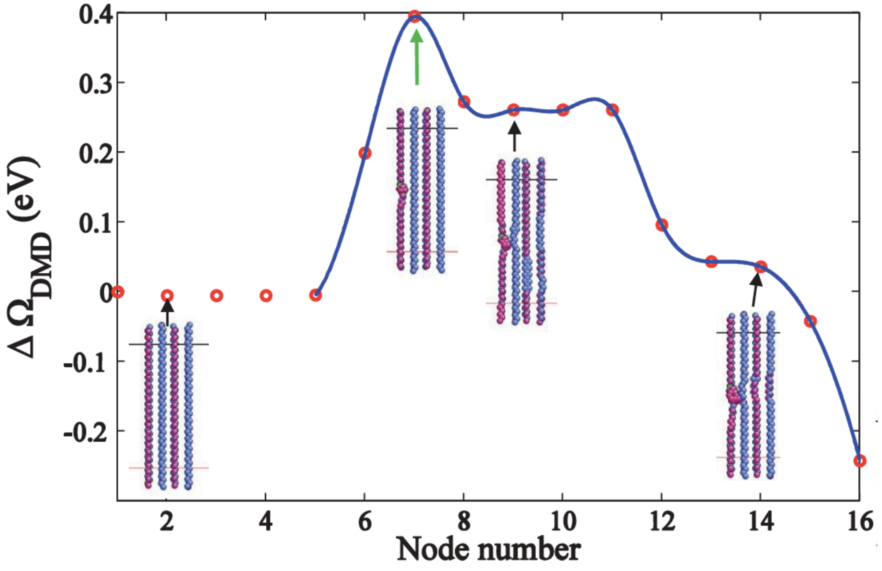

Nudged Elastic Band calculation of free-energy barrier in extended {$\mathbf{X}_i$, α_i, $\mathbf{c}_i$} space in grand-canonical ensemble

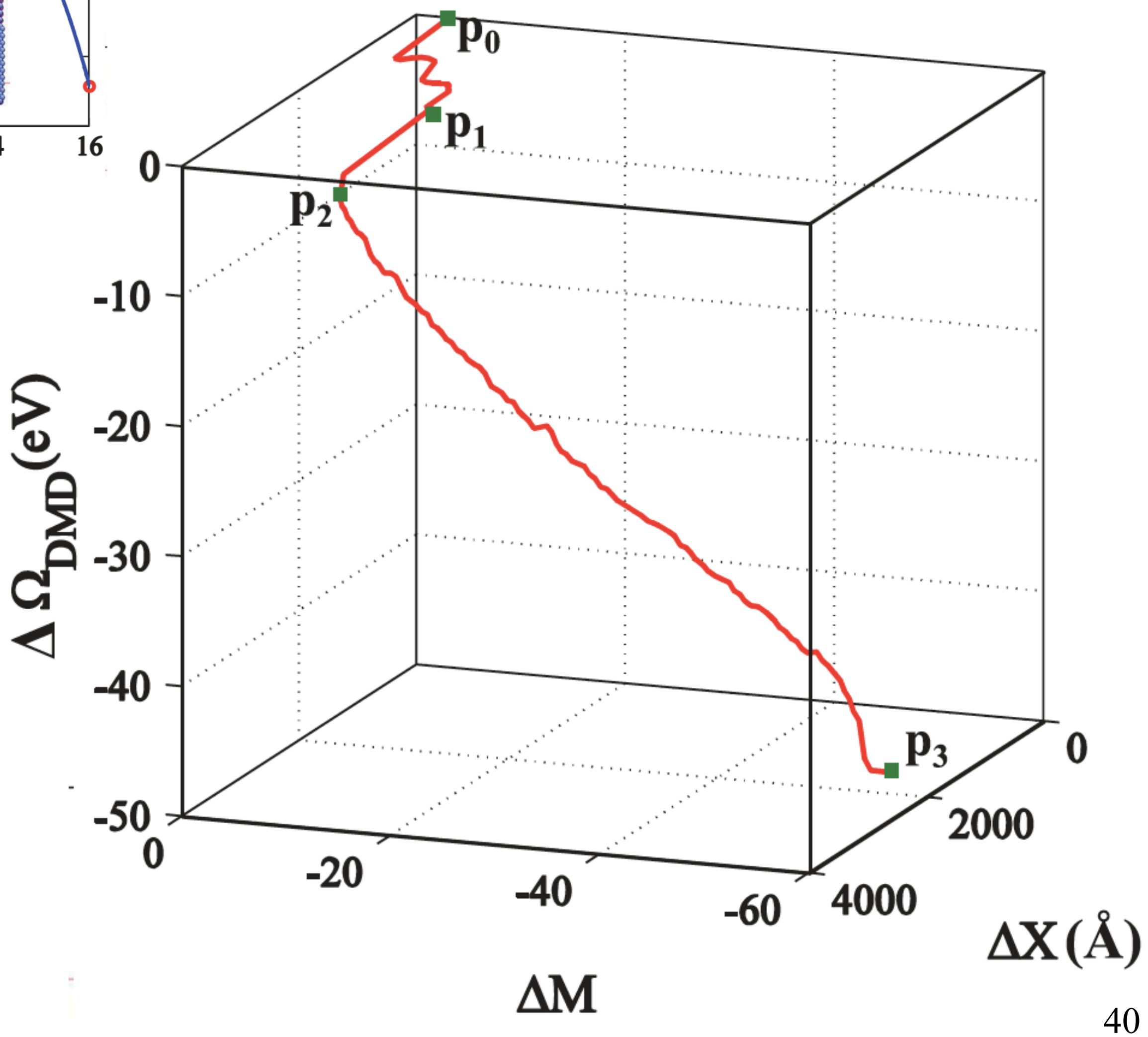

Sarkar et al, *Phys. Rev. B* **86** (2012) 014115

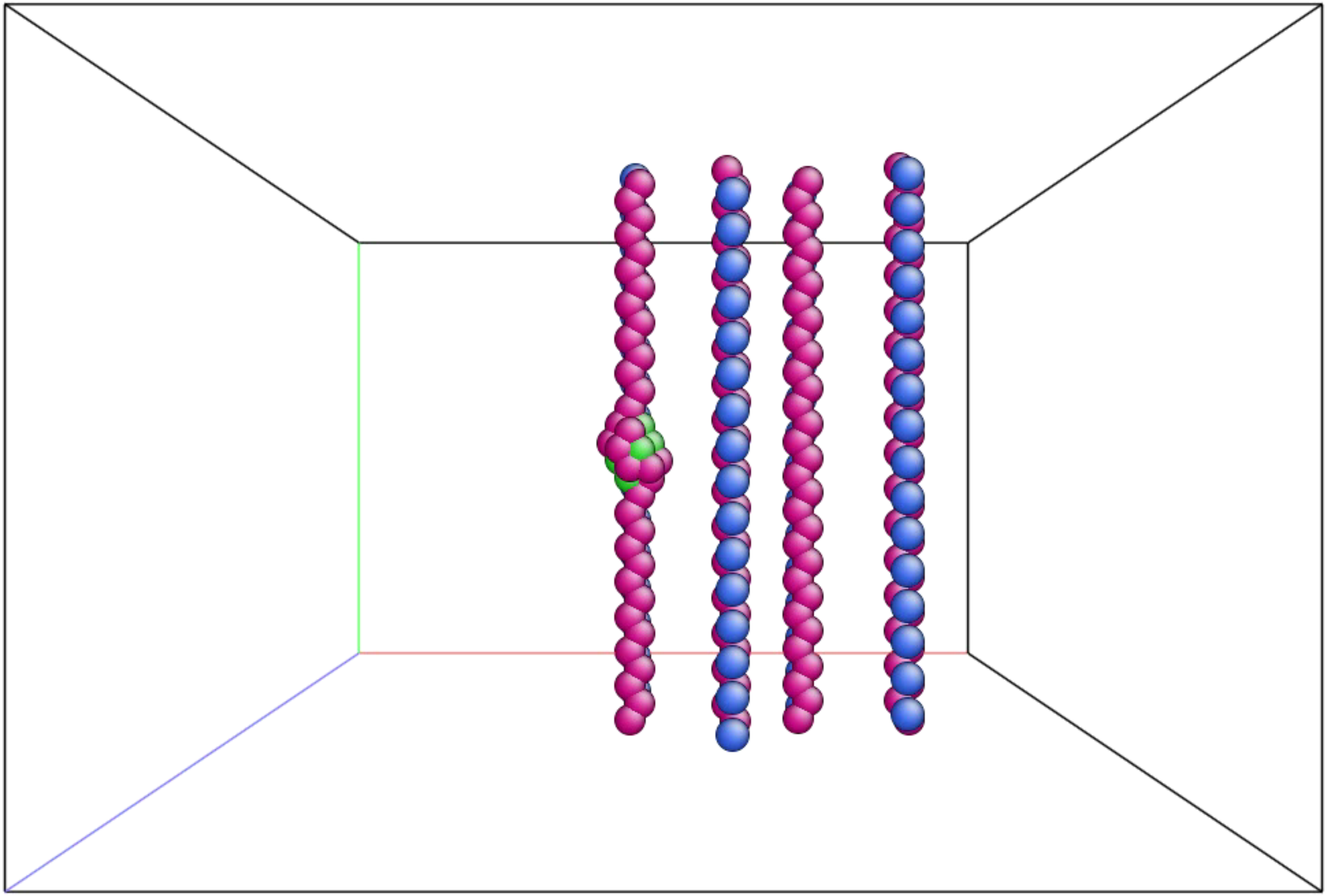

Nano-indentation at slower indentation rate and small contact radius (higher temperature)

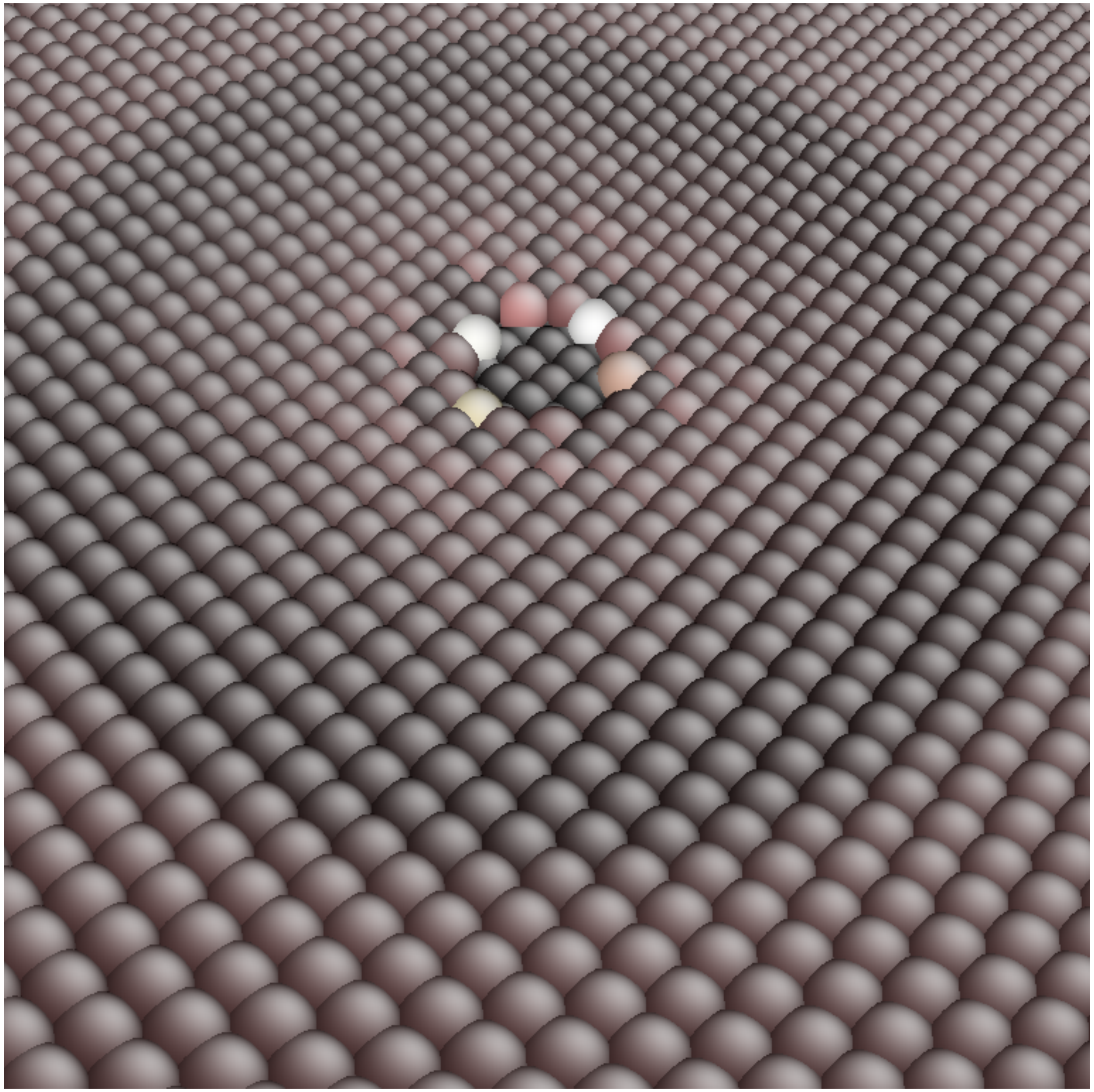

Surface Diffusional Creep:

Surface terrace formed by surface ***vacancy accretion***

Purely diffusive accommodation of slow indentation displacement rate

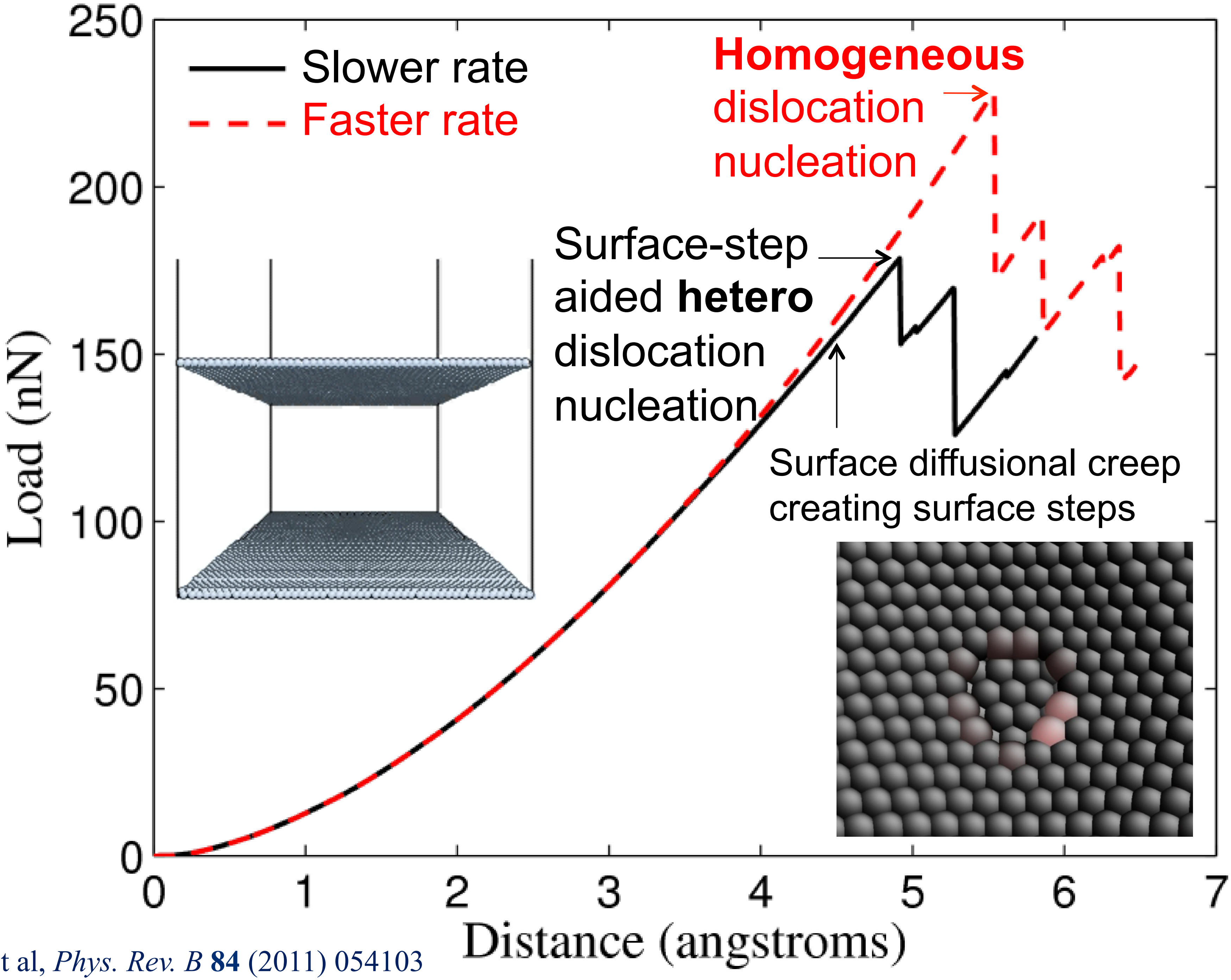

Homogeneous dislocation nucleation

Surface-step aided **hetero** dislocation nucleation

Surface diffusional creep creating surface steps

Li et al, *Phys. Rev. B* **84** (2011) 054103

Purely diffusive

Onset of hybrid displacive-diffusional

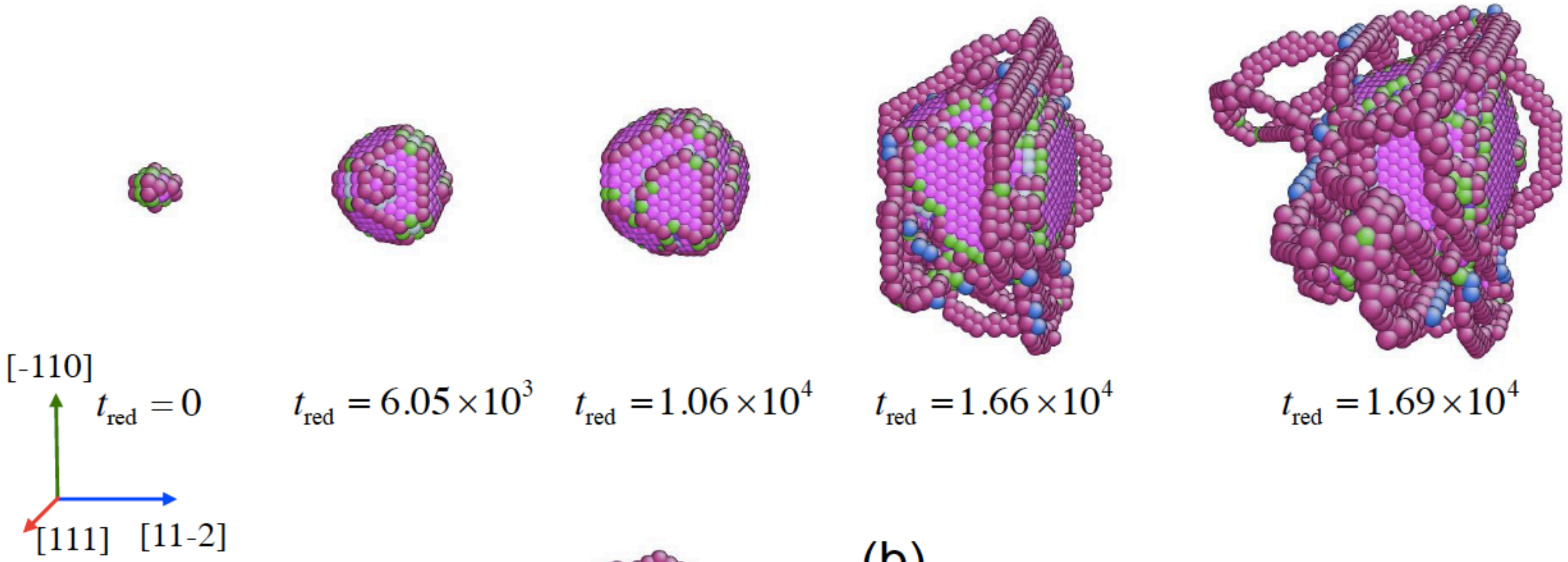

$t_{\mathrm{red}} = 0$ $t_{\mathrm{red}} = 6.05 \times 10^3$ $t_{\mathrm{red}} = 1.06 \times 10^4$ $t_{\mathrm{red}} = 1.66 \times 10^4$ $t_{\mathrm{red}} = 1.69 \times 10^4$

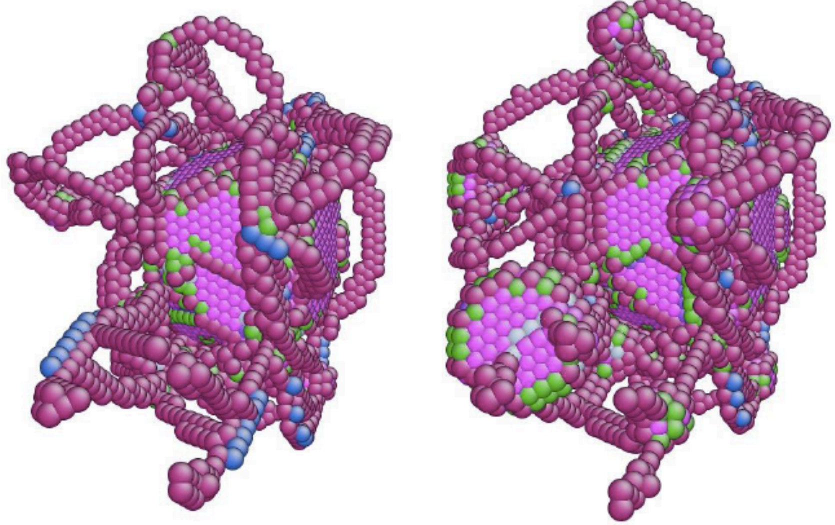

$t_{\mathrm{red}} = 1.72 \times 10^4$ $t_{\mathrm{red}} = 1.78 \times 10^4$

(b)

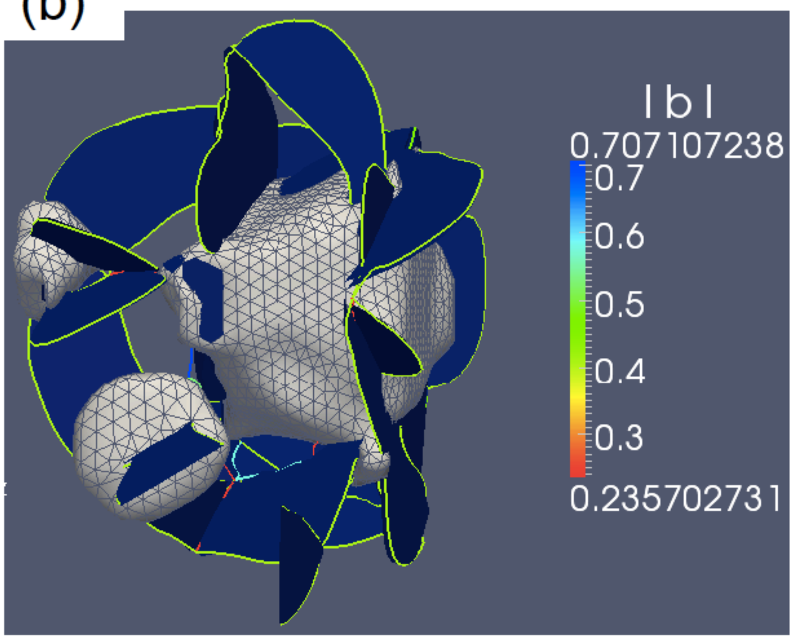

Sanket Sarkar et al, to be submitted

Solute-defect interactions in Al-Mg alloys from diffusive variational Gaussian calculations

E. Dontsova,[1,*] J. Rottler,[2] and C. W. Sinclair[1]
[1]*Department of Materials Engineering, The University of British Columbia, Vancouver, British Columbia, Canada V6T 1Z4*
[2]*Department of Physics and Astronomy, The University of British Columbia, Vancouver, British Columbia, Canada V6T 1Z1*

(Received 29 July 2014; revised manuscript received 16 October 2014; published 5 November 2014)

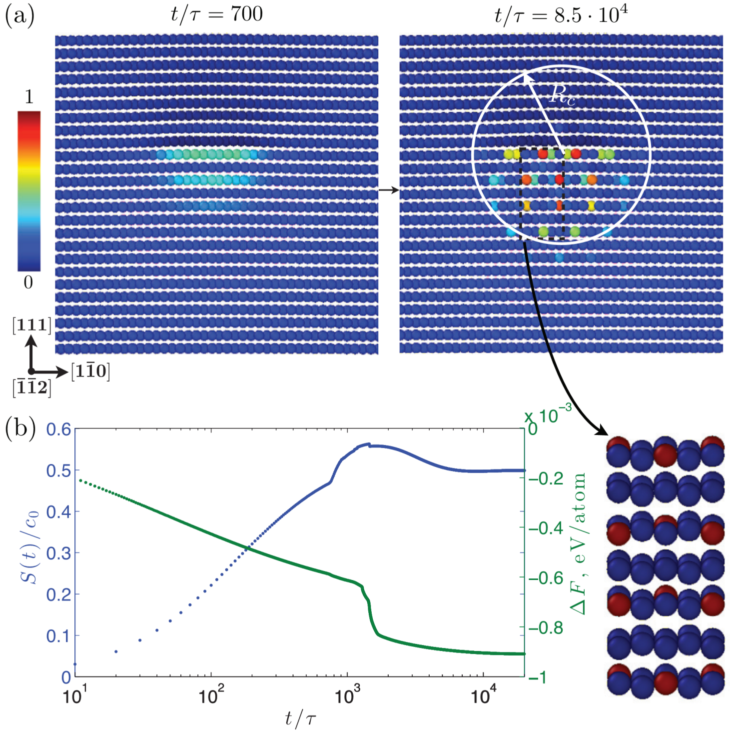

D7 (Al7Mg)
intermetallic
compound:
True surprise!

FIG. 9. (Color online) (a) Two snapshots from DMD simulations (times indicated above the figures) for solute segregation near the split edge dislocation for $c_0 = 10\%$ at $T = 600$ K. The unit cell of a fully ordered precipitate obtained from cooling this system to a lower temperature is shown at the bottom right. (b) Time evolution of the normalized excess solute concentration (blue symbols) in the region indicated by the white circle in (a) and the free-energy difference (green symbols) between the current and initial states.

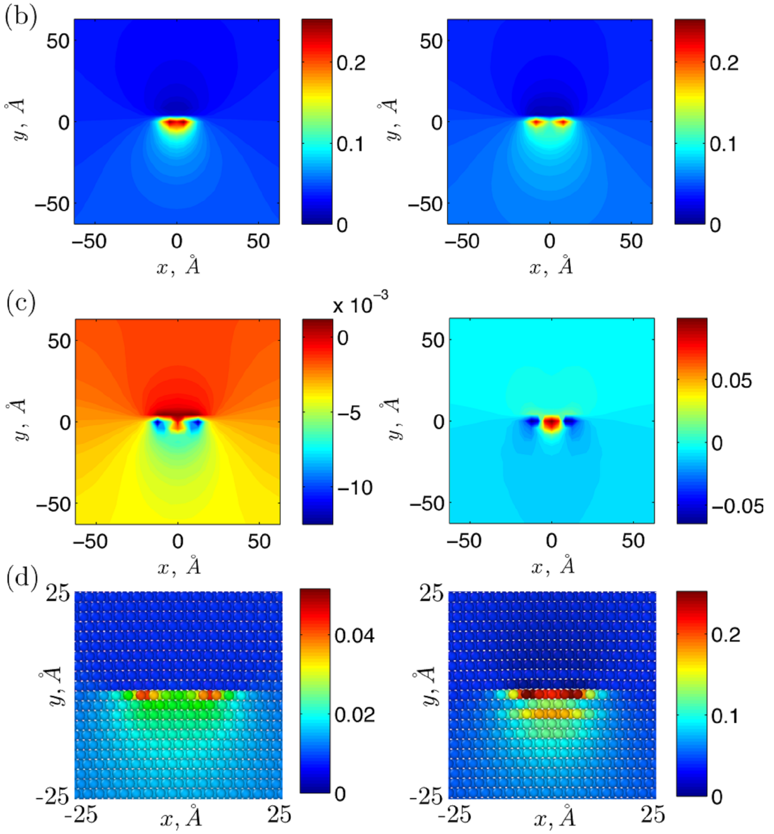

FIG. 6. (Color online) Contour plots of solute concentration near the split edge dislocation from DMD calculation (left) and from the hydrostatic pressure field existing prior to segregation (right) for (a) $c_0 = 1\%$ and (b) 5% at $T = 600$ K. (c) Contour plots of the difference between these results and (d) magnified snapshots of the concentration field illustrating the details of the solute distribution for 1% Mg (left) and 5% Mg (right).

Dontsova, Rottler, Sinclair, *Phys. Rev. B* **90** (2014) 174102

Example: Dislocation Glide in FeH

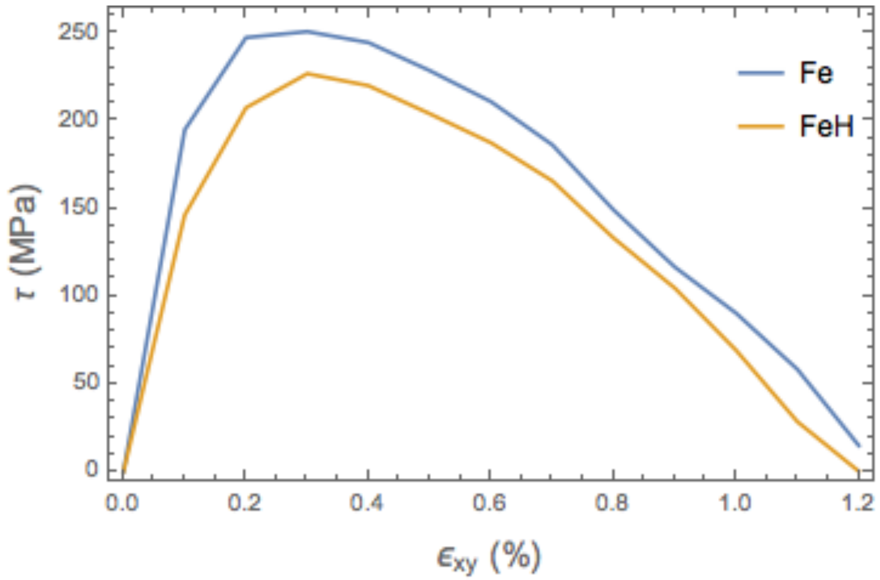

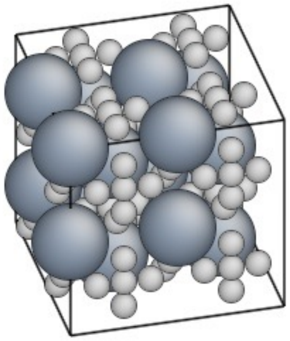

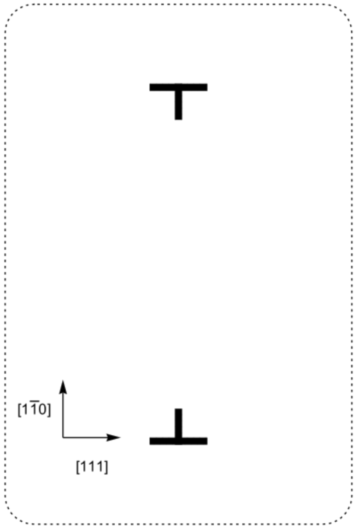

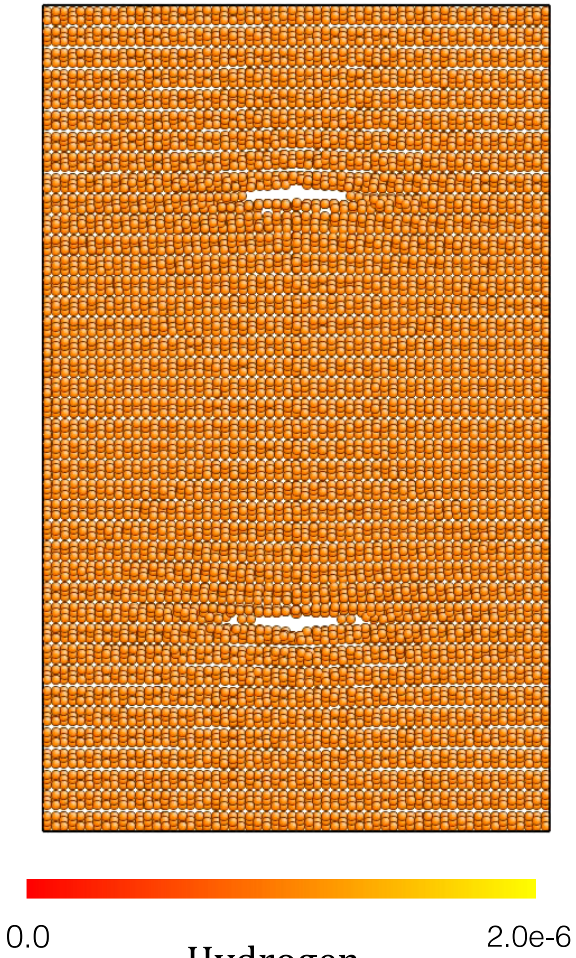

Hydrogen
Concentration
Distribution

- 19920 sites (2340 Fe + 17580 H)
- H sites $c=10^{-6}$
- Fe sites $c=1$

Sina Moeni, MIT

DMD analysis model for precipitation around dislocation core

Shuhei Shinzato, Shigenobu Ogata,
Osaka University

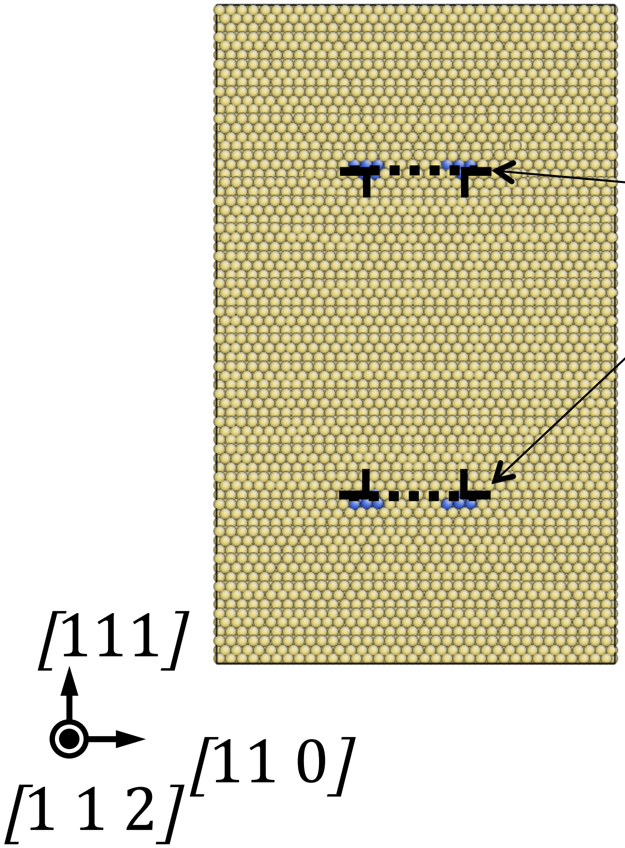

Ni-Al binary system

Introduce edge dislocation dipole

☐ Conditions

- ✓ 20448 atoms
- ✓ Temperature : 1000 K
- ✓ Back concentration of Al : 3,5,10at%
- ✓ Vacancy concentration : 0.001 at%
- ✓ Interatomic interaction : EAM

Ni--Al EAM potential from
Y. Mishin, “Atomistic modeling of the γ and γ’-phases of the Ni--Al system,” *Acta Mater.* **52** (2004) 1451-

Time evolution of composition distribution around dislocation core

- Ni-3at%Al

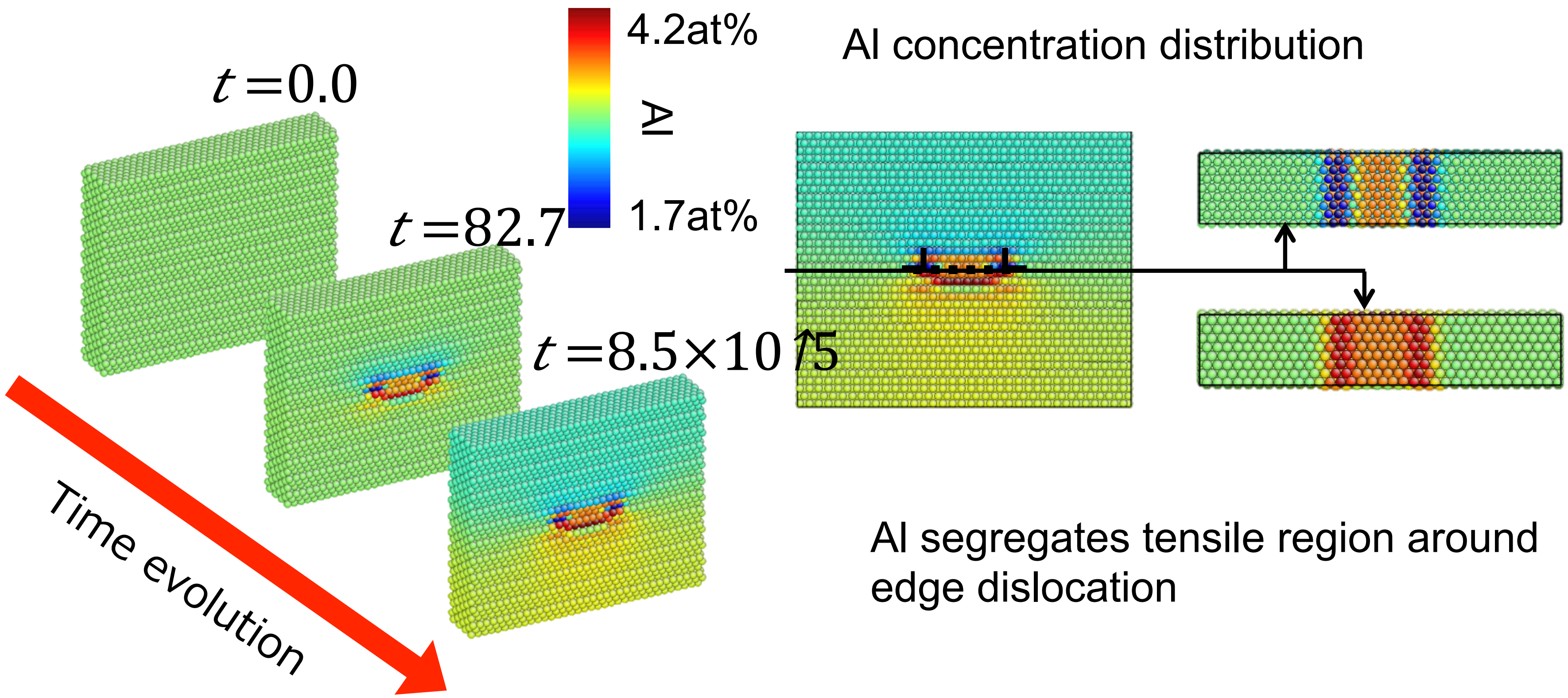

Al segregates tensile region around edge dislocation

Time evolution of Al color in Ni-3%Al alloy

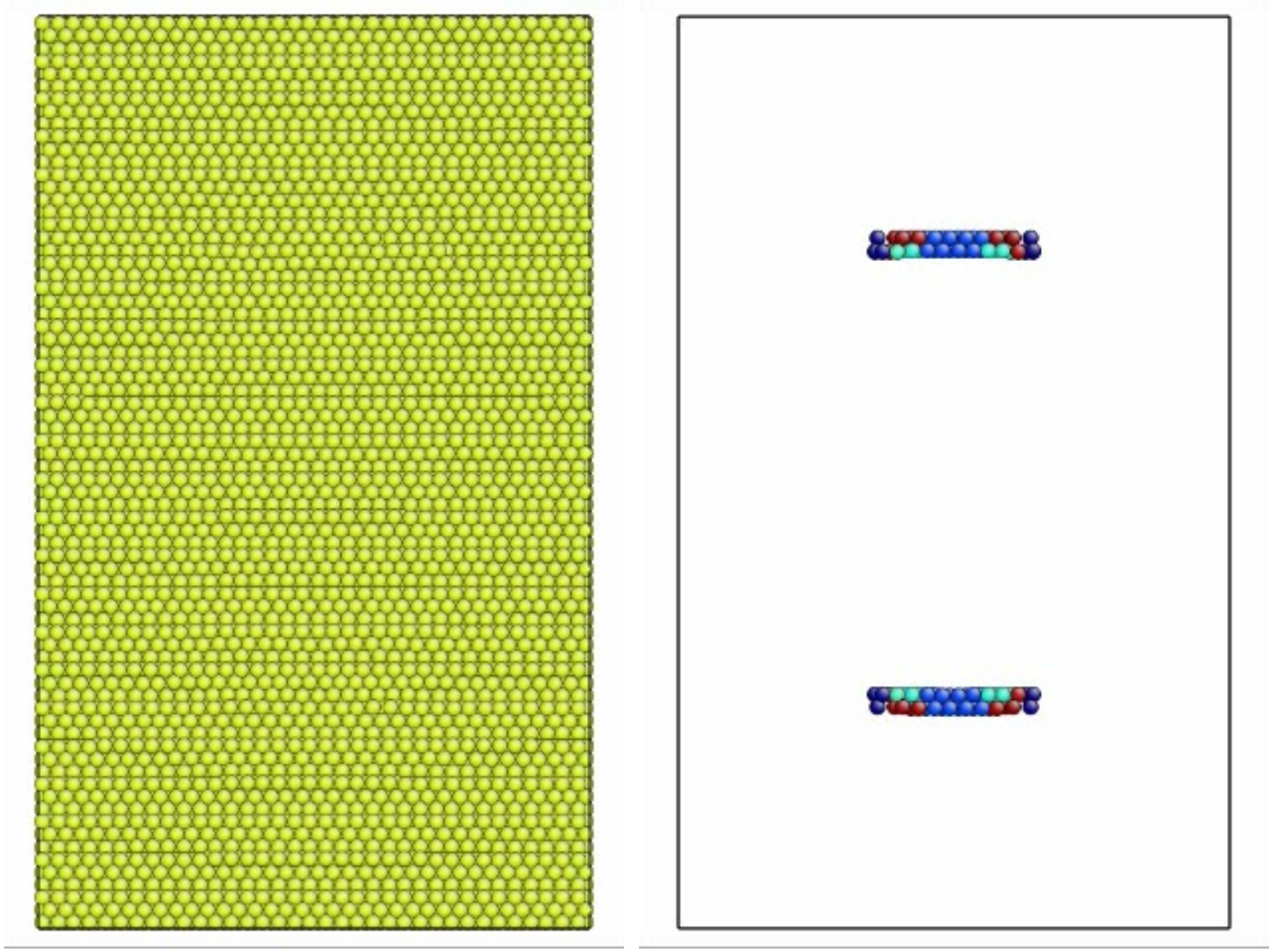

Color of Al

Central symmetry parameter

Stacking fault size increases by Al segregation

Time evolution of composition distribution around dislocation core

- ☐ Ni-5at%Al

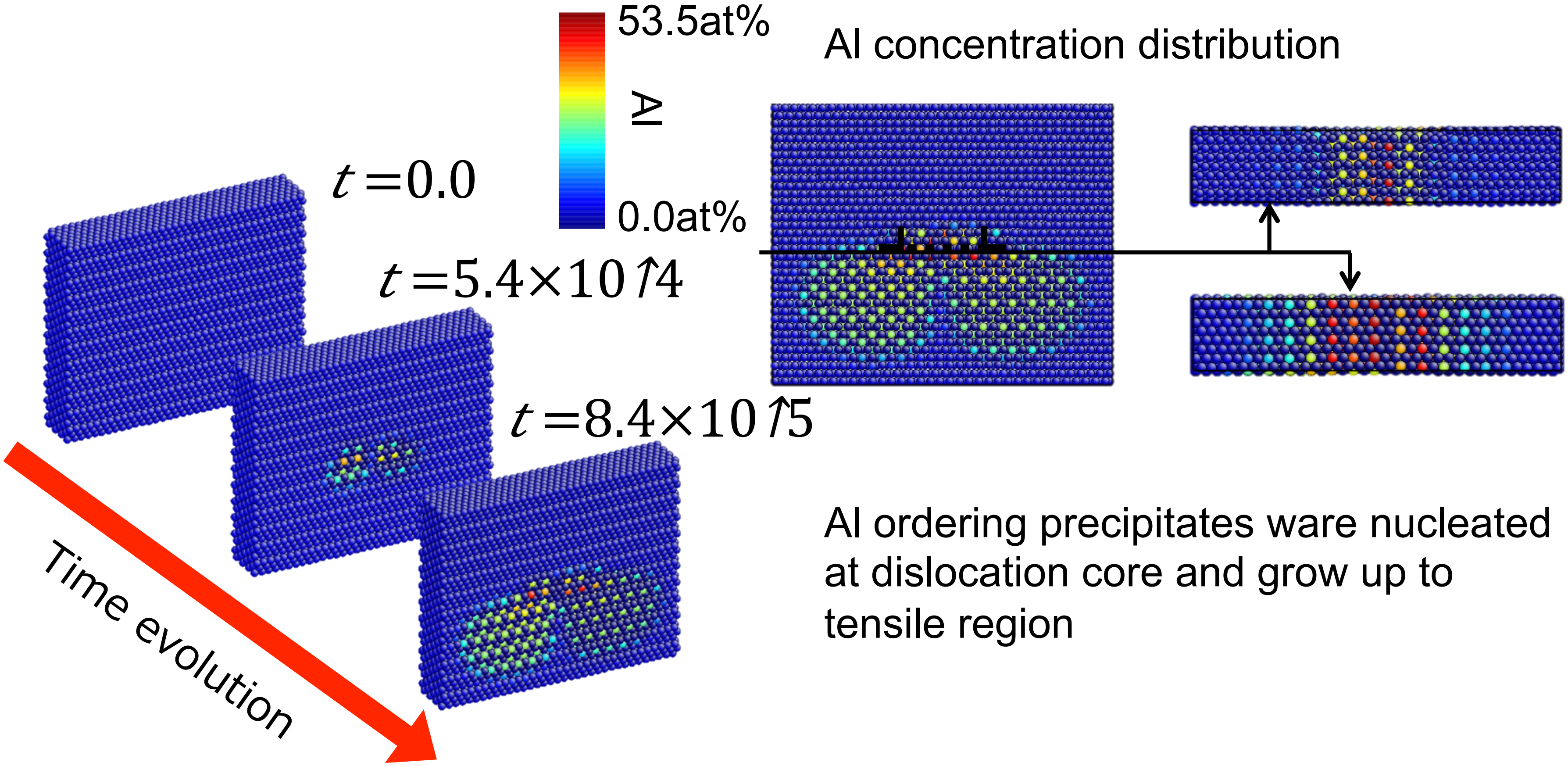

Al ordering precipitates ware nucleated at dislocation core and grow up to tensile region

Projection DMD result to MD configuration

Substitute Ni atom to Al atom being consistent with back concentration in DMD simulation

The substitute sites are stochastically selected based on site occupation probability obtained from DMD simulation

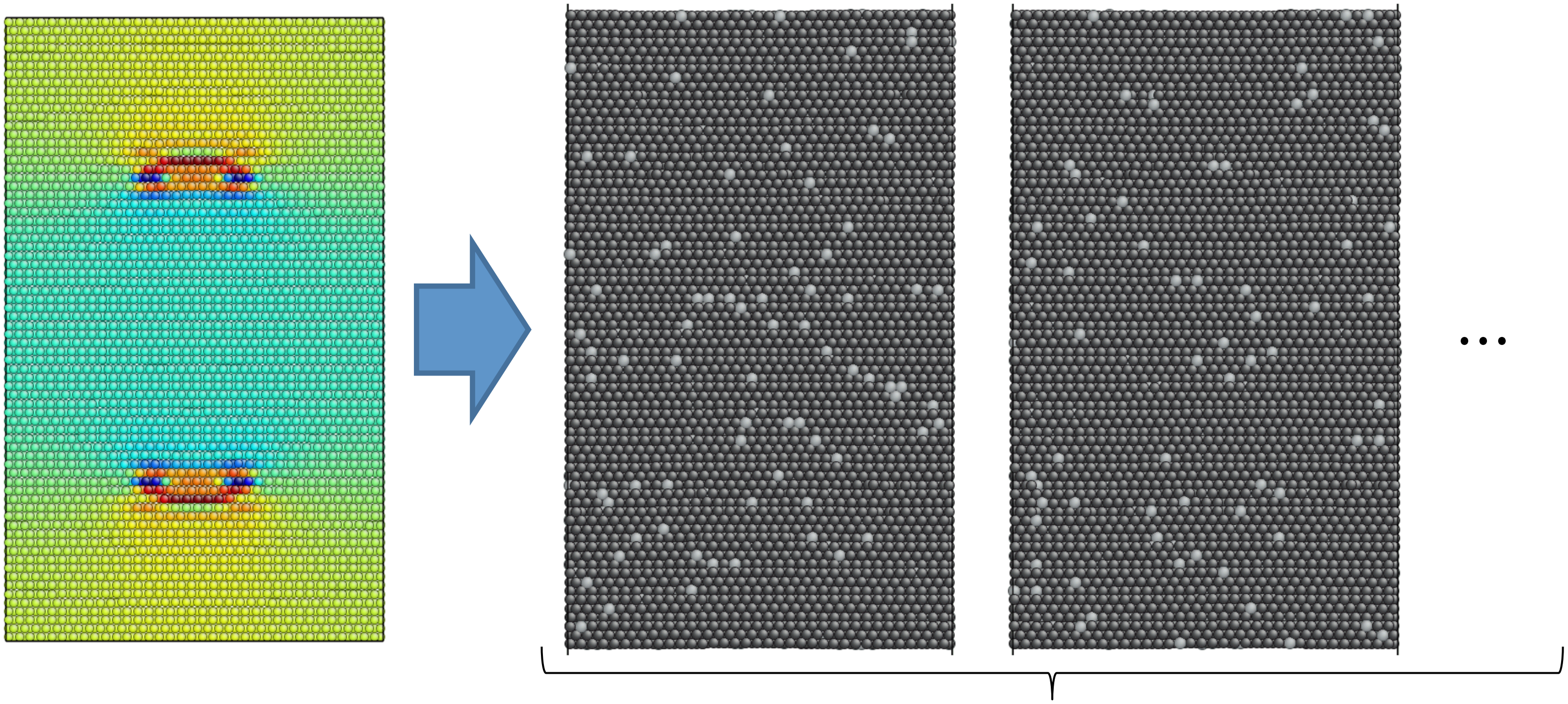

10 different configurations are generated in each concentration

Estimation of Peierls stress as a function of Al composition

☐ Peierls stress estimation model

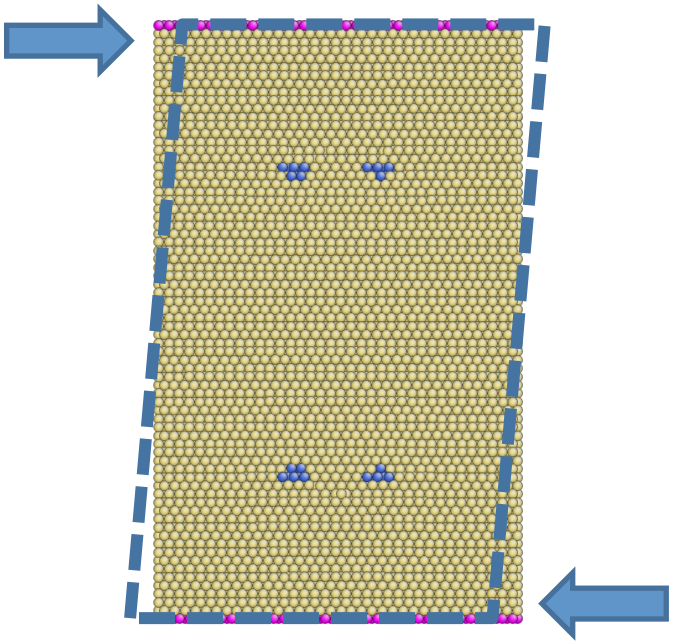

- Shear load applied on top and bottom 3 atomic layers
- Peierls stress is determined as the lowest stress at which dislocation starts to move

☐ Peierls stress as a function of Al composition

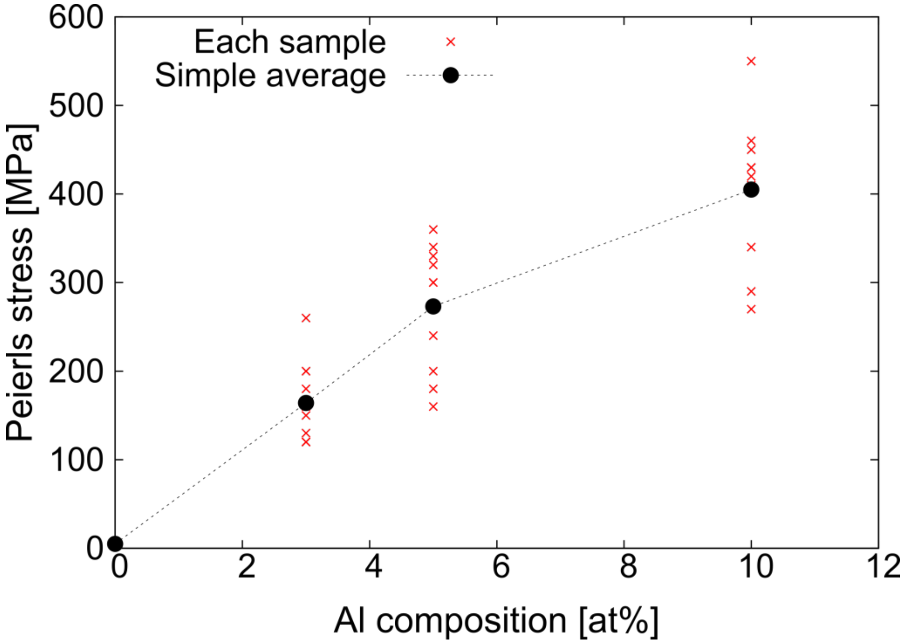

Peierls stress increases with increasing Al composition

a Problem is discovered….

Time evolution of composition distribution around dislocation core

☐ Ni-10at%Al

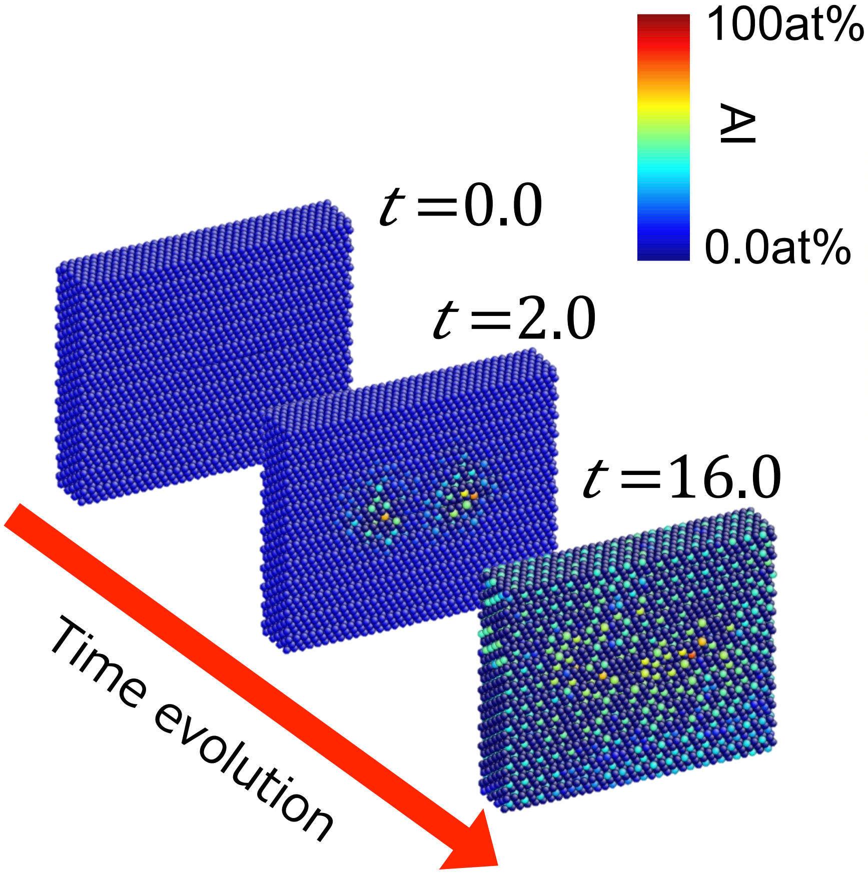

Al concentration distribution

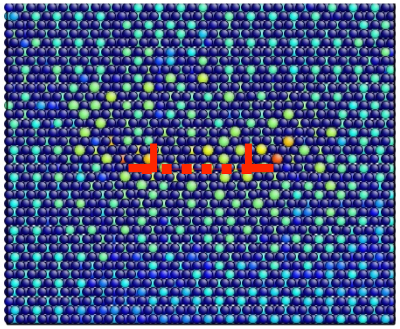

Once Al aggregates around dislocation, ordered precipitate rapidly become bigger,
and bigger, and bigger…

Free energy as a function of composition(1)

Calculate $g(x)$, $x=\#\mathrm{Al}/(\#\mathrm{Ni}+\#\mathrm{Al})$, for fcc Ni-Al and bcc Ni-Al

☐ fcc Ni-Al (864 atoms)

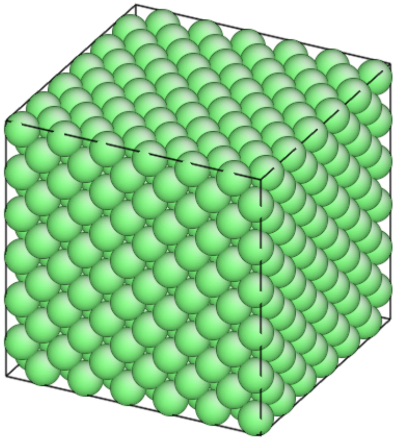

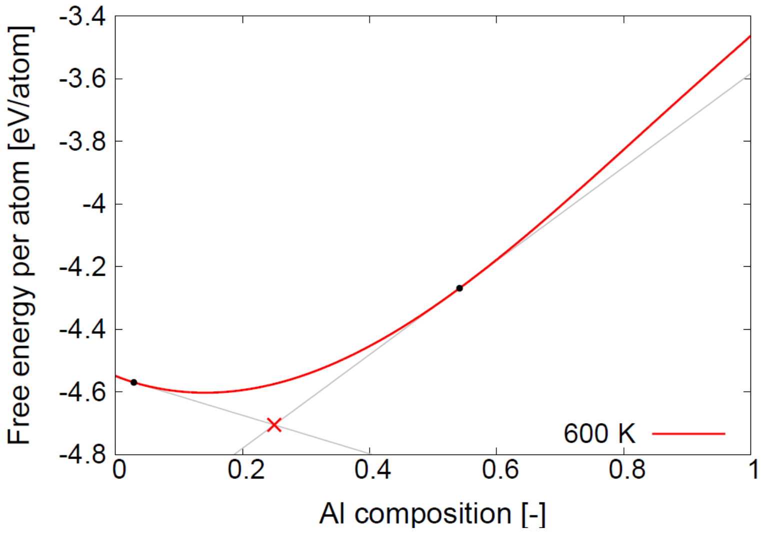

Set $c_{\mathrm{Al}}=x$ at all sites

Calculate free energy of each system from $c_{\mathrm{Al}}=0$ to $c_{\mathrm{Al}}=1$

Red line:
Free energy at each composition of Al calculated by DMD

Red cross:
Energy of ordering γ' phase (25%Al,$L1_2$ structure)

Gray line:
tangent through red cross

Black point:
contact point between tangent and FE curve

Free energy as a function of composition(2)

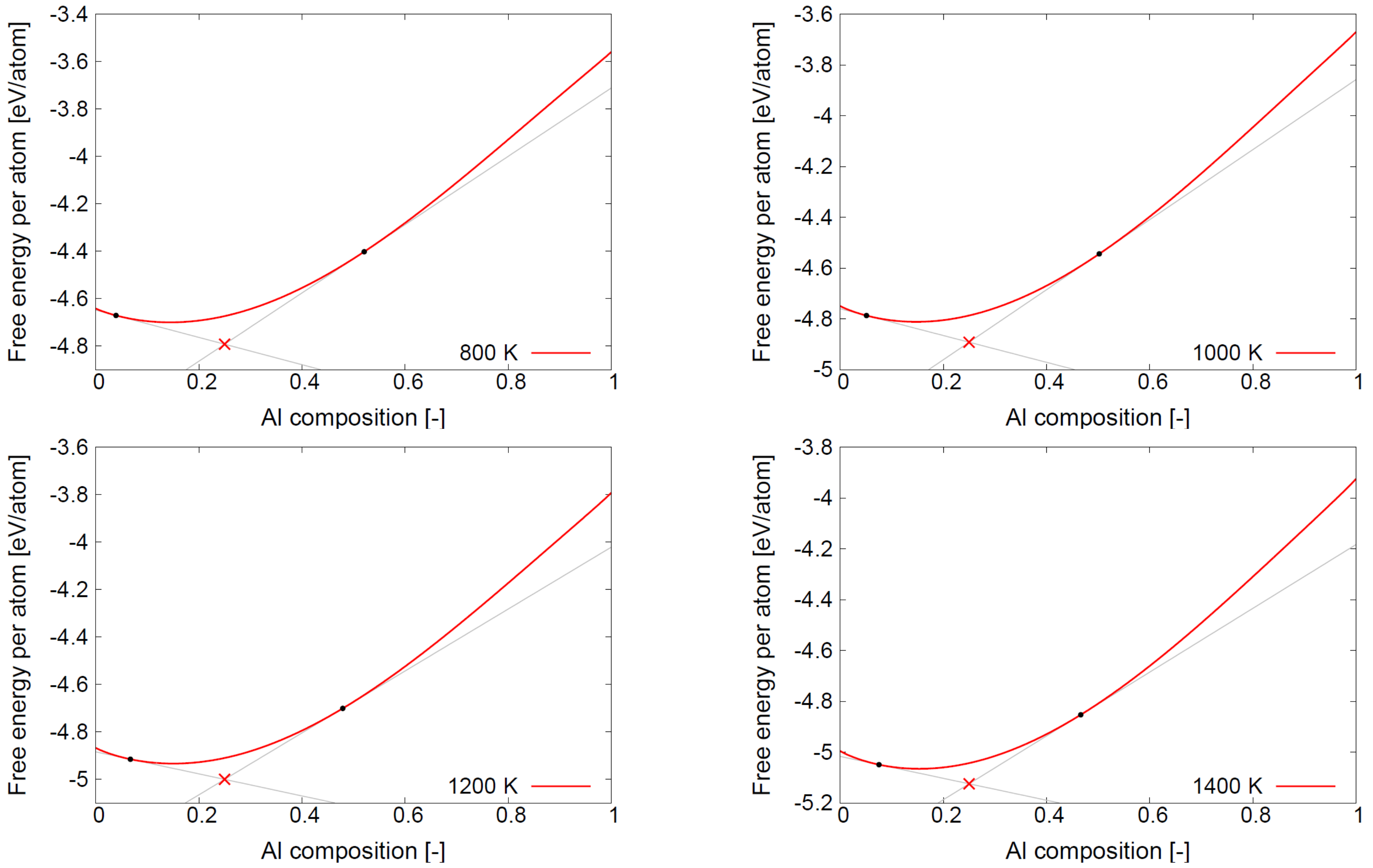

× Free energy of $L1_2$ structure ● Contact point of tangent

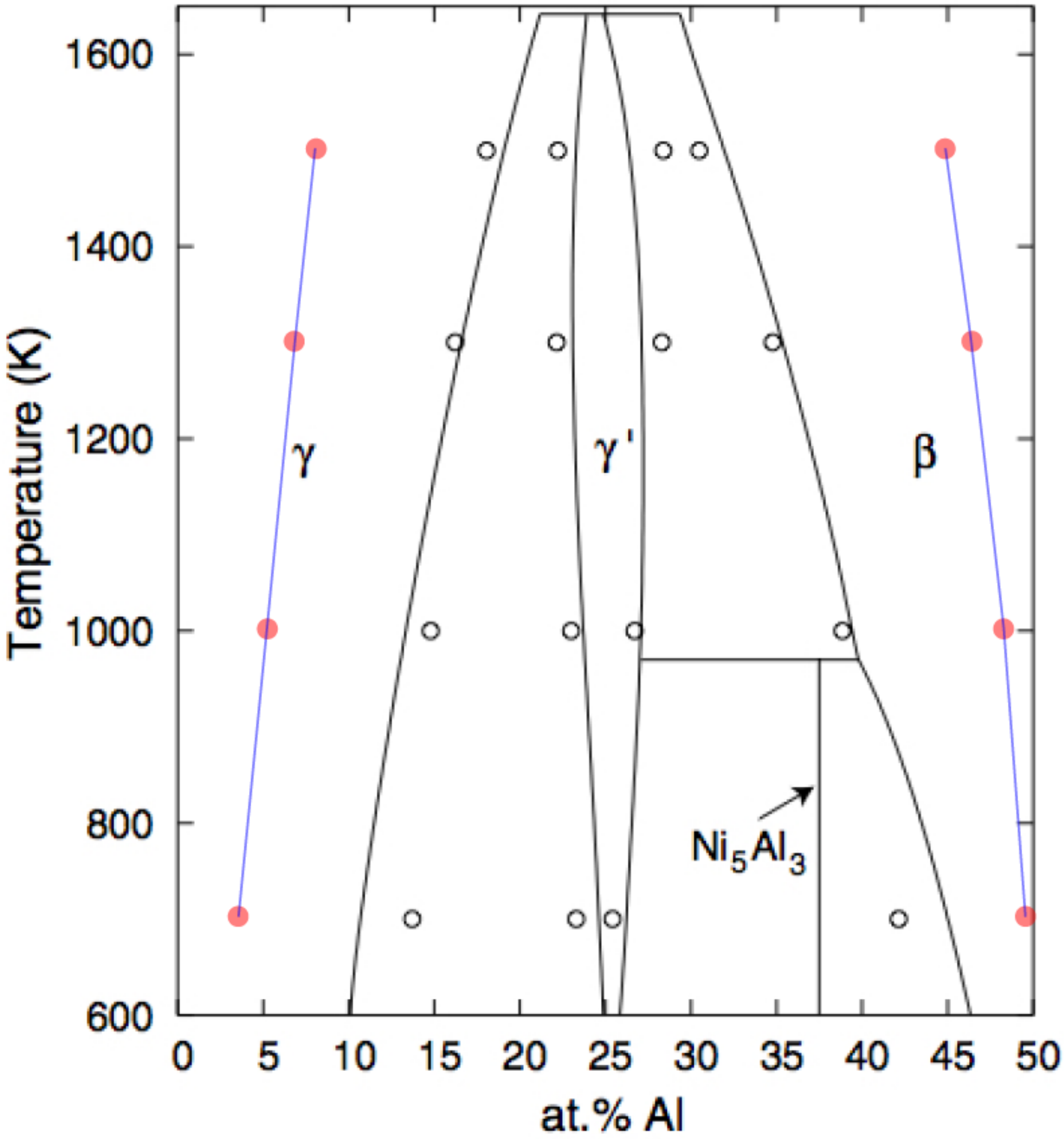

Temperature (K)
1600
1400
1200
1000
800
600
0
5
10
15
20
25
30
35
40
45
50
at.% Al
γ
γ '
β
Ni_5Al_3

$\boxed{T\text{=1300K}}$

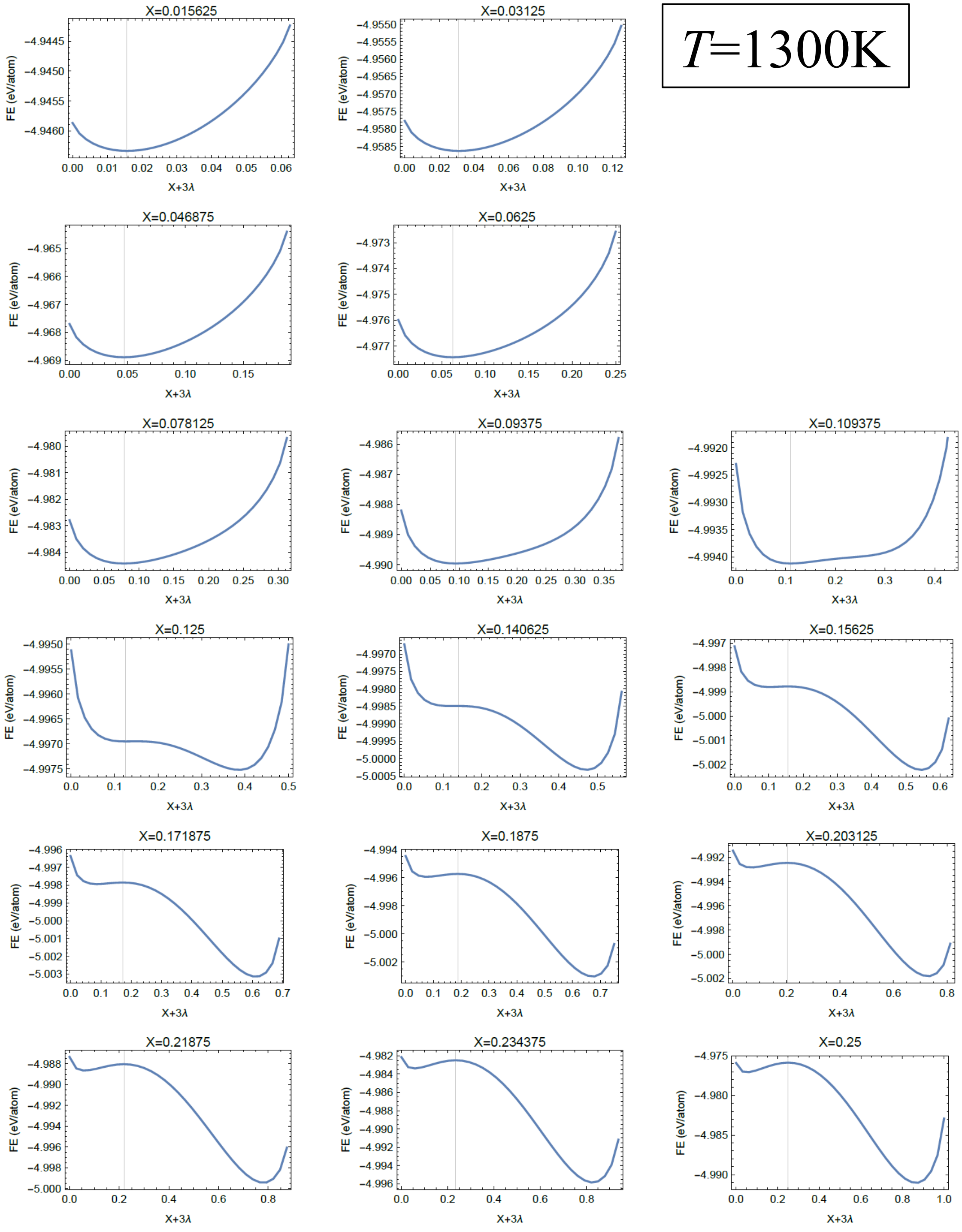

Given X (supercell Al fraction):

monopartite

$$\mathbf{o}_i = \mathbf{o}_j = \begin{bmatrix} 1-X \\ X \end{bmatrix}$$

c

bipartite

$$\mathbf{o}_i = \begin{bmatrix} 1-X-3\lambda \\ X+3\lambda \end{bmatrix} \text{ for sublattice 1}$$

$$\mathbf{o}_j = \begin{bmatrix} 1-X+\lambda \\ X-\lambda \end{bmatrix} \text{ for sublattice 2}$$

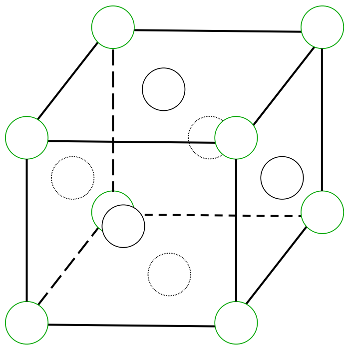

Site lattice with different occupants

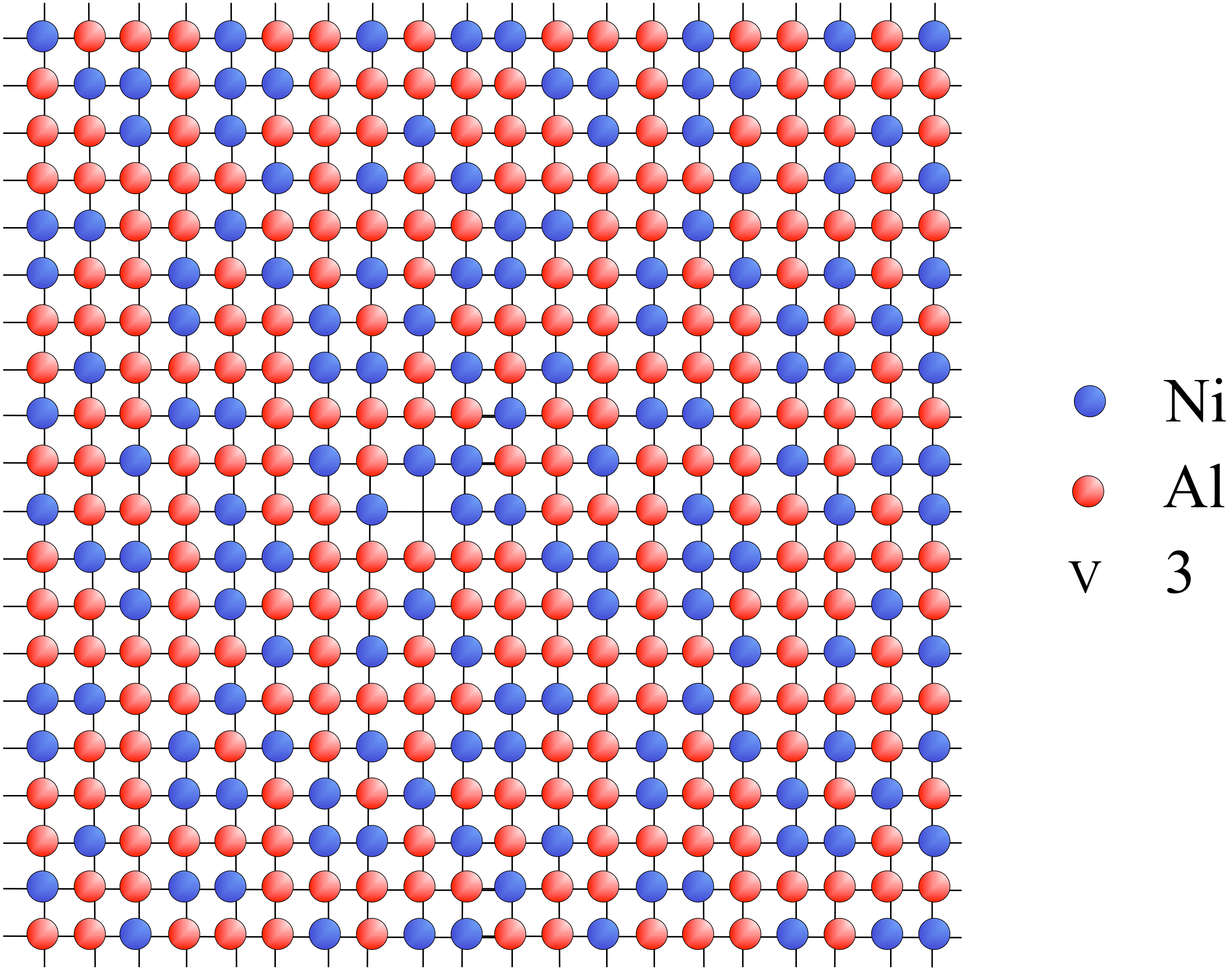

Site lattice with different occupants

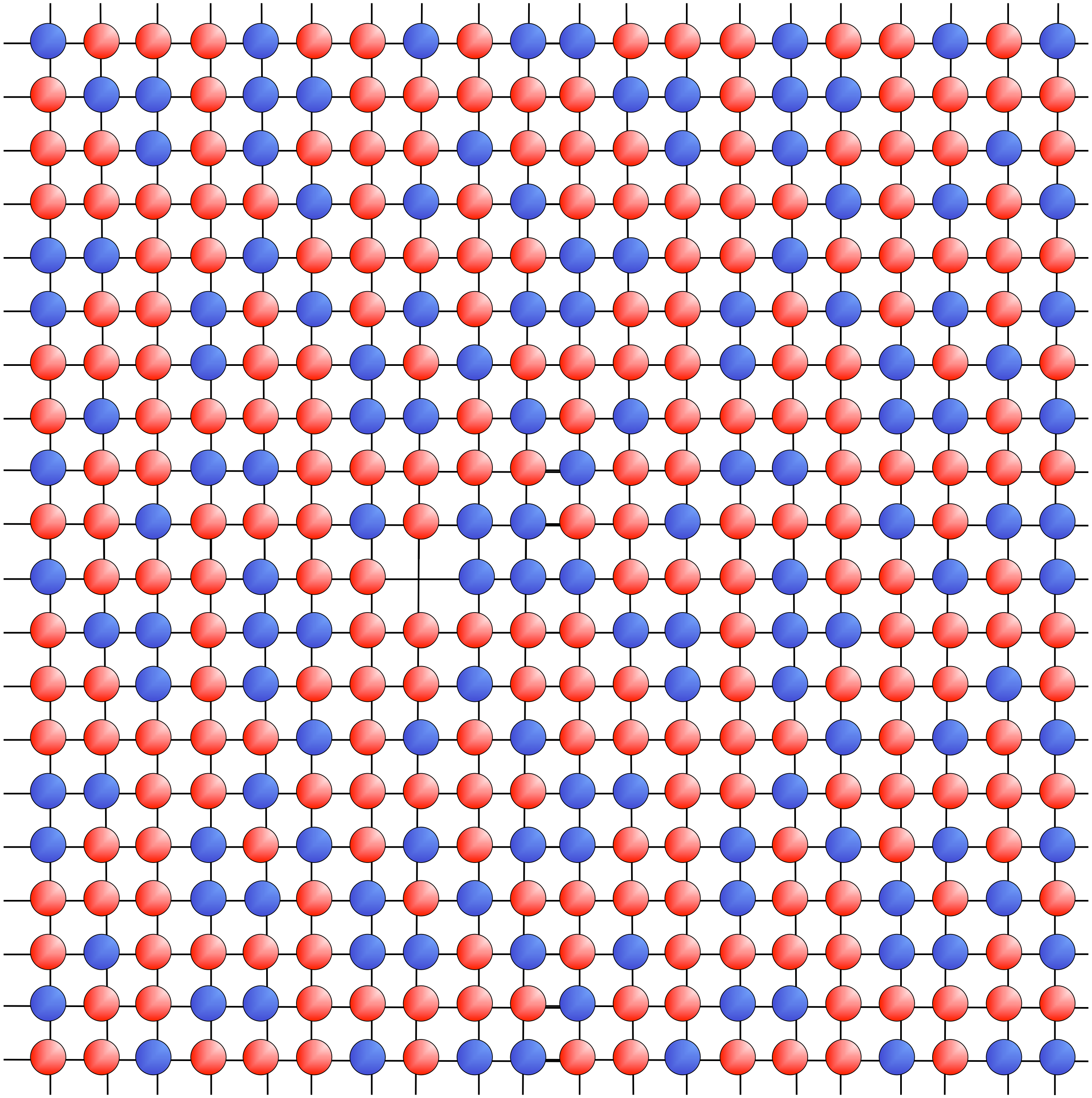

🔵 Ni

🔴 Al

v 3

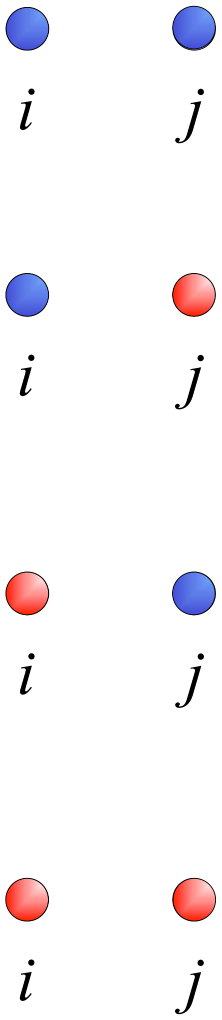

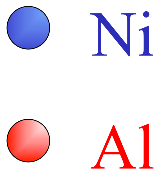

$$\begin{bmatrix}1\\0\end{bmatrix} \quad \begin{bmatrix}1\\0\end{bmatrix} \quad \begin{pmatrix}1&0\\0&0\end{pmatrix}$$

$$\begin{bmatrix}1\\0\end{bmatrix} \quad \begin{bmatrix}0\\1\end{bmatrix} \quad \begin{pmatrix}0&1\\0&0\end{pmatrix}$$

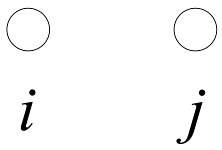

$$\begin{bmatrix}0\\1\end{bmatrix} \quad \begin{bmatrix}1\\0\end{bmatrix} \quad \begin{pmatrix}0&0\\1&0\end{pmatrix}$$

$$\begin{bmatrix}0\\1\end{bmatrix} \quad \begin{bmatrix}0\\1\end{bmatrix} \quad \begin{pmatrix}0&0\\0&1\end{pmatrix}$$

$$\downarrow \qquad \downarrow \qquad \downarrow$$

$$\mathbf{o}_i = \begin{bmatrix}0.7\\0.3\end{bmatrix} \quad \mathbf{o}_j = \begin{bmatrix}0.4\\0.6\end{bmatrix} \quad \mathbf{B}_{ij} = \begin{pmatrix}0.3&0.4\\0.1&0.2\end{pmatrix}$$

constraints

$$\sum_{n=1}^{C} B_{ij}^{mn} = o_i^m \quad \text{and} \quad \sum_{m=1}^{C} B_{ij}^{mn} = o_j^n$$

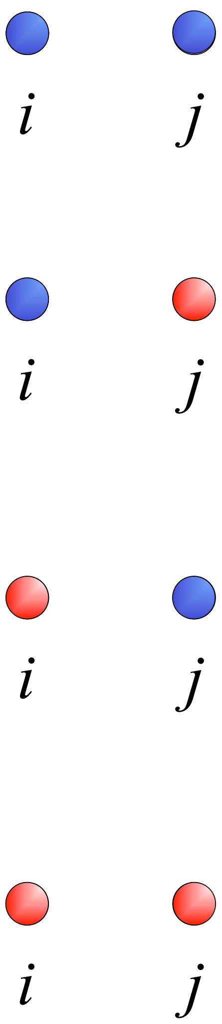

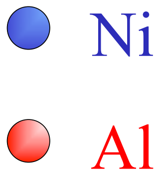

$$\begin{bmatrix}1\\0\end{bmatrix} \quad \begin{bmatrix}1\\0\end{bmatrix} \quad \begin{pmatrix}1 & 0\\0 & 0\end{pmatrix}$$

$$\begin{bmatrix}1\\0\end{bmatrix} \quad \begin{bmatrix}0\\1\end{bmatrix} \quad \begin{pmatrix}0 & 1\\0 & 0\end{pmatrix}$$

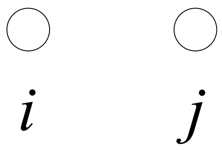

$$\begin{bmatrix}0\\1\end{bmatrix} \quad \begin{bmatrix}1\\0\end{bmatrix} \quad \begin{pmatrix}0 & 0\\1 & 0\end{pmatrix}$$

$$\begin{bmatrix}0\\1\end{bmatrix} \quad \begin{bmatrix}0\\1\end{bmatrix} \quad \begin{pmatrix}0 & 0\\0 & 1\end{pmatrix}$$

constraints

$$\sum_{n=1}^{C} B_{ij}^{mn} = o_i^m \text{ and } \sum_{m=1}^{C} B_{ij}^{mn} = o_j^n$$

$$\mathbf{o}_i = \begin{bmatrix}0.7\\0.3\end{bmatrix} \quad \mathbf{o}_j = \begin{bmatrix}0.4\\0.6\end{bmatrix} \quad \mathbf{B}_{ij} = \begin{pmatrix}0.3 & 0.4\\0.1 & 0.2\end{pmatrix} \quad \mathbf{B}_{ij}^{\mathrm{MF}} \equiv \mathbf{o}_i\mathbf{o}_j^T = \begin{pmatrix}0.28 & 0.42\\0.12 & 0.18\end{pmatrix}$$

🔵 Ni

🔴 Al

🔵 i 🔵 j $\begin{bmatrix}1\\0\end{bmatrix}$ $\begin{bmatrix}1\\0\end{bmatrix}$ $\begin{pmatrix}1 & 0\\0 & 0\end{pmatrix}$

🔵 i 🔴 j $\begin{bmatrix}1\\0\end{bmatrix}$ $\begin{bmatrix}0\\1\end{bmatrix}$ $\begin{pmatrix}0 & 1\\0 & 0\end{pmatrix}$

○ i ○ j

🔴 i 🔵 j $\begin{bmatrix}0\\1\end{bmatrix}$ $\begin{bmatrix}1\\0\end{bmatrix}$ $\begin{pmatrix}0 & 0\\1 & 0\end{pmatrix}$

🔴 i 🔴 j $\begin{bmatrix}0\\1\end{bmatrix}$ $\begin{bmatrix}0\\1\end{bmatrix}$ $\begin{pmatrix}0 & 0\\0 & 1\end{pmatrix}$

↓ ↓ ↓

$$\mathbf{o}_i = \begin{bmatrix}0.7\\0.3\end{bmatrix} \quad \mathbf{o}_j = \begin{bmatrix}0.4\\0.6\end{bmatrix} \quad \mathbf{B}_{ij} = \begin{pmatrix}0.3 & 0.4\\0.1 & 0.2\end{pmatrix}$$

0.02: “self-love” SRO

‖

$$\mathbf{B}_{ij} \equiv \mathbf{B}_{ij}^{\mathrm{MF}} + \begin{pmatrix}\eta & -\eta\\ -\eta & \eta\end{pmatrix}$$

Correlation correction

constraints

$$\sum_{n=1}^{C} B_{ij}^{mn} = o_i^m \quad \text{and} \quad \sum_{m=1}^{C} B_{ij}^{mn} = o_j^n$$

$$\mathbf{B}_{ij}^{\mathrm{MF}} \equiv \mathbf{o}_i \mathbf{o}_j^T = \begin{pmatrix}0.28 & 0.42\\0.12 & 0.18\end{pmatrix}$$

$$o_i^m o_j^n w_{mn}(|\mathbf{X}_i - \mathbf{X}_j|, \alpha_i^m, \alpha_j^n) \Rightarrow B_{ij}^{mn} w_{mn}(|\mathbf{X}_i - \mathbf{X}_j|, \alpha_i^m, \alpha_j^n)$$

$$\sum_{i=1}^{S}\sum_{m=1}^{C} o_i^m E_m\left(\sum_{j=1}^{S}\sum_{n=1}^{C} o_j^n \psi_{mn}(|\mathbf{X}_i - \mathbf{X}_j|, \alpha_i^m, \alpha_j^n)\right) \Rightarrow$$

$$\sum_{i=1}^{S}\sum_{m=1}^{C} o_i^m E_m\left(\sum_{j=1}^{S}\sum_{n=1}^{C} \frac{B_{ij}^{mn}}{o_i^m} \psi_{mn}(|\mathbf{X}_i - \mathbf{X}_j|, \alpha_i^m, \alpha_j^n)\right)$$

Conditional probability

$$k_{\mathrm{B}}T\sum_{i=1}^{S}\sum_{m=1}^{C} o_i^m \ln o_i^m \Rightarrow$$

always positive under **constraints**

$$\sum_{n=1}^{C} B_{ij}^{mn} = o_i^m \quad \text{and} \quad \sum_{m=1}^{C} B_{ij}^{mn} = o_j^n$$

$$k_{\mathrm{B}}T\sum_{i=1}^{S}\sum_{m=1}^{C} o_i^m \ln o_i^m + \boxed{k_{\mathrm{B}}T\sum_{ij\in N}\sum_{m=1}^{C}\sum_{n=1}^{C} B_{ij}^{mn} \ln \frac{B_{ij}^{mn}}{o_i^m o_j^n}}$$

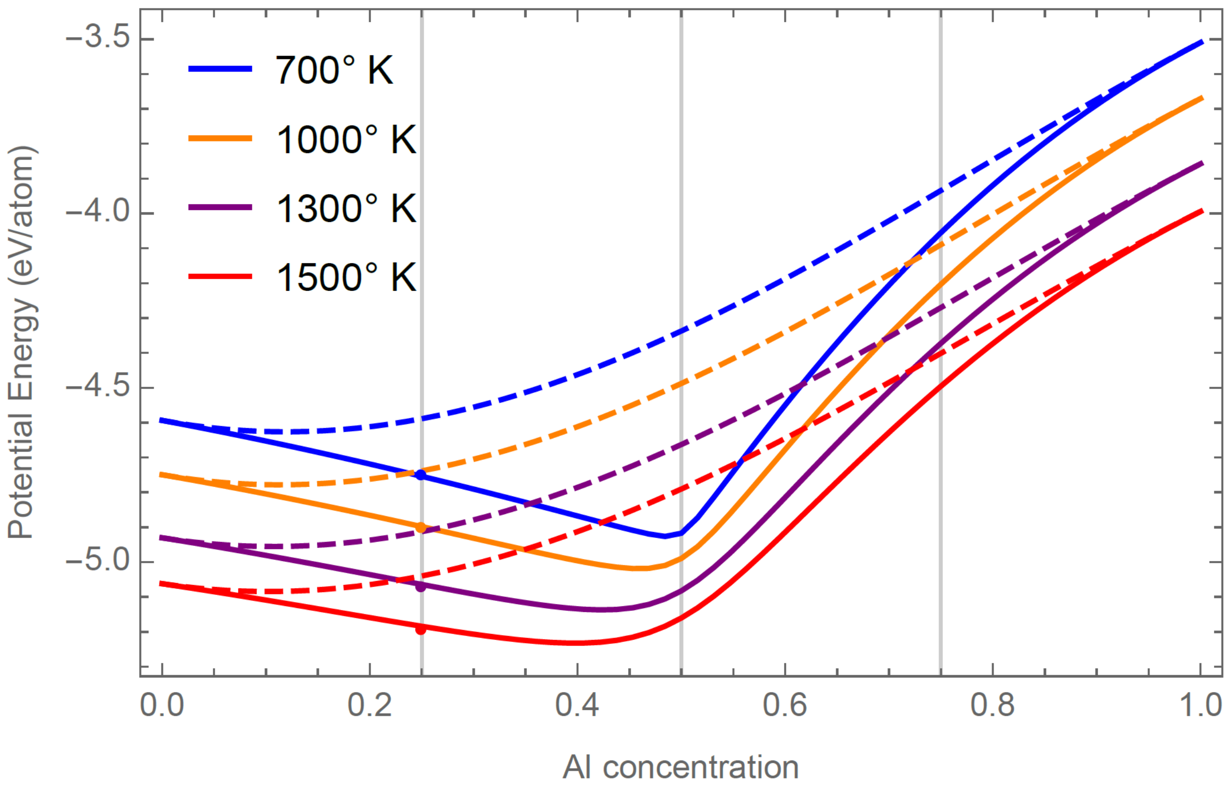

−3.5
−4.0
−4.5
−5.0
0.0
0.2
0.4
0.6
0.8
1.0
Potential Energy (eV/atom)
Al concentration
700° K
1000° K
1300° K
1500° K

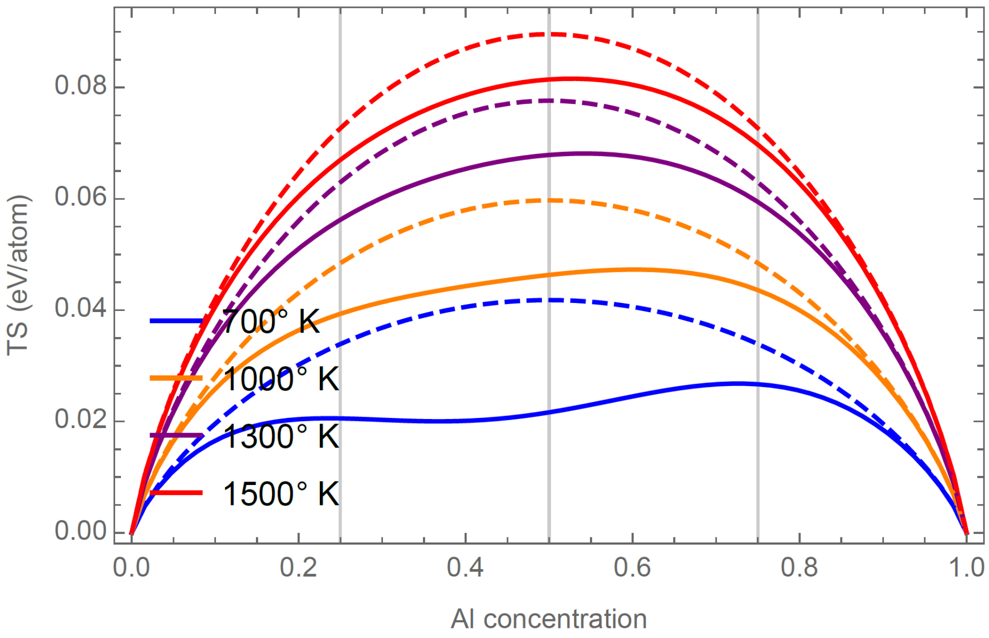

0.00
0.02
0.04
0.06
0.08
0.0
0.2
0.4
0.6
0.8
1.0
TS (eV/atom)
Al concentration
700° K
1000° K
1300° K
1500° K

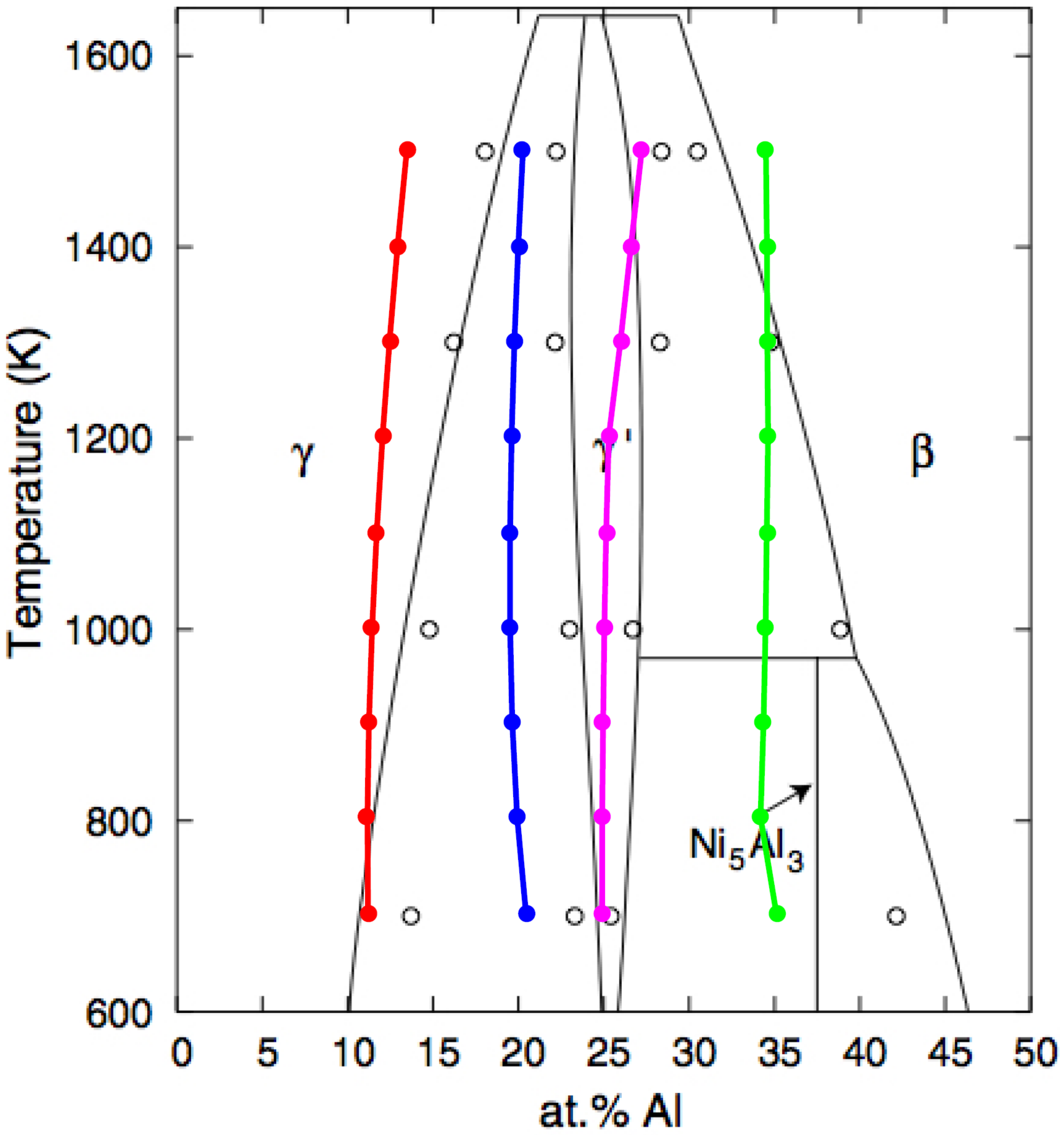

$$\Delta S_{ij}^{mn} = -2B_{ij}^{mn}\log\left(B_{ij}^{mn}\right) + \left(B_{ij}^{mn} + o_i^m o_j^n\right)\log\left(o_i^m o_j^n\right)$$

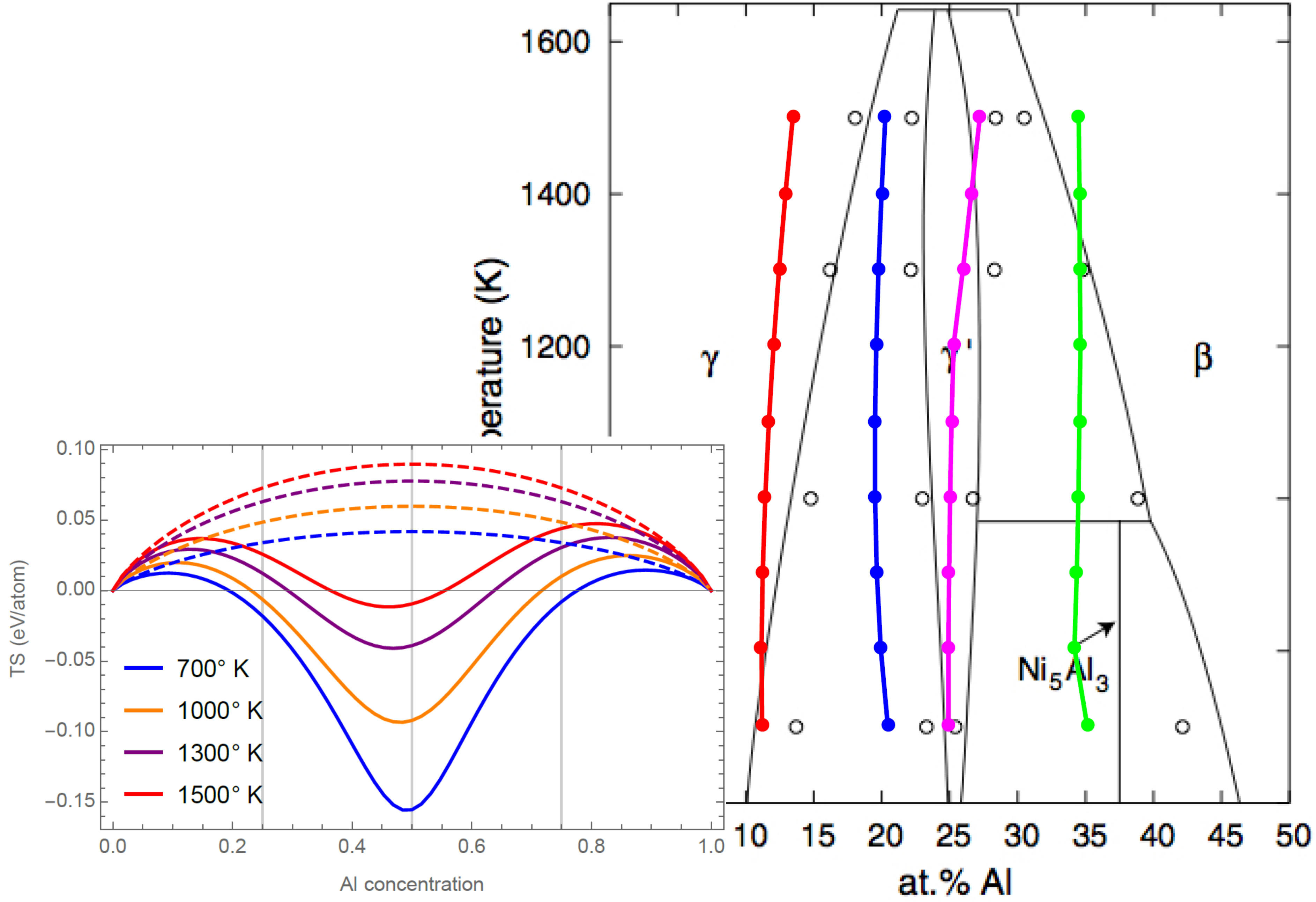

$$\Delta S_{ij}^{mn} = -2B_{ij}^{mn}\log\left(B_{ij}^{mn}\right) + \left(B_{ij}^{mn} + o_i^m o_j^n\right)\log\left(o_i^m o_j^n\right)$$

LDA → GGA

$\kappa = 0.1$

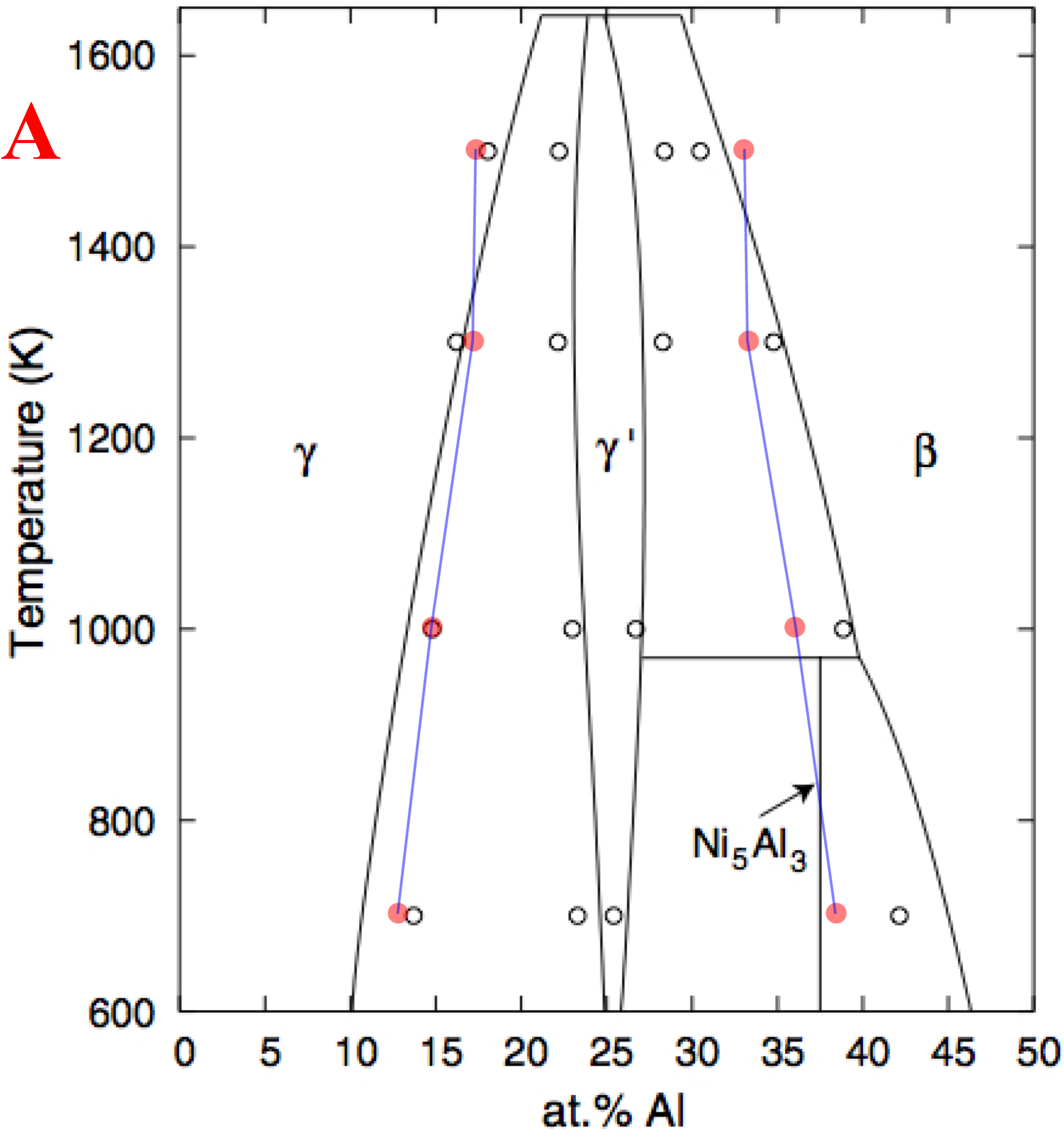

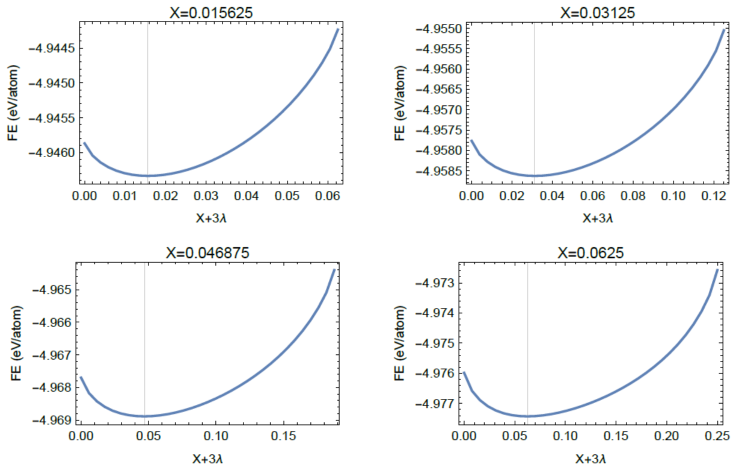

T=1300K

Given *X* (supercell Al fraction):

monopartite

$$\mathbf{o}_i = \mathbf{o}_j = \begin{bmatrix} 1-X \\ X \end{bmatrix}$$

c

bipartite

$$\mathbf{o}_i = \begin{bmatrix} 1-X-3\lambda \\ X+3\lambda \end{bmatrix} \quad \text{for sublattice 1}$$

$$\mathbf{o}_j = \begin{bmatrix} 1-X+\lambda \\ X-\lambda \end{bmatrix} \quad \text{for sublattice 2}$$

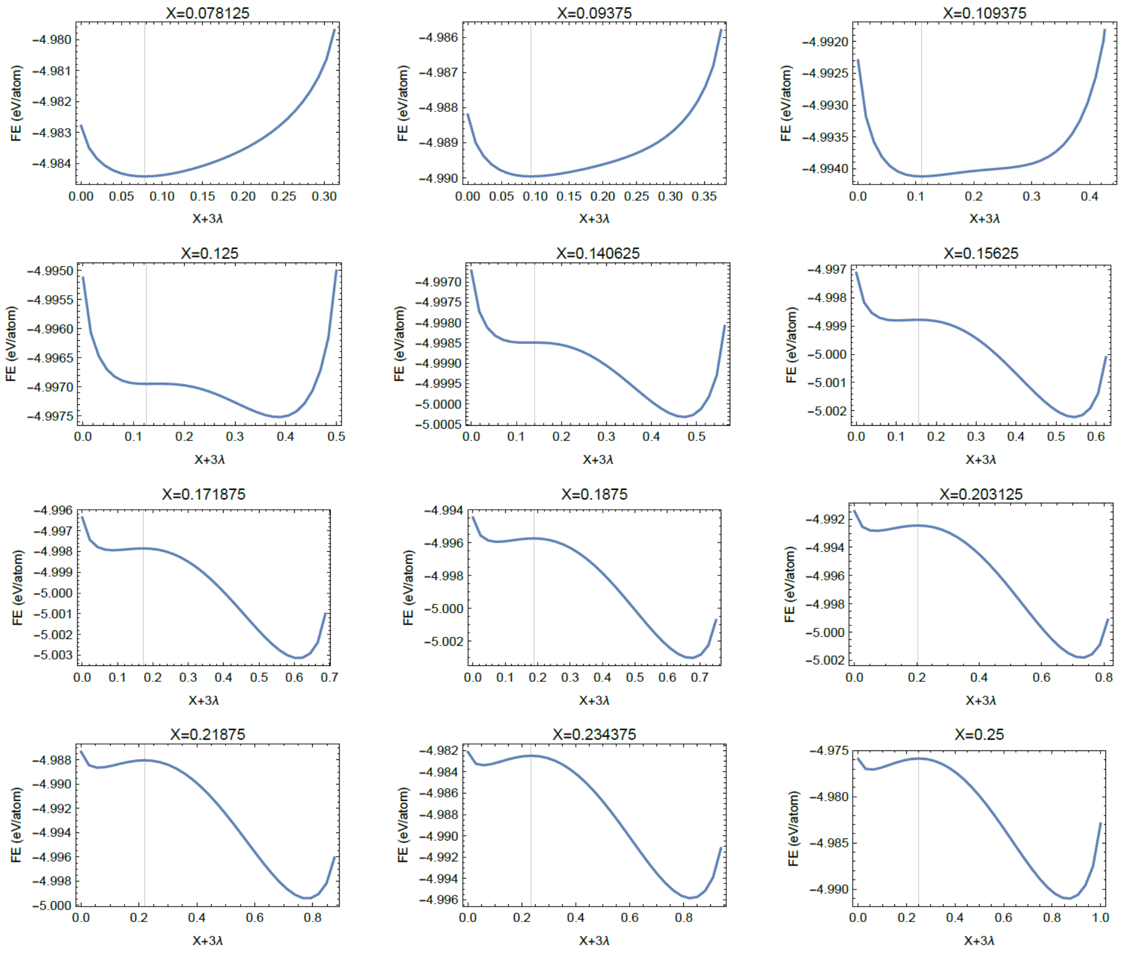

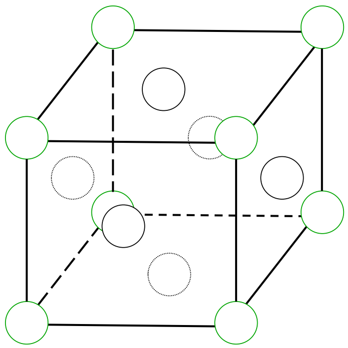

LDA → GGA

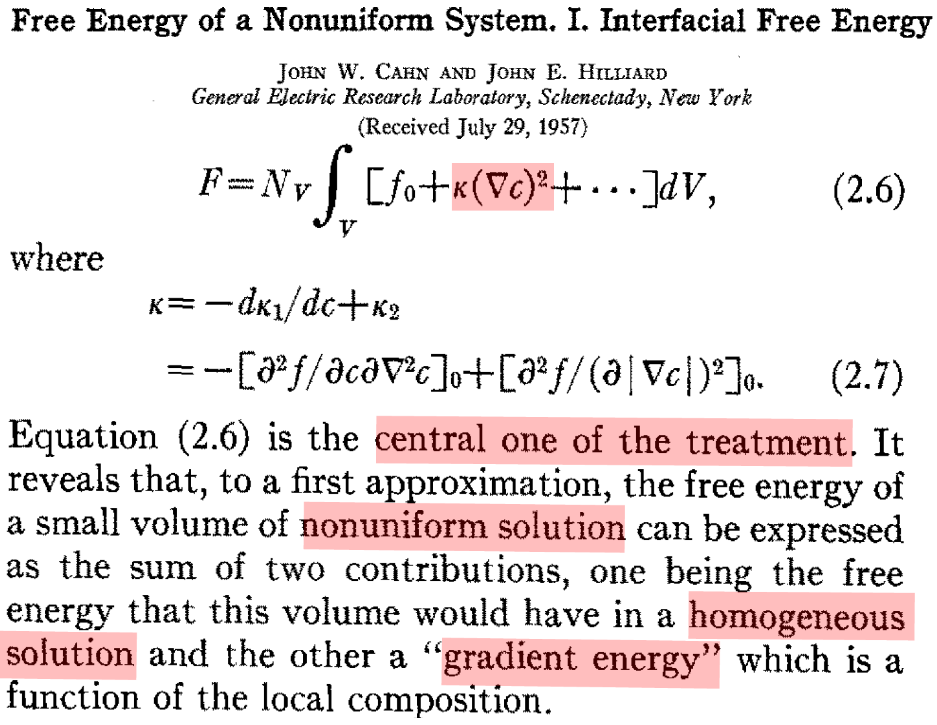

Free Energy of a Nonuniform System. I. Interfacial Free Energy

JOHN W. CAHN AND JOHN E. HILLIARD
General Electric Research Laboratory, Schenectady, New York
(Received July 29, 1957)

$$F=N_V\int_V[f_0+\kappa(\nabla c)^2+\cdots]dV, \qquad (2.6)$$

where

$$\begin{aligned}\kappa&=-d\kappa_1/dc+\kappa_2\\&=-[\partial^2 f/\partial c\partial\nabla^2 c]_0+[\partial^2 f/(\partial|\nabla c|)^2]_0.\end{aligned} \qquad (2.7)$$

Equation (2.6) is the central one of the treatment. It reveals that, to a first approximation, the free energy of a small volume of nonuniform solution can be expressed as the sum of two contributions, one being the free energy that this volume would have in a homogeneous solution and the other a "gradient energy" which is a function of the local composition.

$$o_i^m o_j^n w_{mn}(|\mathbf{X}_i-\mathbf{X}_j|,\alpha_i^m,\alpha_j^n) \Rightarrow$$

$$o_i^m o_j^n w_{mn}(|\mathbf{X}_i-\mathbf{X}_j|,\alpha_i^m,\alpha_j^n)\times\left(1-\frac{\kappa}{2}|\mathbf{o}_i-\mathbf{o}_j|^2\right)$$

$$\sum_{i=1}^{S}\sum_{m=1}^{C} o_i^m E_m\left(\sum_{j=1}^{S}\sum_{n=1}^{C} o_j^n \psi_{mn}(|\mathbf{X}_i-\mathbf{X}_j|,\alpha_i^m,\alpha_j^n)\right)\Rightarrow$$

$$\sum_{i=1}^{S}\sum_{m=1}^{C} o_i^m E_m\left(\sum_{j=1}^{S}\sum_{n=1}^{C} o_j^n \psi_{mn}(|\mathbf{X}_i-\mathbf{X}_j|,\alpha_i^m,\alpha_j^n)\times\left(1-\frac{\kappa}{2}|\mathbf{o}_i-\mathbf{o}_j|^2\right)\right)$$

- DMD thermodynamics formulated as a **density functional theory**. Atomic realization of regular solution model, w/ gradient thermodynamics, long-range elastic & short-range coordination interactions

- Pair, triplet, … **correlations** ignored. **Cluster expansion** calculation should give more accurate $F_{\mathrm{DMD}}(\{\mathbf{X}_i,\alpha_i,\mathbf{c}_i\})$

- DMD kinetics "solves Cahn-Hilliard equation on a moving atom grid", with **atomic spatial resolution**, but at **diffusive timescales**. *Time-Dependent DFT*

- Another view: DMD guides **atom creation** and **atom annihilation operators** in MD or VG simulations by chemical potential gradient

Li et al, *Phys. Rev. B* **84** (2011) 054103; Sarkar et al., *Phys. Rev. B* **86** (2012) 014115

- Explores mass-action, **coupled diffusive-displacive mechanisms** (Wang & Li, *Acta Mater*. **58** (2010) 1212) **cheaply**

- Code order-*N*, 95% similar as MD

- Uses EAM potentials: Most accurate, efficient as *T*✸0

- No need to pre-build event catalog.
  competitive in speed against kinetic Monte Carlo

- Correlation effect by adding *one* **atomistic gradient coefficient**, that greatly improves phase diagram.

- The “quasi-continuum” version of DMD can be coupled to well-established diffusion - microelasticity equation solvers such as **finite-element** or **phase-field** method

Li et al, *Phys. Rev. B* **84** (2011) 054103; Sarkar et al., *Phys. Rev. B* **86** (2012) 014115

Adaptive grid **down to the atom** - Quasicontinuum DMD?

continuum
diffusion-elasticity
(phase field)
equation solver
with adaptive
meshing

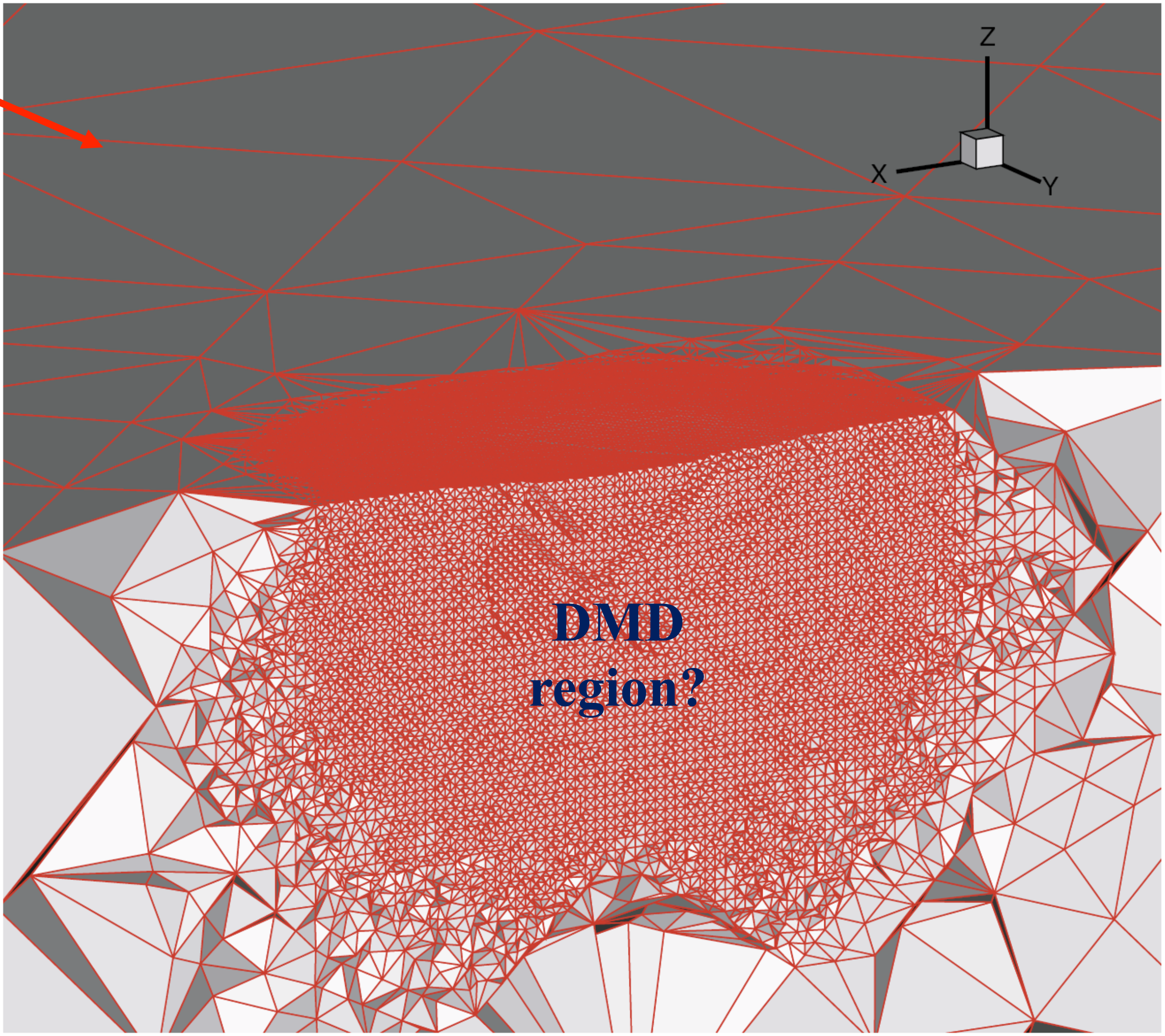

image taken from Knap and Ortiz, *Phys. Rev. Lett*. **90** (2003) 226102.

MIT Atomistic Parallel Package (MAPP)

- Open-source MD / Diffusive MD code
- Written in C++ / MPI
- up to 30% faster than LAMMPS on 100 processors for metallic potentials.
- New parallelization schemes for faster data transfer between processors
- New minimization algorithm (L-BFGS)

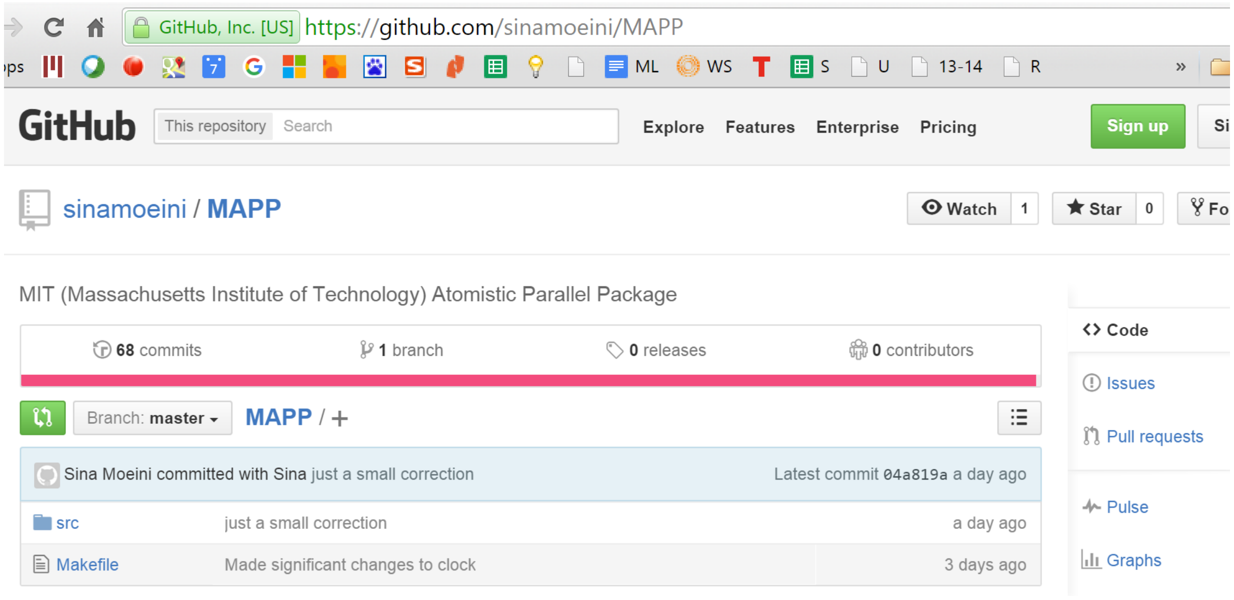

https://github.com/sinamoeini/MAPP

sinamoeini / **MAPP**

MIT (Massachusetts Institute of Technology) Atomistic Parallel Package

68 commits | **1** branch | **0** releases | **0** contributors

Sina Moeini committed with Sina just a small correction — Latest commit `04a819a` a day ago

src	just a small correction	a day ago
Makefile	Made significant changes to clock	3 days ago

http://Li.mit.edu/mapp

Riding on coattail of Fall MRS

A small workshop on

December 2 (Saturday) 2017

at MIT

For simplicity, assume $\Omega - \Omega_V^f = 0$

Take one beam out of this construction scaffold, what will happen?

Answer: *Nothing…*

Remove a brick inside this rubble, what will happen?

This is the case with **grain boundaries**, **liquids**, **and metallic glasses**, which do not preserve **sites**.

Crystal lattice tends to preserve **sites** – ***a most important distinction***

Gas diffusion: lots of free volume

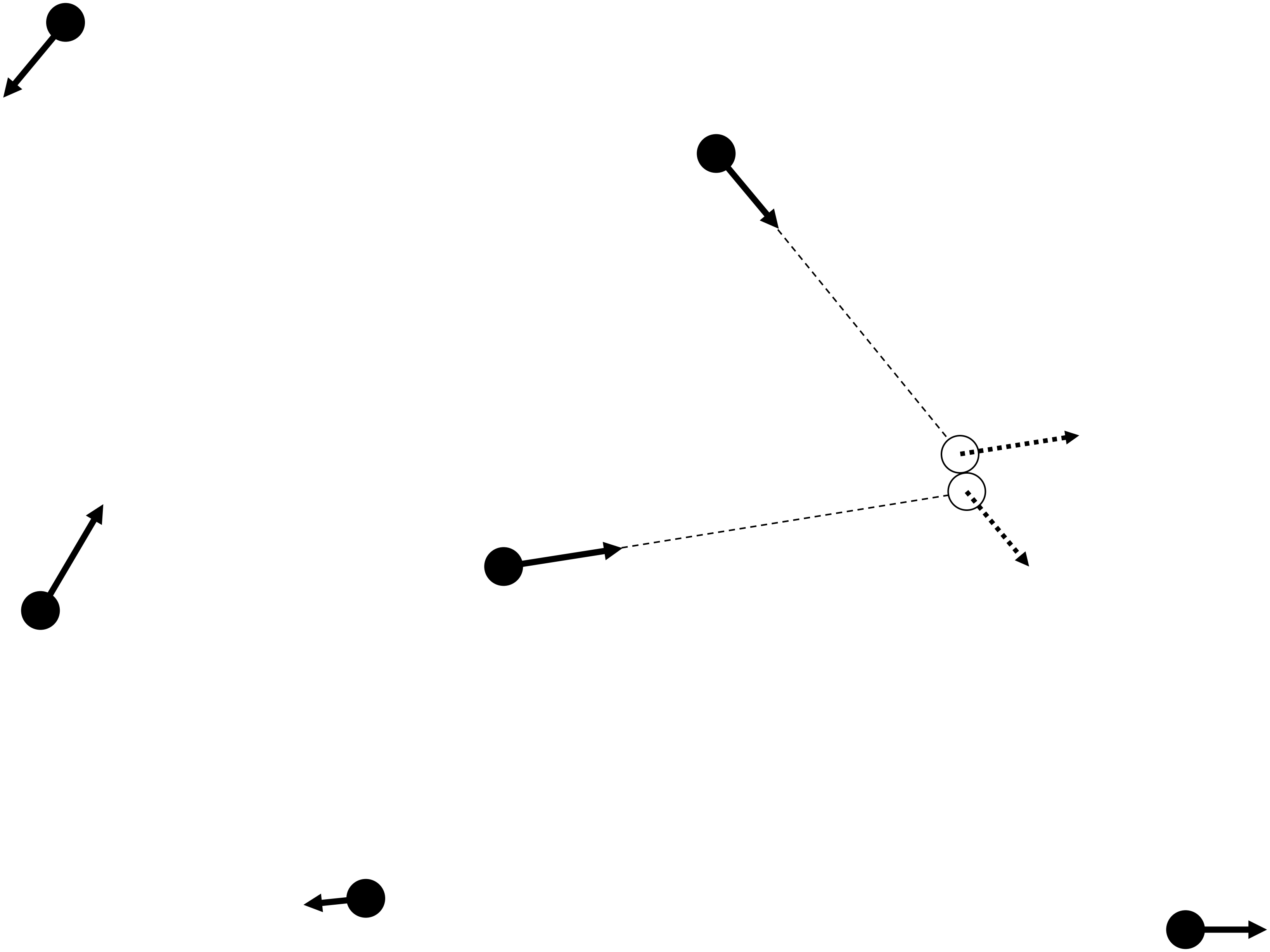

Diffusion in crystal: free volume localized as vacancy

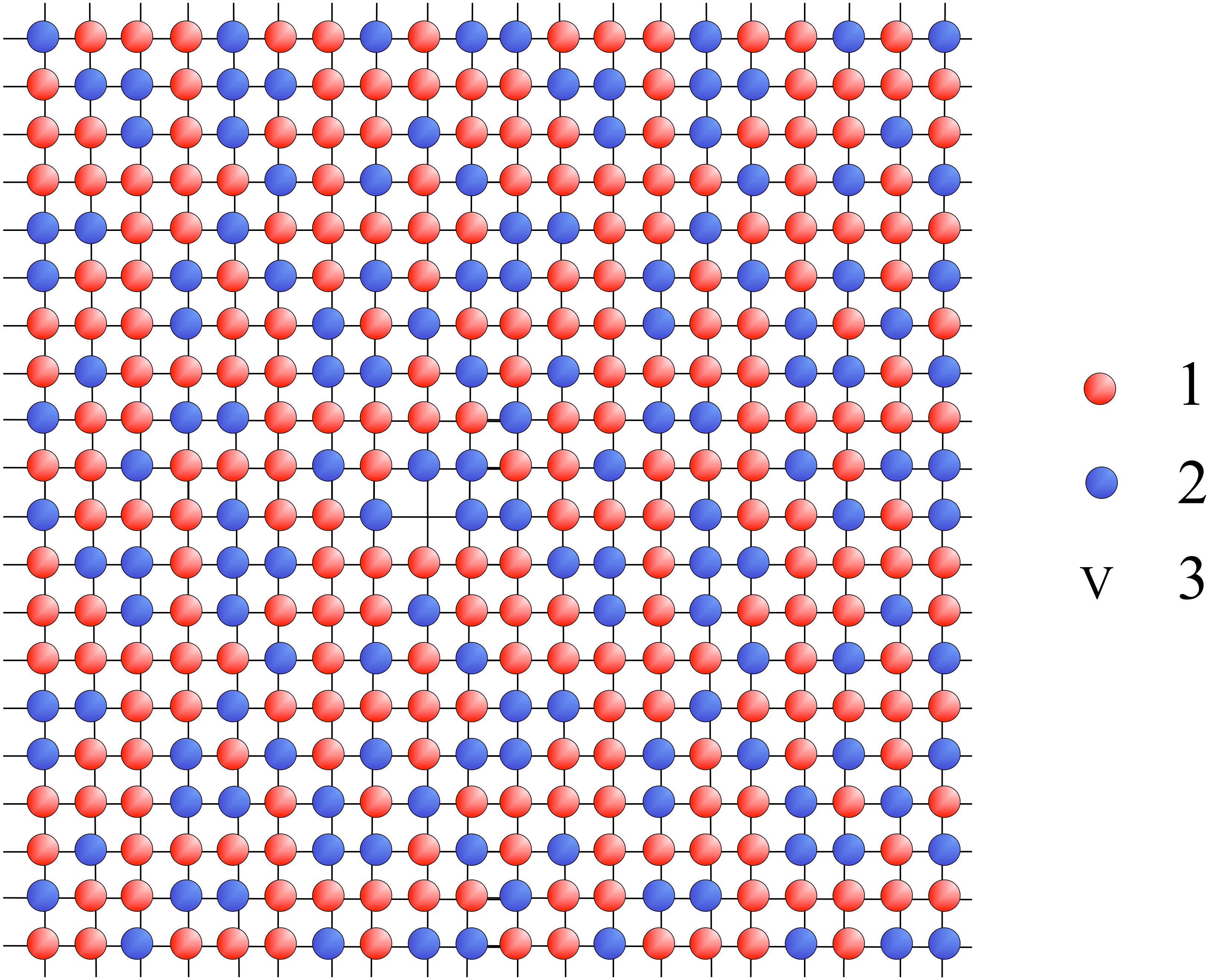

Liquid diffusion: less free volume and shared between atom clusters

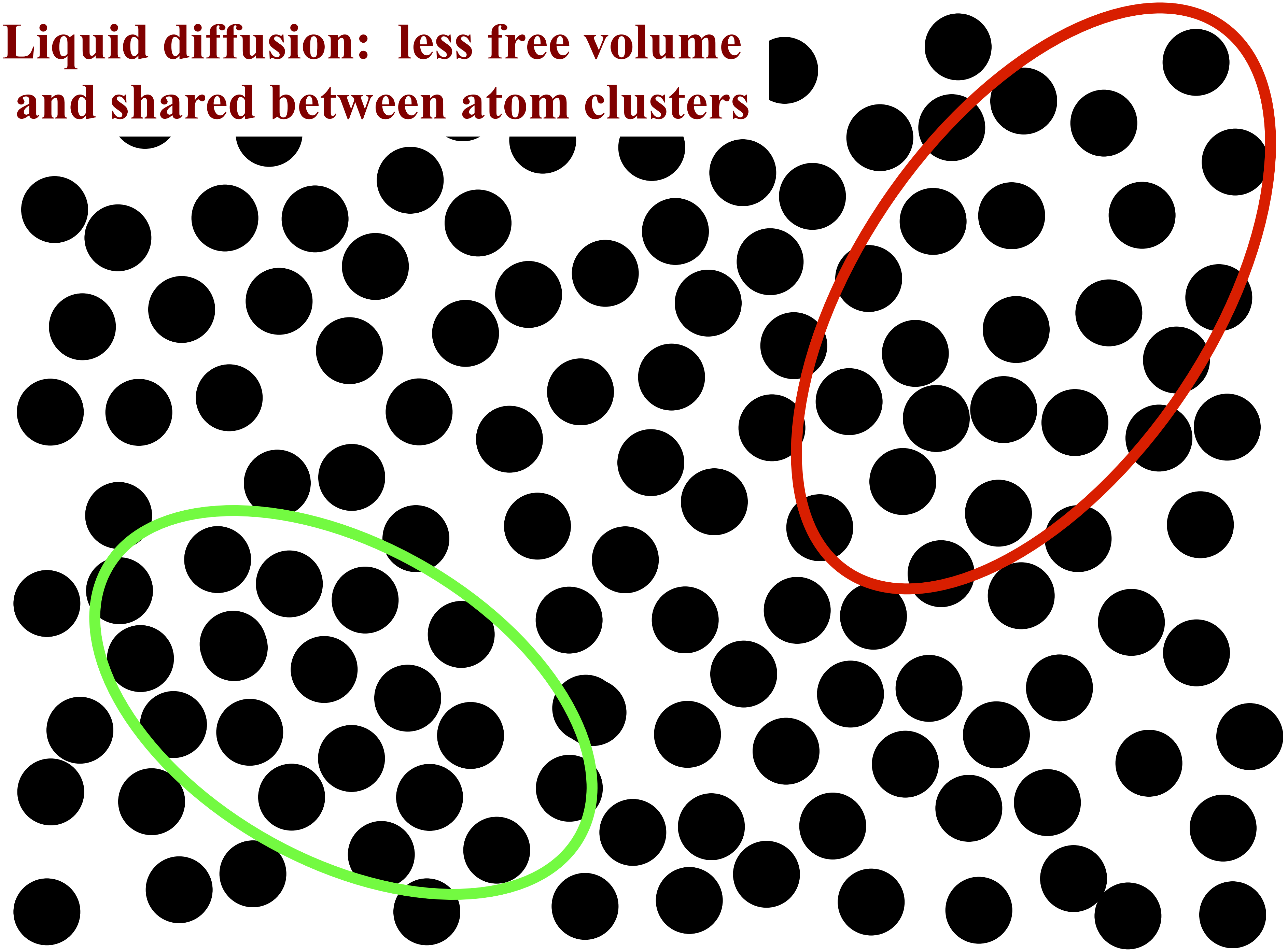

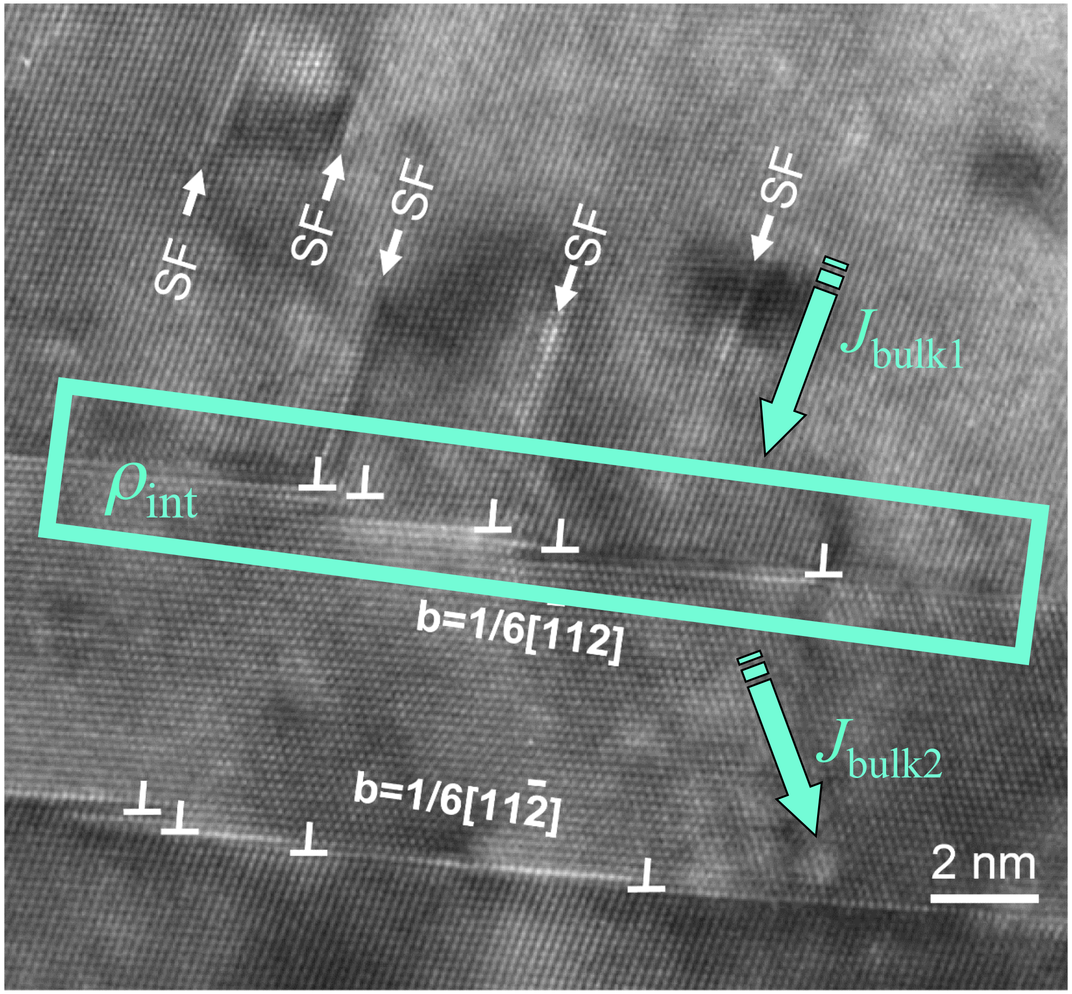

Absorption-Desorption-Transmission kinetics for interfacial dislocation density ρ_{int} evolution:

$$J_{\text{bulk1}} = J_{\text{abs}}(\tau, \rho_{\text{int}}) + J_{\text{tms}}(\tau, \rho_{\text{int}})$$

$$J_{\text{bulk2}} = J_{\text{tms}}(\tau, \rho_{\text{int}}) + J_{\text{des}}(\tau, \rho_{\text{int}})$$

$$\frac{d\rho_{\text{int}}}{dt} = J_{\text{abs}}(\tau, \rho_{\text{int}}) - J_{\text{des}}(\tau, \rho_{\text{int}})$$

$$-\log J(\tau, \rho_{\text{int}}) \propto Q(\tau, \rho_{\text{int}}):$$

Atomistic calculation	Exp't measurement
$\frac{\partial Q(\tau, \rho_{\text{int}})}{\partial \tau} \propto -\Omega \longrightarrow$	strain-rate sensitivity *m*
$\frac{\partial Q(\tau, \rho_{\text{int}})}{\partial \rho_{\text{int}}} \propto \Pi \longrightarrow$	strain-hardening coefficient Θ

1. The variables should really be tensors to denote dislocation types, here we use scalar for simplicity.

2. $J_{\text{bulk}}(\tau)$'s are boundary conditions for dislocation-density aware bulk crystal plasticity models (e.g. Arsenlis, Parks, Becker, Bulatov, *JMPS* 52 (2004) 1213).

Comparison of yield stress, activation volume and strain-rate sensitivity between experimental measurements and atomistic calculation

		yield stress	activation volume Ω	strain-rate sensitivity *m*
Nano-twinned Copper	Uniaxial tension [Lu04]	~ 1 GPa		$m \equiv \frac{\partial \ln \sigma}{\partial \ln \dot{\varepsilon}} = \frac{k_B T}{\sigma \Omega}$
	Nanoindentation [Lu05]	> 700 MPa*	$12 - 22b^3$	$0.025 - 0.036$
	Atomistic calculation	780 MPa	$24 - 44b^3$	$0.013 - 0.023$
Diffusion-controlled processes			$\sim 0.1b^3$	~ 1
Bulk forest hardening		$\sim \mu b \sqrt{\rho_{\text{bulk}}}$	$100 - 1000b^3$	$0 - 0.005$

[*] extracted from measured hardness H as $\frac{H}{3}$.

PNAS **104** (2007) 3031

atomistic calculation can provide strain-rate sensitivity information, at experimentally realistic strain rate of ~10^{-4}/s.

Self-learning $\Delta V(r)$ → Metadynamics: Ishii, Ogata, Kimizuka & Li, "Adaptive-boost molecular dynamics simulation of carbon diffusion in iron," *Phys. Rev. B* **85** (2012) 064303

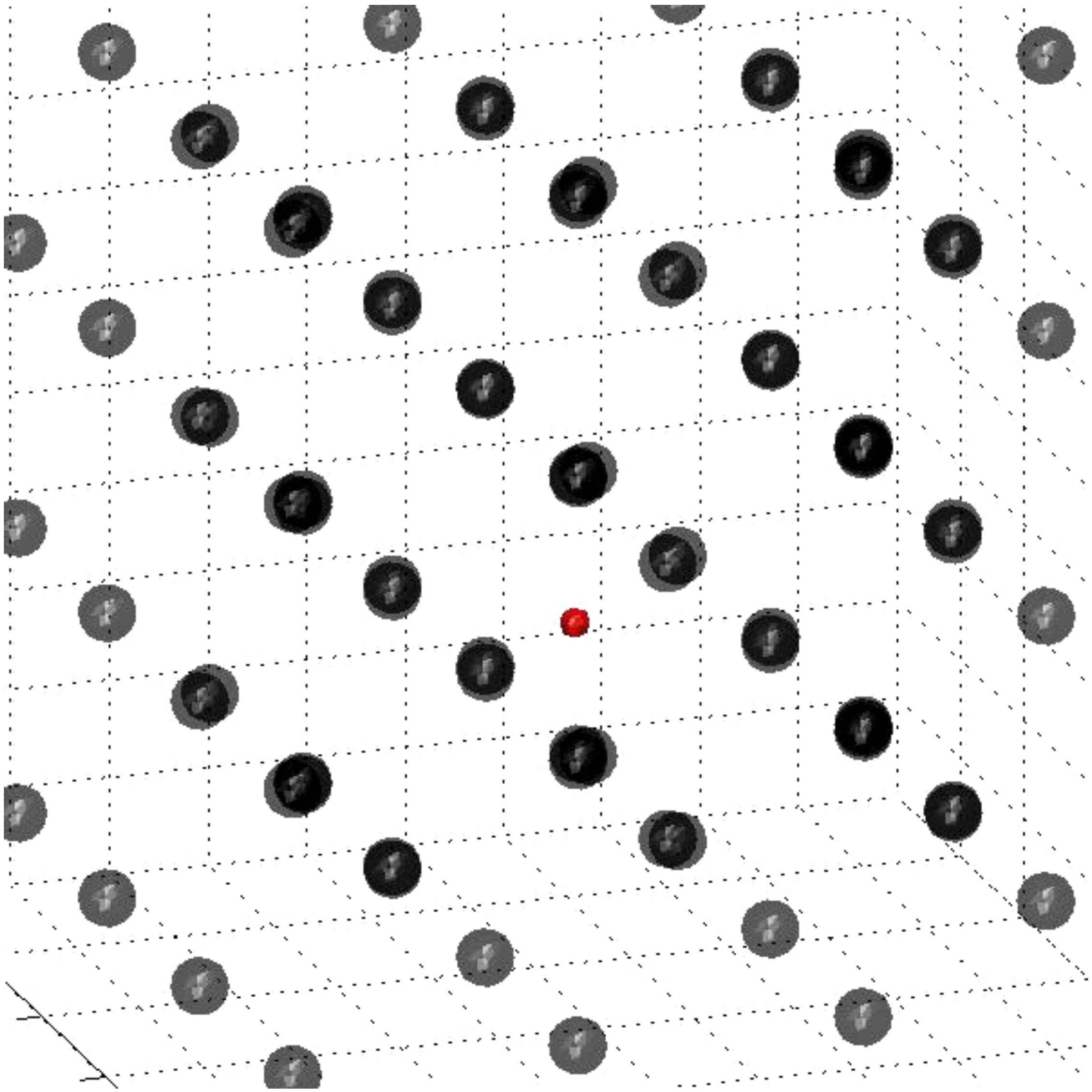

$$\rho(\hat{\boldsymbol{A}}) = \frac{\int \cdots \int \delta(\boldsymbol{A}(\boldsymbol{r}) - \hat{\boldsymbol{A}}) \exp(-\beta\mathcal{H}) d\boldsymbol{r}\, d\,\boldsymbol{p}}{\int \cdots \int \exp(-\beta\mathcal{H}) d\boldsymbol{r}\, d\,\boldsymbol{p}}$$

$$F(\boldsymbol{A}) = -k_{\mathrm{B}} T \ln \rho(\boldsymbol{A})$$

$$\Delta V(\boldsymbol{A}(\boldsymbol{r})) = \Delta V(\boldsymbol{A}) = k_{\mathrm{B}} T \ln \rho(\boldsymbol{A})$$

Density Field Estimator

Eapen, Li & Yip,
“Statistical Field Estimators for Multiscale Simulations,”
Phys. Rev. E **72** (2005) 056712.

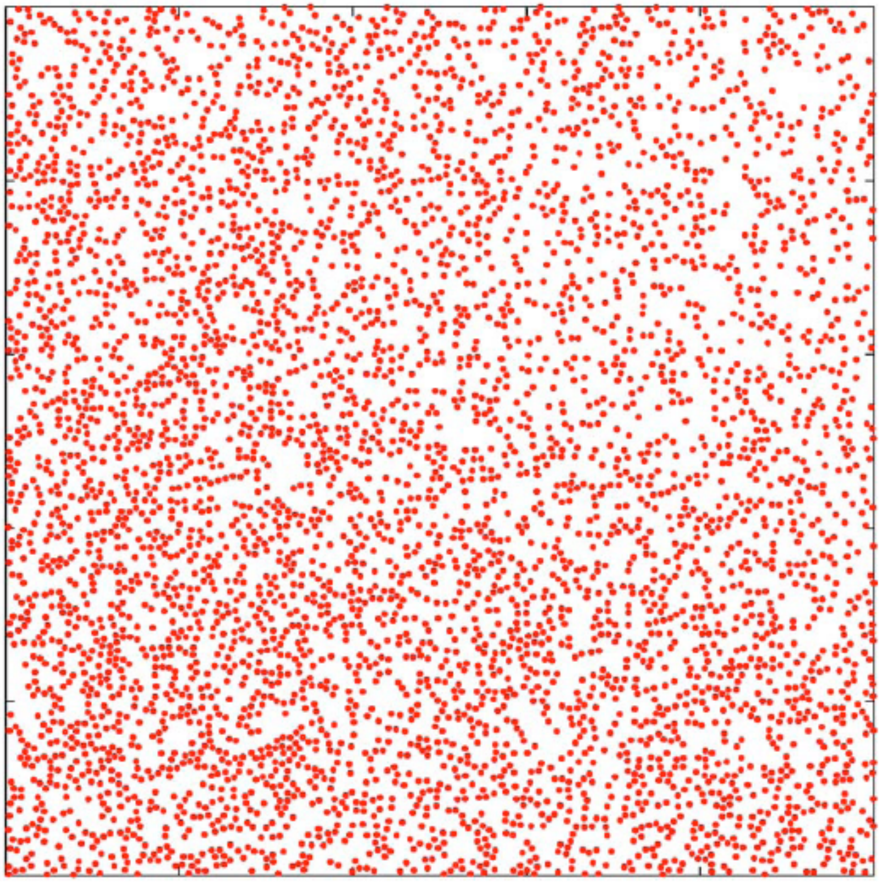

Maximum-entropy density estimator

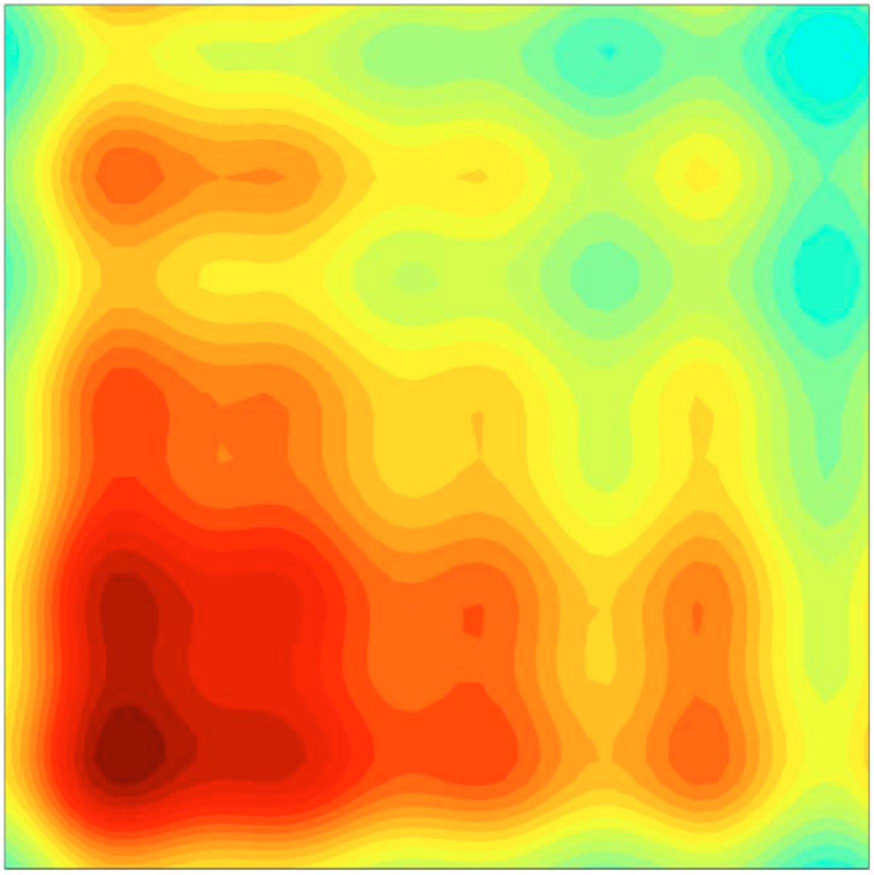

Gaussian smearing
not necessarily the best approach

Phys. Rev. B **85** (2012) 064303

Energy Landscape **Topology**: Glass Viscosity

$$\textbf{Green-Kubo}\ \text{Viscosity} = \frac{\Omega}{k_{\mathrm{B}}T}\int_0^{\infty} d\tau \left\langle \sigma(t)\sigma(t+\tau)\right\rangle$$

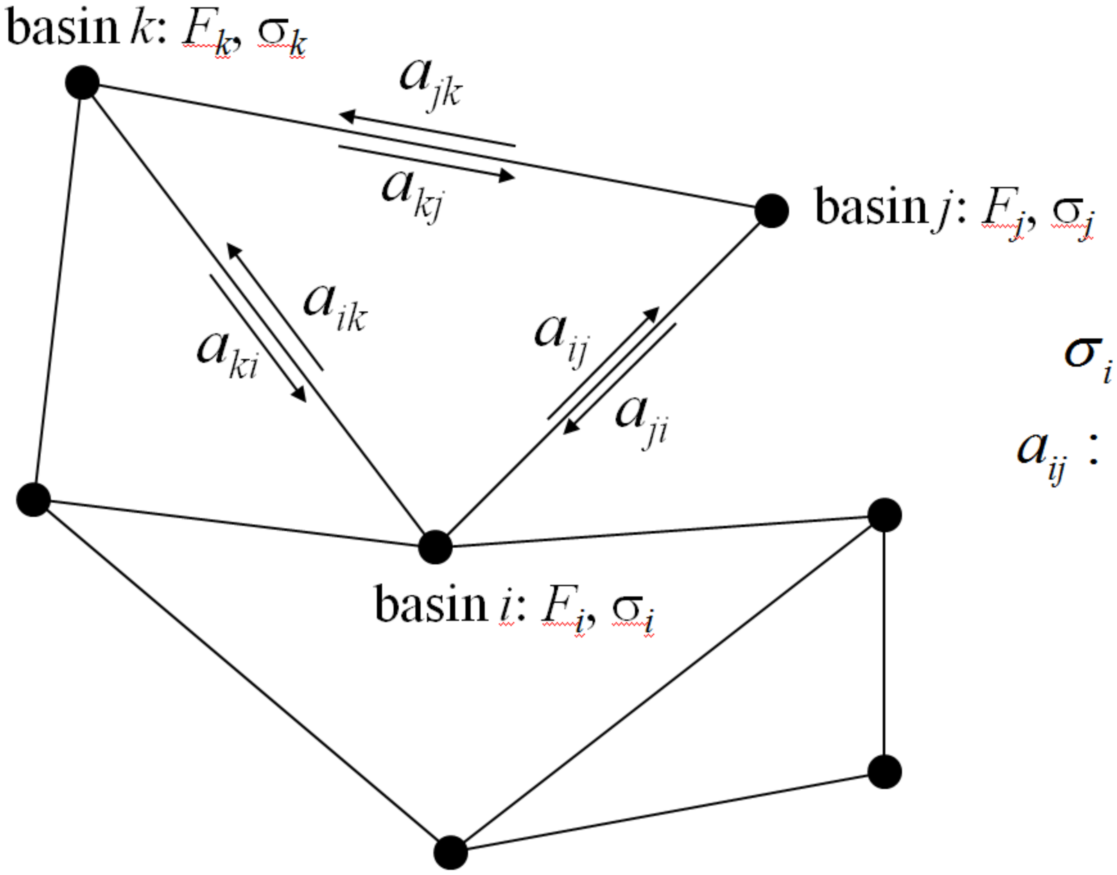

Markov Network Model
of Connected Minima

PLoS ONE **6** (2011) e17909

σ_i : inherent stress of basin i

a_{ij} : thermally activated hopping rate from basin $i \rightarrow j$

$$\left(\mathbf{A}(\omega)\right)_{ij} \equiv \delta_{ij} - \frac{a_{ij}}{\omega + a_j}$$

$$\text{Viscosity} = \frac{\Omega}{k_{\mathrm{B}}T}\sum_i P_i \sigma_i \frac{1}{a_i}\left(\mathbf{A}(\omega = 0^{+})^{-1}\boldsymbol{\sigma}\right)_i$$

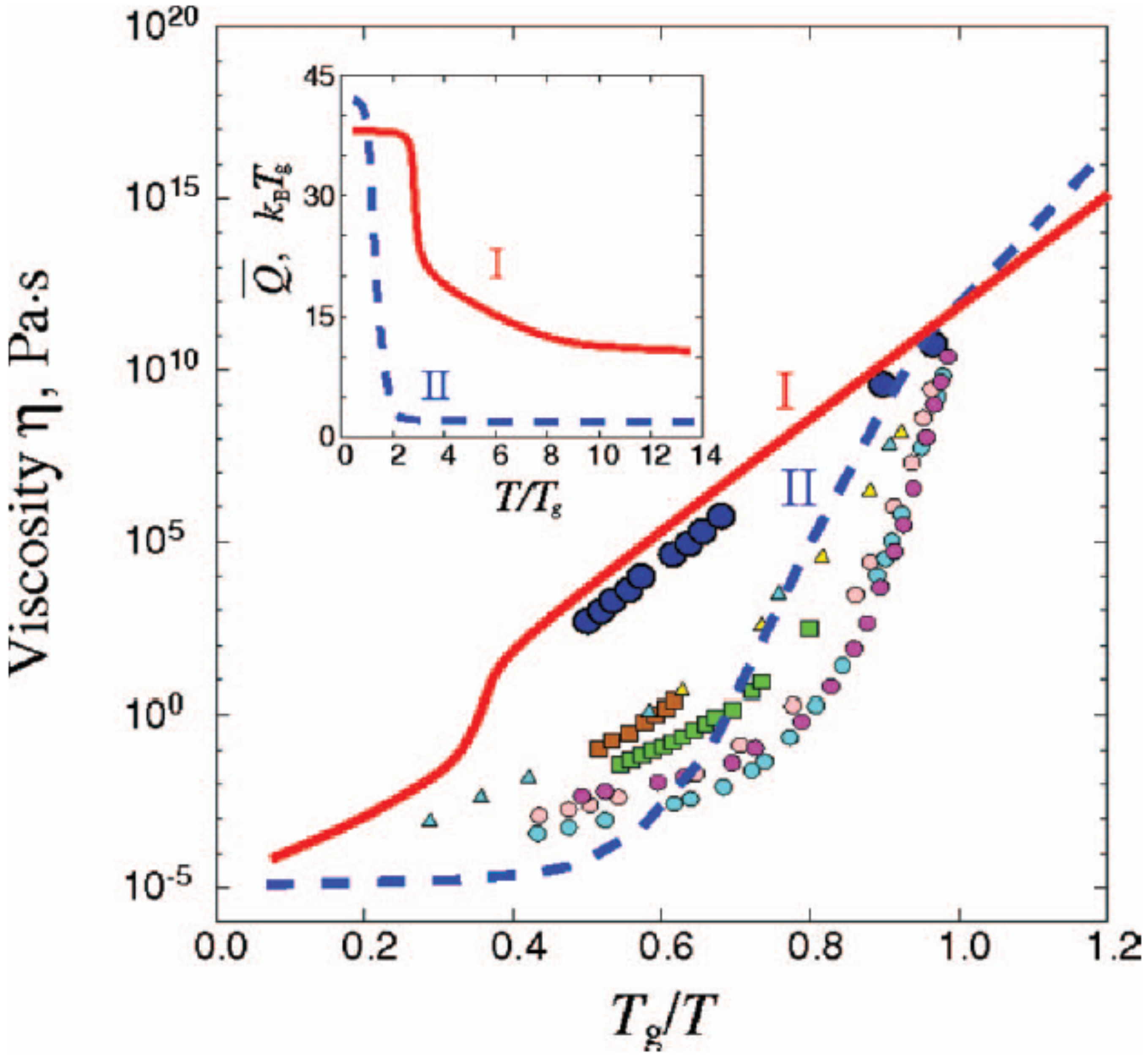

Comparison of viscosity calculations for SiO_2 and BLJ with experimental data on SiO_2 (circles) and fragile glass formers (O-terphenil, propanol, propylene carbonate, etc.)

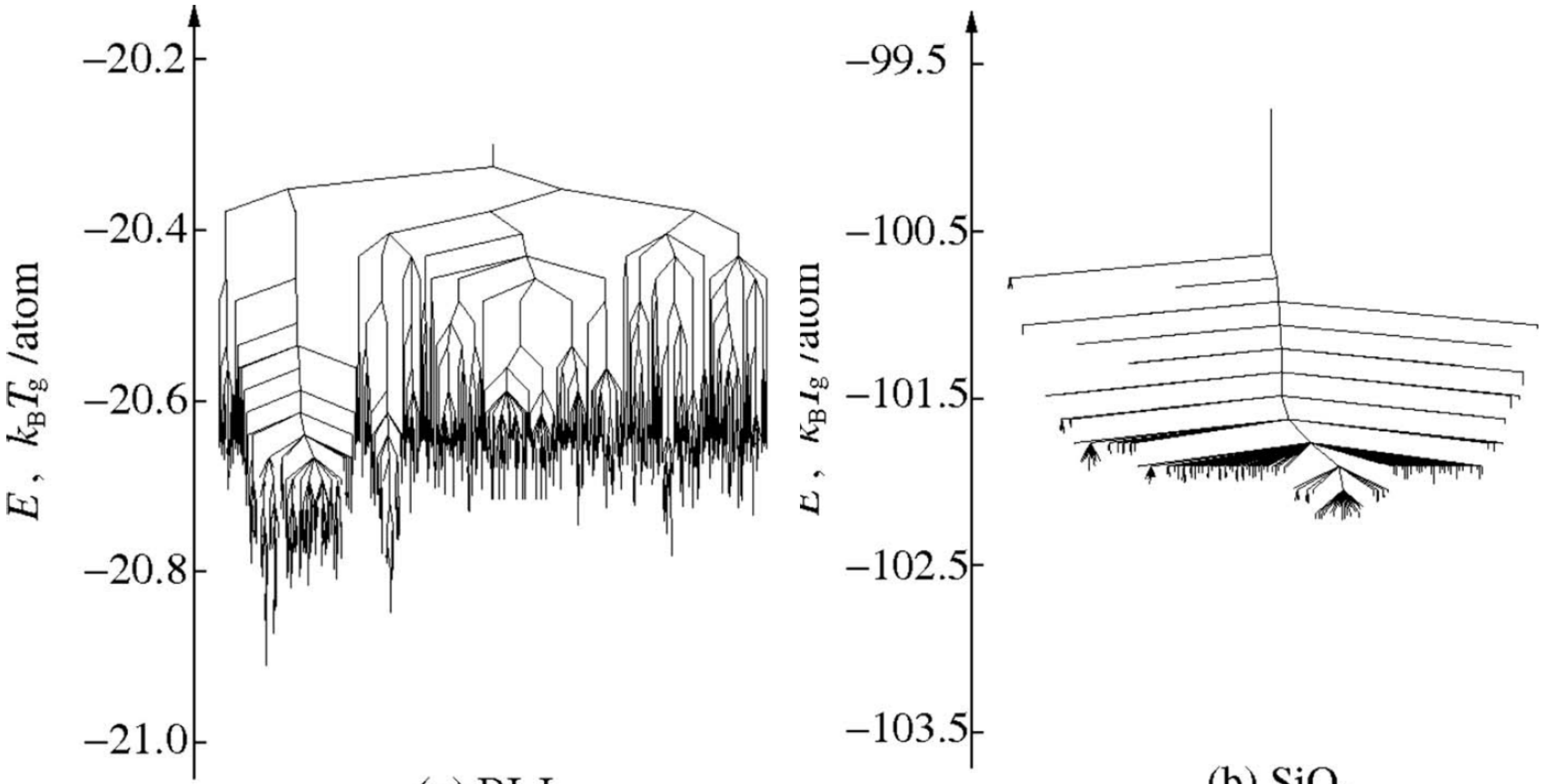

(a) BLJ

(b) SiO_2

Fragile glass former

Strong glass former

Disconnectivity graphs mapped out by Autonomous Basin Climbing

J. Chem. Phys. **131** (2009) 164505

Inventing “Wheels” on Energy Landscape

Inventing “Wheels” on Energy Landscape

How do you know your glass ageing kinetics with Lennard-Jones potential is **unlike** this trek?

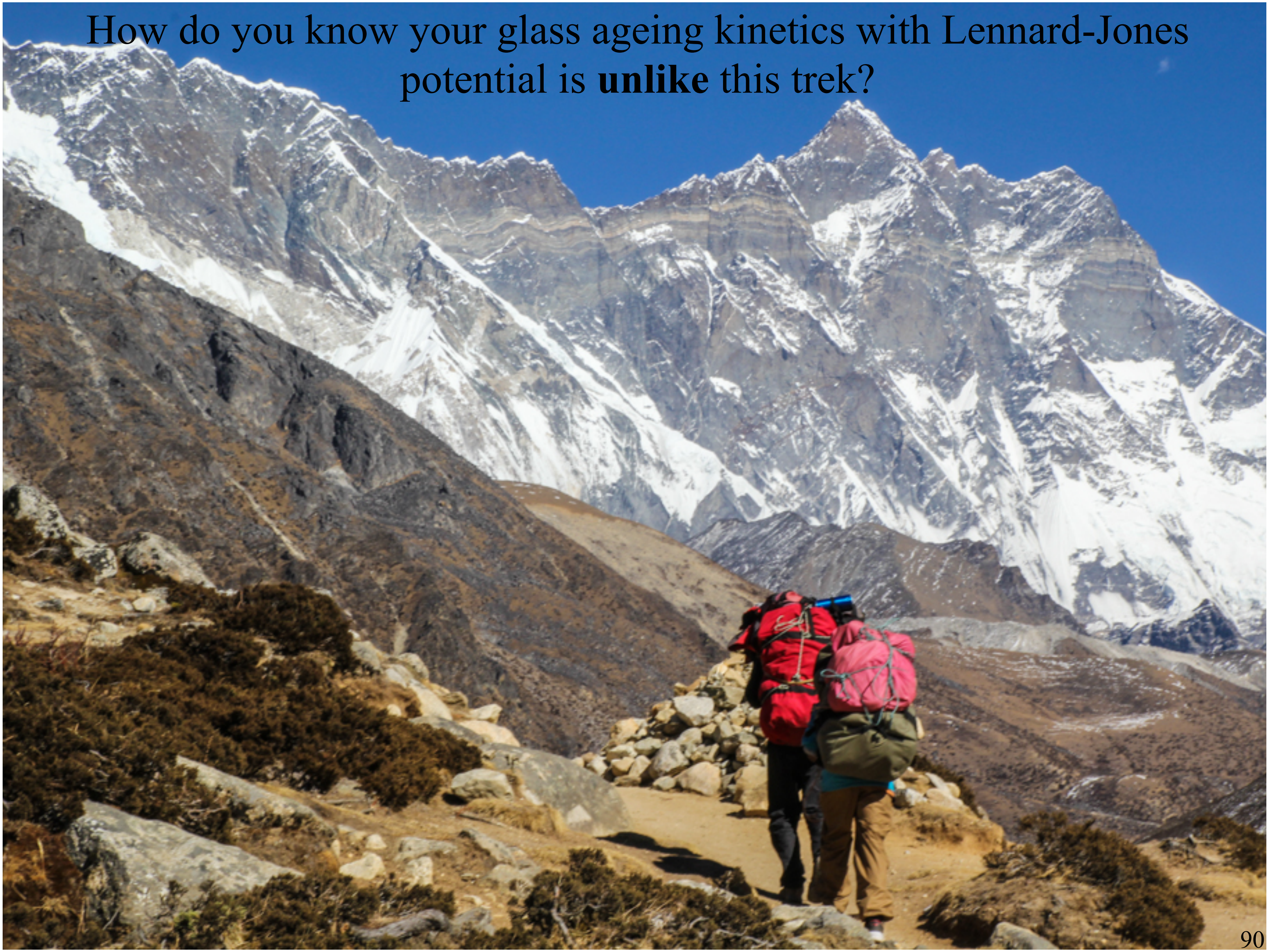

How do you know your glass ageing kinetics with Lennard-Jones potential is **unlike** this trek?

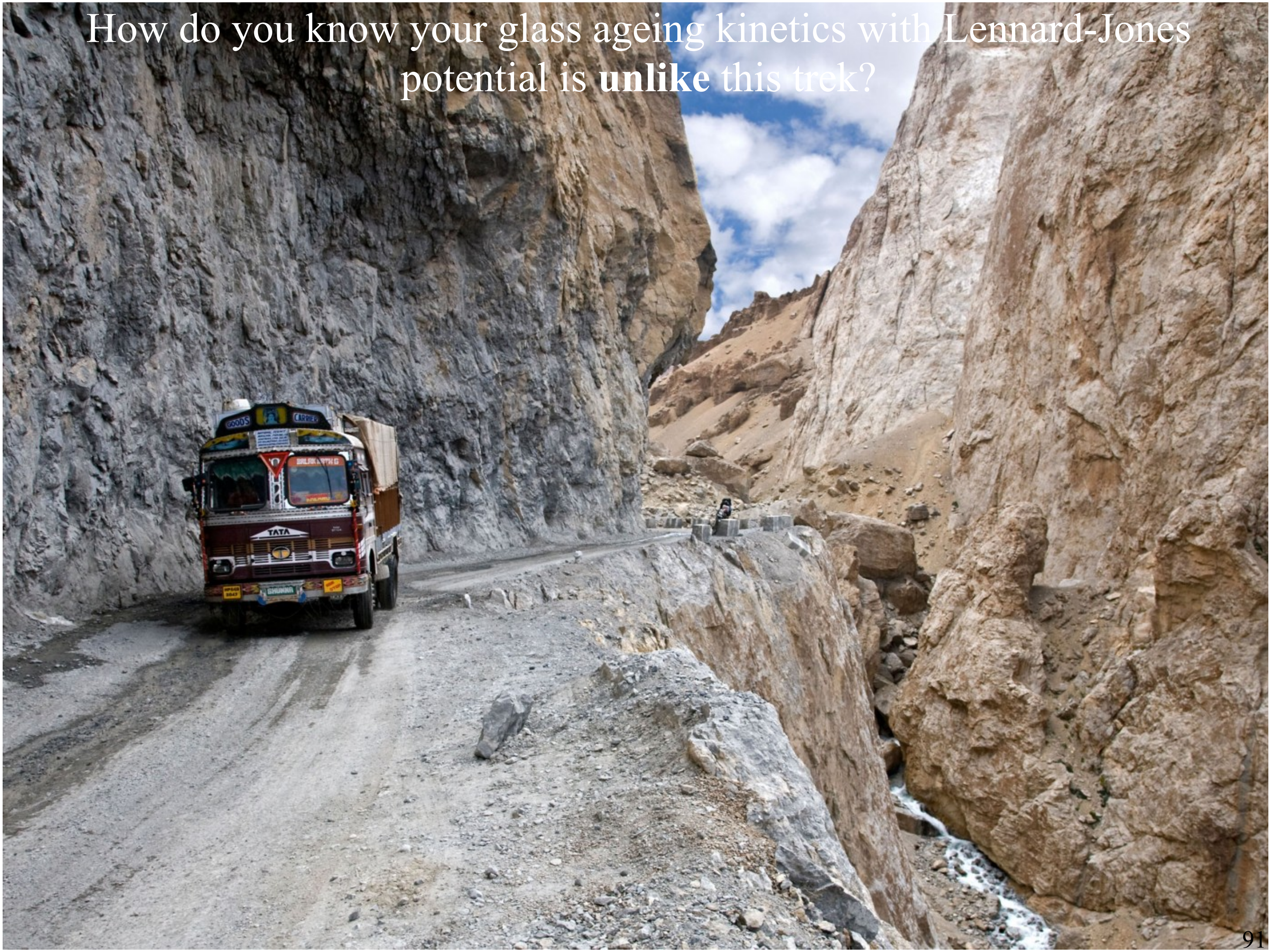

We need freaking wheels, of various sizes

What is a wheel in 1-dimensional energy landscape?

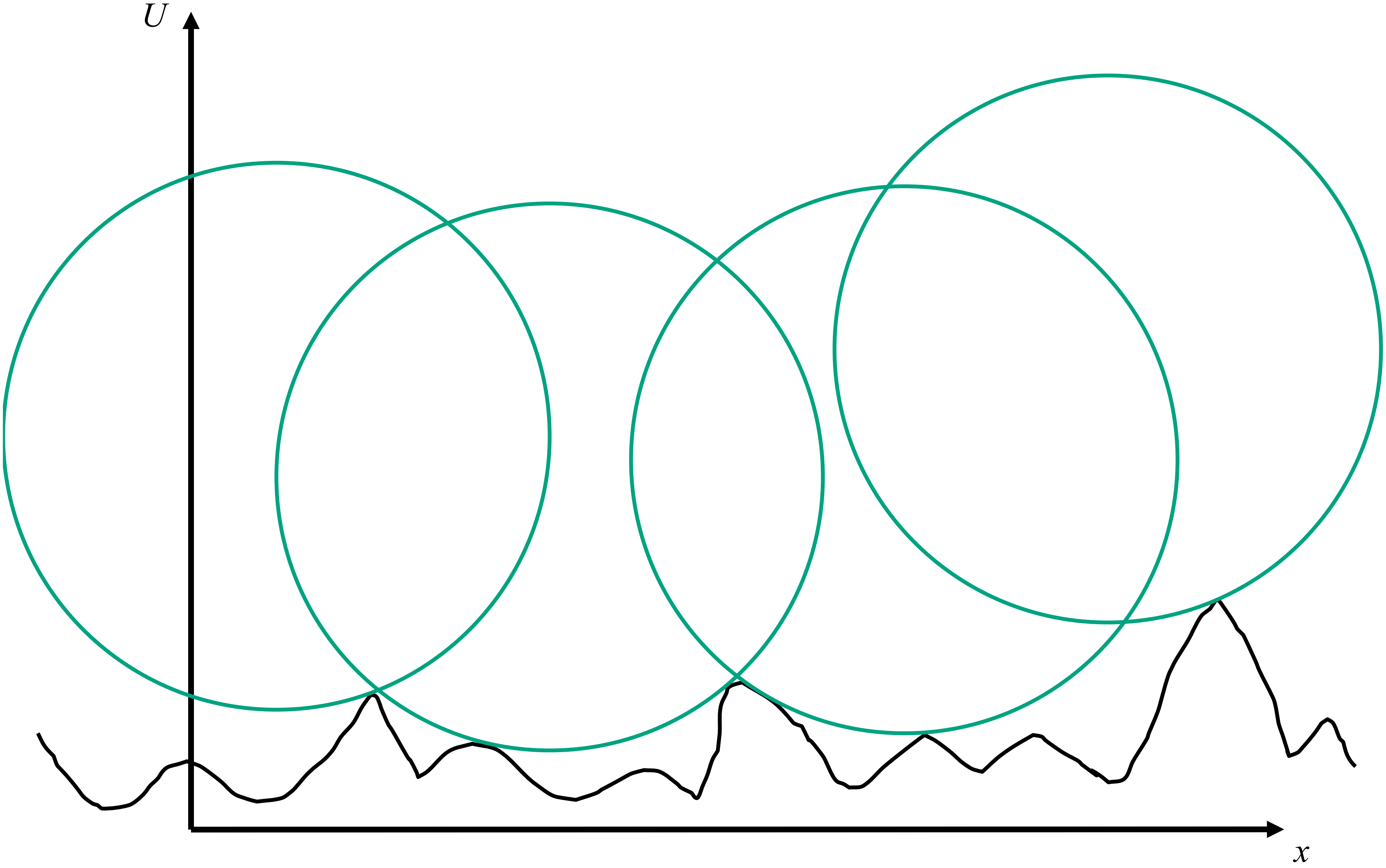

What is a wheel in 3N-dimensional energy landscape? It is a 3N-sphere, and when stable it is contacting 3N+1 **support points** on energy landscape

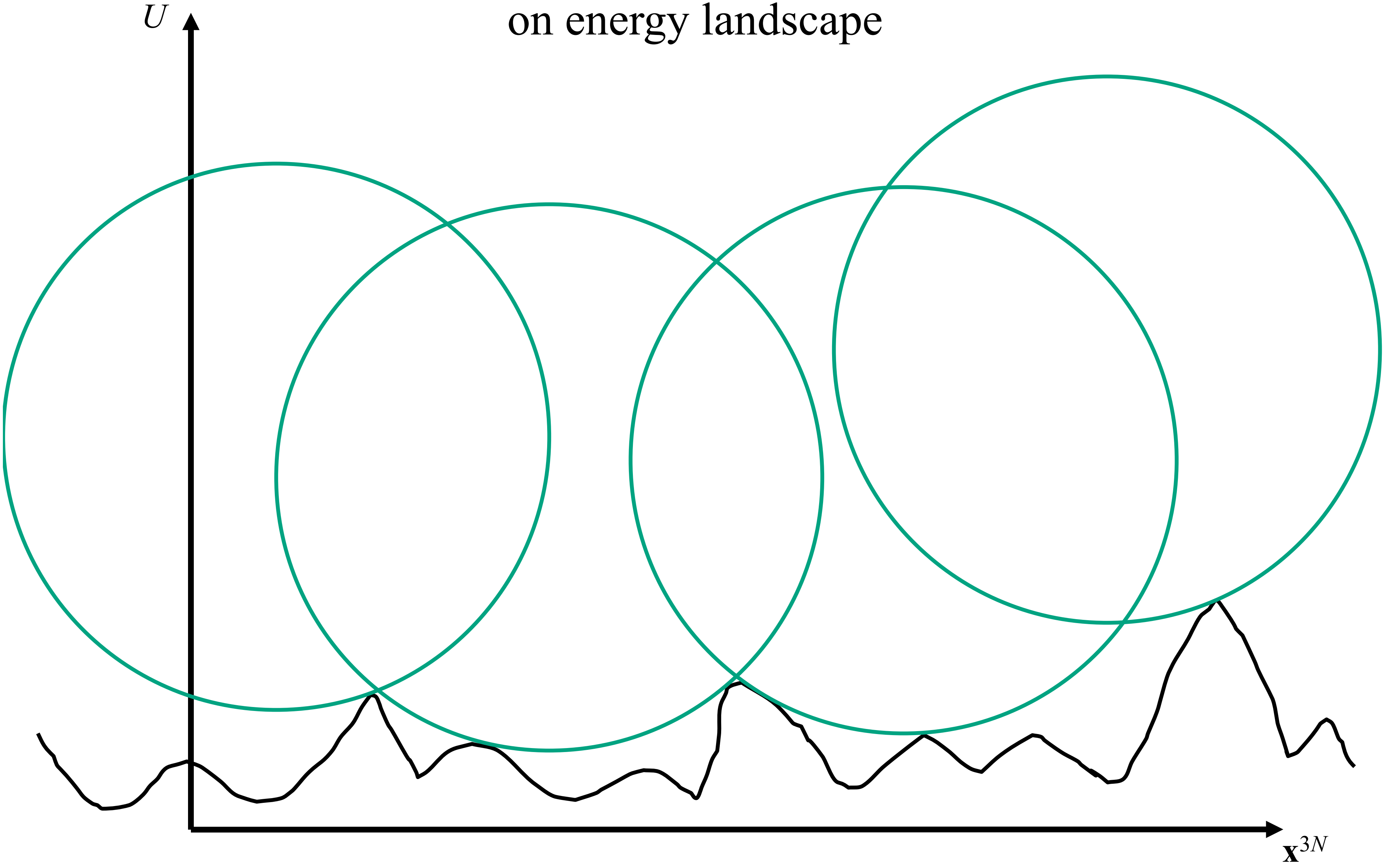

For glass ageing, I want to release a large $3N$-sphere on energy landscape

Then I don’t care *too much* **the exact** pavement pattern

The $3N$-sphere has mass M, radius R, some **support points** $\{\mathbf{x}_{\text{support}}{}^{3N+1}\}$, center location $\mathbf{X}^{3N+1}$, velocity $\mathbf{V}^{3N+1}$, moment of inertia $\mathbf{J}^{3N+1}$

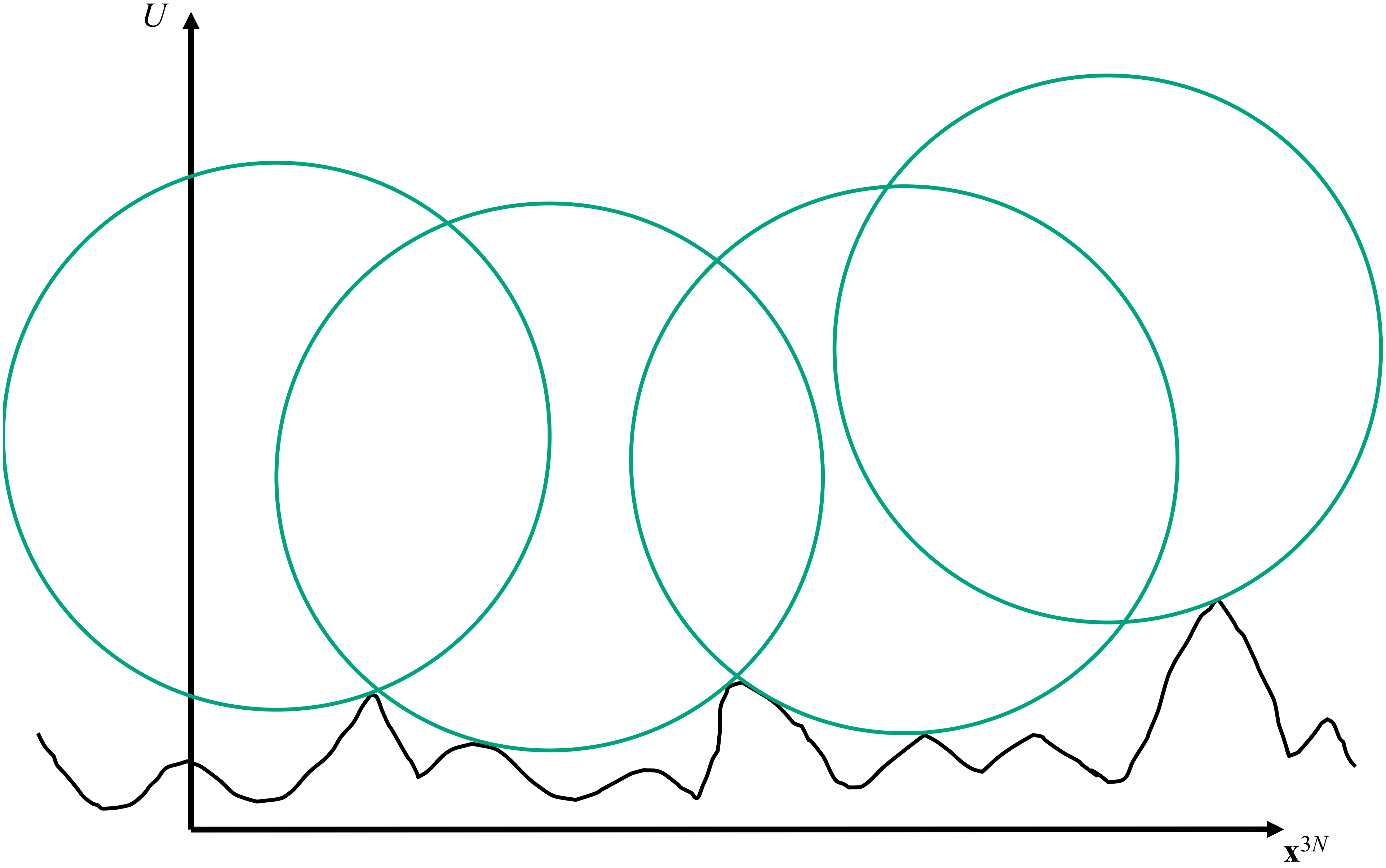

I want to implement a literal dynamical equation of motion
for this 3*N*-ball…
with efficient numerical computation

with rubber tire… damping (car suspension)…
The rubber literally need to hit the “ground” (landscape)

Quite Literal

The key is quick contact points estimation... that is we need to estimate which part of the hypersphere is likely to make "landfall" with a new support point on the energy landscape. The hyperspace "soccer ball" is following rigid-body motion with angular momentum and some damping.

Suppose we have 1000 particles, so the hyperspace soccer ball will need to track 3001 support points, each having 3000 coordinates, so the memory requirement is 3001x3000=10^7 which is tolerable. Of course, we can have a wheel instead of ball that emphasizes fewer "reaction coordinate" and maybe fewer contact points, but this wheel probably need to "turn" after running for a while. For simplicity, let us just release a ball first.

The algorithm also need to choose a “gravitational constant” g that equals $\Delta U \propto g\Delta z$. This potential energy – real spatial distance conversion, and the collectivity of the swarm of points, seem to be the key features of this approach.